Fisheries New Zealand
Tini a Tangaroa

Quantifying benthic biodiversity: using seafloor image data to build single-taxon and community distribution models for Chatham Rise, New Zealand

New Zealand Aquatic Environment and Biodiversity Report No. 235

D.A. Bowden
O.F. Anderson
P. Escobar-Flores
A.A. Rowden
M.R. Clark

ISSN 1179-6480 (online)
ISBN 978-1-99-000888-7 (online)

October 2019

New Zealand Government

Requests for further copies should be directed to:

Publications Logistics Officer
Ministry for Primary Industries
PO Box 2526
WELLINGTON 6140

Email: brand@mpi.govt.nz
Telephone: 0800 00 83 33
Facsimile: 04-894 0300

This publication is also available on the Ministry for Primary Industries websites at:
http://www.mpi.govt.nz/news-and-resources/publications
http://fs.fish.govt.nz go to Document library/Research reports

TABLE OF CONTENTS

EXECUTIVE SUMMARY 1

1. INTRODUCTION 3
1.1 Background 3
1.2 Habitat suitability modelling 3
1.3 Project objectives 4

2. Methods 5
2.1 Study area 5
2.2 Benthic faunal data 5
2.3 Selection of environmental predictor variables 6
2.4 Selection of taxa for single-taxon models 8
2.5 Single-taxon models 10
Spatial autocorrelation 10
Random Forest models 11
Boosted Regression Tree models 11
Hurdle models and uncertainty 11
Model performance 11
Ensemble models 12
Single-taxon model evaluation 12
2.6 Community models 13
Regions of Common Profile 13
Gradient Forests 14
Community model evaluation 15

3. Results 15
3.1 Environmental predictor variables 15
3.2 Single-taxon models 16
Variable selection and influence 16
Model performance 17
Model predictions 18
3.3 Community models 30
Regions of Common Profile 30
Gradient Forests 32
Community model evaluation 38
3.4 Assessing research trawl survey catch records as test-data 41

4. DISCUSSION 42
Future directions 45
Conclusions 46

5. Acknowledgments 47

6. REFERENCES 47

7. APPENDIX 1 – Single-taxon models 53

8. APPENDIX 2 – Regions of Common Profile 55

9. APPENDIX 3 – Gradient Forests 57

EXECUTIVE SUMMARY

Bowden, D.A.; Anderson, O.A.; Escobar-Flores, P.; Rowden, A.A.; Clark, M.R. (2019).
Quantifying benthic biodiversity: using seafloor image data to build single-taxon and community distribution models for Chatham Rise, New Zealand.

***New Zealand Aquatic Environment and Biodiversity Report No. 235*. 65 p.**

Understanding the spatial distribution of seabed biodiversity is essential for effective management of the effects of human activities including fishing and mining. Distributions of individual species, patterns of variability in species richness and abundance, and locations of sensitive or vulnerable habitats are essential inputs into marine spatial planning and risk assessment processes. Chatham Rise is an important deep-sea fishing region in New Zealand. Lying at the convergence of Sub-Tropical and Sub-Antarctic water masses, it has a highly diverse and dynamic physical environment, supporting high levels of biological production and encompassing a broad range of benthic habitats and fauna. Existing knowledge about seabed faunal distributions on Chatham Rise comes from records of museum specimens, fisheries and research trawl bycatch, and increasing from photographic surveys. Data from museum and trawl databases have been used to build models that predict species and community distributions in unsampled space but because the models are based on presence-only data from disparate sources and do not incorporate population density data, their predictions are considered uncertain.

To reduce uncertainty in predictions, we used a new, spatially extensive, fully quantitative, and taxonomically consistent dataset of benthic invertebrate occurrence developed by merging data from five seabed photographic surveys, to inform development of improved predictive models at both single-taxon and community levels. Two independent modelling methods were used for each level: Boosted Regression Trees (BRT) and Random Forests (RF) for single-taxa, and Regions of Common Profile (RCP) and Gradient Forests (GF) for communities, enabling ensemble model predictions for single taxa and comparison between classification methods for communities. For single-taxon models, the 'hurdle' model technique was used, combining predictions from presence-absence and abundance models to reduce bias associated with zero-inflated data. Sets of explanatory environmental variables (12 for single-taxon models, 18 for GF, and 9 for RCP) were selected from an initial set of 58 candidate layers and the 354 invertebrate taxa identified from the seabed image surveys were condensed into a set of 69 taxa by aggregation to higher taxonomic levels and exclusion of rarer and non-benthic taxa. Single-taxon models were produced for 20 taxa, selected according to their sensitivity or vulnerability to human-induced environmental impacts, while all 69 taxa were included in community models.

Outputs from the single-taxon models are presented as maps showing predicted occurrences as densities (individuals 1000 m^{-2}) with associated estimates of model precision (CV) and cross-validation metrics. All models performed well by these criteria but a comparison using invertebrate bycatch data from the *trawl* database was inconclusive for most taxa modelled because of inadequate abundance information in the test data. While predictions for most of the taxa modelled have clear similarities with those of previous models, they also show differences, often driven by inclusion of density data. Outputs from the community models are presented as spatial classifications of the study area, analogous to existing spatial classifications such as the Marine Environments Classification and derivatives. RCP divided the area into 7 classes, whereas a hierarchical clustering method allowed GF results to be assessed at class levels from 7 to 50 classes and compared visually against existing classifications.

These predictions are the best-informed representations of seabed distributions at regional scales in the New Zealand Exclusive Economic Zone to date and provide a resource that will have applications in marine environmental management and ecosystem research. Potential applications include quantification of benthic impacts from bottom-contact fishing gear and other anthropogenic agencies, informing spatial management of biodiversity through, for example, the design of marine protected areas, and informing research into ecosystem linkages between water-column and seabed processes. A further obvious

application and test of the predictions will be to use the modelled relationships developed here to predict faunal distributions across seabed areas beyond Chatham Rise.

1. INTRODUCTION

1.1 Background

In New Zealand, as in other parts of the world, concern about the environmental effects of deep-sea bottom trawling is an escalating issue (Clark 2010, Clark et al. 2016, Kaiser et al. 2006). The Marine Stewardship Council has identified benthic effects as a concern that is not being addressed adequately for eco-certification, and public concern about the effects of bottom trawling has been heightened by increasing awareness of impacts on iconic seabed habitats such as cold-water corals on seamounts (Clark et al. 2019). Key knowledge required to understand and manage the ecosystem impacts of bottom-contact fishing and other seabed disturbances is quantitative baseline information about the distribution and abundance of benthic species and communities. Because such information represents fundamental knowledge about biodiversity, it is also required by government agencies to conform with New Zealand's Biodiversity Strategy (https://www.mfe.govt.nz/publications/biodiversity/new-zealand-biodiversity-strategy) and meet commitments under international agreements including the Convention on Biodiversity Aichi Targets (https://www.cbd.int/sp/targets/).

Because detailed quantitative data on benthic distributions are generally sparse in depths beyond the coastal zone, there has been increasing interest in the use of habitat suitability models, also known as species distribution models (SDM, Reiss et al. 2015, Vierod et al. 2014) in which sophisticated non-linear correlations between point-sampled distributions of benthic fauna and grids of environmental variables are developed to predict probabilities of suitable habitat occurring in unsampled areas. However, the very sparseness of data that has prompted development and use of such models can also result in high levels of uncertainty associated with their predictions, especially at broader spatial scales (Araujo & Guisan 2006). This uncertainty has limited the usefulness of modelled distribution data in environmental management, and in some cases in New Zealand has contributed to potentially over-cautious management decisions in relation to proposed seabed activities (e.g., EPA 2015).

1.2 Habitat suitability modelling

Several methods have been developed to model spatial distributions by defining relationships between point-sampled faunal data and environmental gradients. These methods can be broadly separated into those that model individual taxa (referred to here as 'single-taxon models') and those that model the entire sampled assemblage or community simultaneously (referred to here as 'community models'). Established single-taxon modelling methods include Boosted Regression Trees (BRT, De'ath 2007), Maximum Entropy (MaxEnt, Elith et al. 2011), Random Forests (RF, Breiman 2001), and Generalized Additive Models (GAM), while community modelling methods include Generalised Dissimilarity Modelling (GDM, Ferrier et al. 2007), Gradient Forests (GF, Ellis et al. 2012), and Regions of Common Profile (RCP, Foster et al. 2013). The field is in constant development, however, and no one method has been demonstrated to have clear superiority (Robinson et al. 2017).

For single-taxon models in this study, we selected two classification/regression decision-tree methods in common usage for ecological data: RF and BRT. These are among a number of methods that use a machine-learning (ML) algorithm to learn the relationship between the response and its predictors, rather than relying on the more prescriptive approaches based on statistical methods, and both have been shown to perform well in comparative studies (e.g., Martinez-Rincon et al. 2012, Valle et al. 2013). We also considered how best to work with the type of taxon density data produced from analysis of photographic transects, which are typical of point-sampled ecological data sets in being highly over-dispersed, strongly skewed distributions with an excess of zeros. Parametric models such as Generalized Linear Models (GLMs) can allow for the response variable to have a non-normal error distribution such as quasi-Poisson, while other model types allow for negative binomial and zero-inflated Poisson distributions. A more intuitive approach to dealing with zero-inflated data, however, and one that has been shown in at least one study to outperform such models (Potts & Elith 2006), is the use of 'hurdle' models (Cragg 1971). A hurdle model consists of two component models, a binary model predicting probability of presence using the entire data set, and a regression model predicting counts or density using only data from presence locations; the outputs of the two parts are then combined to produce final predictions. We used the hurdle model approach to predict abundance for all single-taxon models.

While individual taxa can be modelled using common habitat suitability or species distribution modelling methods, it is often important for management and conservation initiatives to be able to map spatial variability in overall community composition. Until recently, it was only possible to model whole-community variability (e.g., for bio-regionalisation), by summarising differences among sites as a matrix of similarities or dissimilarities and then clustering these based on relative similarities. The resulting clusters of sites with self-similar communities could then be plotted in geographic space to visualise distributions, or related to continuous environmental variable data to enable prediction in unsampled areas. The most sophisticated method developed using this approach is GDM, which first defines relative similarities among communities at sample sites (using Bray-Curtis similarity), then develops a generalised linear model to identify transformations of environmental variables that correlate best with the community similarity matrix. In New Zealand, GDM was used to develop the original Marine Environment Classification (MEC, Snelder et al. 2007) and subsequent Benthic-Optimised Marine Environment Classification (BOMEC, Leathwick et al. 2012). However, the reliance of such methods on reducing the full detail of the sampled community data to a matrix of pairwise distances among sites has drawbacks in that the results cannot readily be interpreted in terms of how individual taxa respond to environmental gradients, and that there is no robust method to quantify uncertainty in the resulting classifications.

More sophisticated techniques have been developed recently that use novel statistical approaches to model multiple species simultaneously in relation to environmental variables. Of these, we chose for this study two that have become established as accessible methods for community modelling of this type: RCP and GF. GF develops RF analyses for each taxon in the community dataset, describing relationships between the sampled distribution of that taxon and a set of available environmental layers. Results from these individual analyses are then aggregated and used to develop transformations for each environmental predictor that maximise their correspondence with overall community variability, or beta diversity. Outputs from GF are similar in form to those from GDM in that each cell in the spatial grid of the study area is associated with transformed values for each of the environmental predictor variables. This approach enables mapping of the area at different spatial resolutions; from a map at grid-resolution representing gradients in taxon turnover, to hard-boundary classifications developed using appropriate clustering algorithms to group grid cells based on their transformed environmental values (Compton et al. 2013, Pitcher et al. 2012, Stephenson et al. 2018). GF has advantages over GDM in that the contributions of individual taxa can be quantified explicitly, resulting in less uncertainty in understanding of what the output classifications represent in terms of taxa likely to be encountered in different regions. RCP attempts to achieve the same result as GDM and GF; classification of space into distinct regions within which community composition is similar but uses a more statistically robust single-stage modelling approach, which enables explicit quantification of uncertainty. Its outputs are in the form of probabilities for each grid cell that a given community type will be present. These probabilities can then be condensed into a hard-boundary spatial classification by assigning each cell to a community type based on a threshold probability value (Foster et al. 2017, Hill et al. 2017).

1.3 Project objectives

The current project has the overall aim of reducing uncertainty in our understanding of the distributions of benthic fauna across Chatham Rise, a key deep-sea fisheries area. It is structured around four research objectives: (1) a dedicated research voyage using cameras and sediment corers to collect new data on seabed habitats and fauna across Chatham Rise; (2) development of a comprehensive dataset of benthic fauna derived from all seabed photographic surveys on Chatham Rise; (3) assessment of the usefulness of existing predictive models, using the new dataset as an independent test set, and (4) development of updated predictive distribution models of benthic fauna and habitats based on all available data.

The results of Objective 1, the voyage to collect new data, are described by Bowden et al. (2017), the dataset of benthic faunal distributions developed from multiple photographic surveys for Objective 2 is described by Bowden et al. (2019), and the assessment of existing predictive models is described by Anderson et al. (2019). Here, we present work under Objective 4, in which we use the dataset developed under Objective 2 to inform development of new single-taxon and community habitat suitability models for Chatham Rise. The work presented here consisted of four main phases: (i) review and selection of available environmental

predictor variables; (ii) selection and development of modelling methods, (iii) construction of models, and (iv) where possible, testing of the models against independent data.

2. Methods

2.1 Study area

Chatham Rise is a continental rise extending eastwards from the South Island of New Zealand for approximately 1000 km, with Mernoo Bank at its western end and the Chatham Islands at the eastern end (Figure 1). The Sub-Tropical Front coincides with, and is partially constrained by the rise, and because of this it is the most biologically productive fisheries region in New Zealand's Exclusive Economic Zone (EEZ) (Clark et al. 2000, Marchal et al. 2009, McClatchie et al. 1997), with intense phytoplankton blooms propagating from west to east along its length (Chiswell 2001, Nodder et al. 2012, Nodder et al. 2007). Commercially important bottom trawl fisheries exploit populations of scampi, hoki (*Macruronus novaezelandiae*), orange roughy (*Hoplostethus atlanticus*), and oreos (*Pseudocyttus maculatus*, *Neocyttus rhomboidalis* and others). Recent summaries of bottom-contact trawl history across Chatham Rise (Baird et al. 2011, Black & Tilney 2015, Black et al. 2013) show highest trawling intensity, primarily from the hoki fishery, at 450–700 m depth west of Mernoo Bank and on the southern and northern central flanks of Chatham Rise. At present, initiatives to protect benthic habitats and fauna are limited to closures, since 2000, of fisheries on some seamounts in the 'Graveyard' and 'Andes' regions on the northwest flank and southeast flanks of the rise, respectively (Clark & Dunn 2012), and establishment in 2007 of two Benthic Protection Areas (BPAs); the Mid Chatham Rise BPA and the East Chatham Rise BPA (Helson et al. 2010).

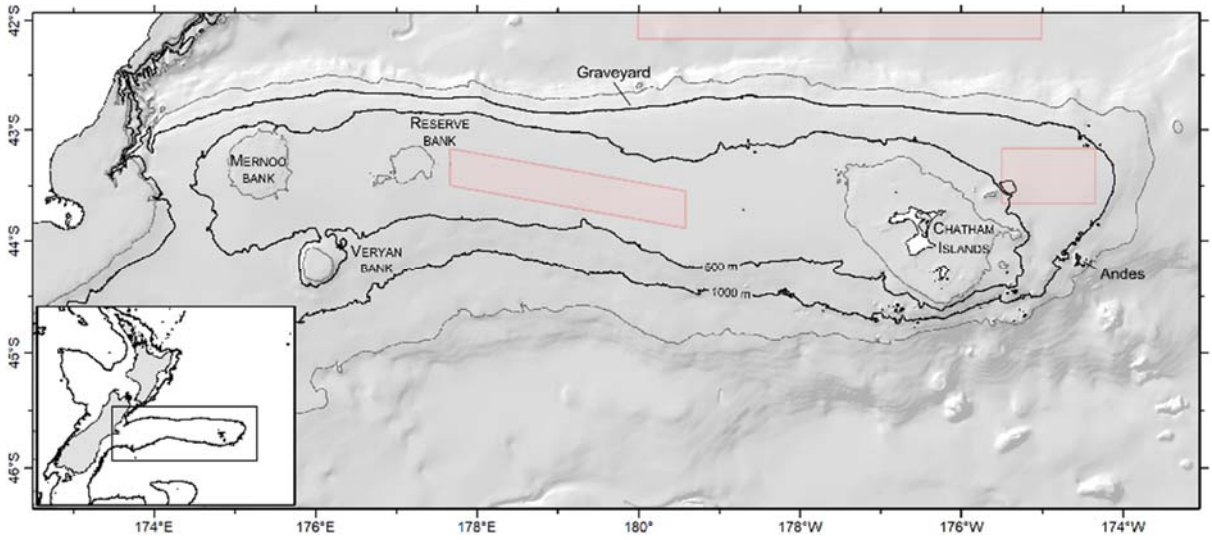

Figure 1: Chatham Rise. Isobaths show 250, 500, 1000, and 1500 metre depths and red polygons show Benthic Protection Areas (BPAs). The three main bank features are named, together with the locations of the Graveyard and Andes seamounts. Inset map shows location of the study area in relation to New Zealand and the 1000 m isobath.

2.2 Benthic faunal data

Faunal sample data for all models were from photographic surveys of Chatham Rise. A comprehensive account of the photographic transect surveys conducted on the Chatham Rise, the image data they collected, and the auditing procedures used to create a combined dataset of faunal densities, is provided by Bowden et al. (2019). For this analysis we selected data from five surveys (Figure 2): a core set of four biodiversity surveys that provided wide spatial coverage of the study area, used the same high-quality imaging system (NIWA's Deep Towed Imaging System, DTIS, Hill 2009), and used consistent methods for logging navigational and observational data, plus one commercial ROV survey of the central Chatham Rise crest

(Rowden et al. 2013), which was designed by NIWA researchers to provide data comparable in extent and quality to the DTIS surveys.

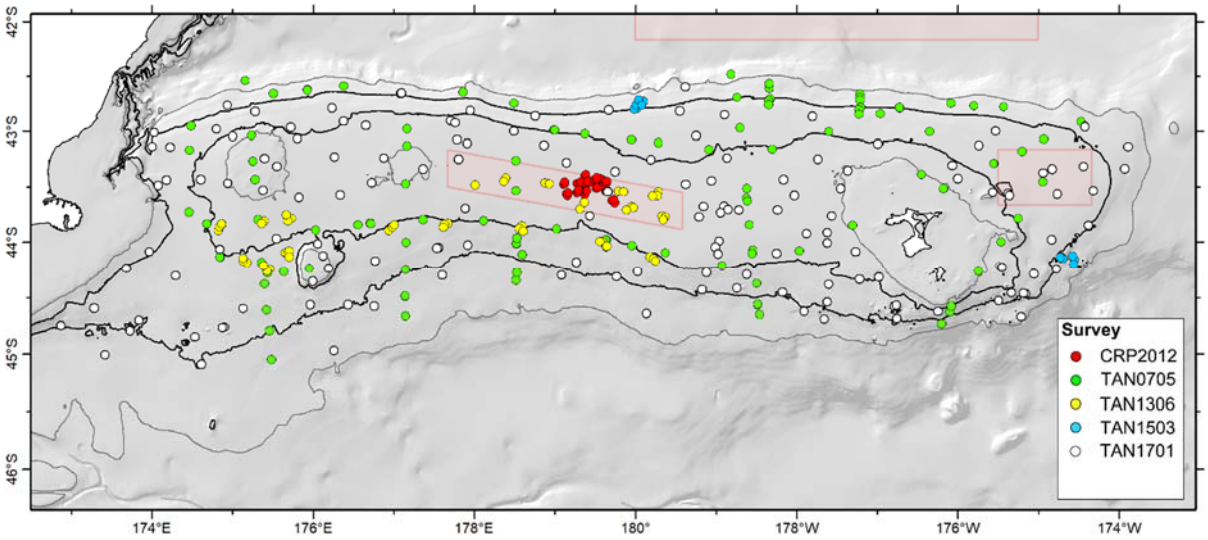

Figure 2: Chatham Rise showing the location of photographic transect stations (colour-coded dots, see legend) for the five voyages examined from which data were used to develop the models. Isobaths show 250, 500, 1000, and 1500 metres, red polygons show Benthic Protection Areas.

Voyages TAN0705 and TAN1701 were broad-scale biodiversity surveys of the Chatham Rise, following stratified random designs. Voyage TAN1306 was designed primarily to survey biodiversity across gradients of fishing intensity, and voyage TAN1503 was focussed on seamounts in the Graveyard and Andes seamount groups on the central northern and eastern flanks of the rise, respectively. Voyage CRP2012 focussed on the phosphorite-rich sediments on the crest of the central portion of the Chatham Rise.

The final data set consisted of 125 658 records of individual benthic organisms from analyses of 358 seabed photographic transects across the five surveys, with 109 161 records from analyses of video, and 15 795 from still images. Data spanned the full extent of Chatham Rise from 172° 50′ E to 173° 53′ W and 42° 29′ S to 45° 5′ S and from 40 m to 1850 m depth. Density estimates for each taxon in the dataset were derived from full counts of individuals throughout each photographic transect (video surveys) or for all analysed image frames (still image surveys), standardised to numbers of individuals 1000 m^{-2} (see Bowden et al. 2019).

2.3 Selection of environmental predictor variables

A set of environmental variables that potentially influence marine organism distributions was generated from regional or global datasets upscaled to a finer resolution based on depth data from a 250 m bathymetry grid for the New Zealand region by Georgian et al. (2019) following the method of Davies & Guinotte (2011). Additional seafloor terrain metrics including measures of depth variability (range, standard deviation, 'ruggedness'), slope (angle, standard deviation), and curvature (convexity or concavity in plan view, profile view, and composite) were derived from this bathymetry grid using Benthic Terrain Modeler in ArcGIS 10.3.1.1 (Table 1). Several other potentially important variables used in earlier modelling studies, including temperature-depth residuals, sediment composition, seamounts, and cumulative trawl intensity were subsequently added to this set.

Temperature residuals were obtained from the residuals of a regression of temperature versus depth, resulting in a variable that provides information about temperature in a form that is uncorrelated with depth and represents deviations from the expected temperature for a given depth. Sample sites were designated as being on a seamount if they were within the footprint of the deepest complete depth contour around any of the seamounts recorded in the NIWA Seamounts database (Rowden et al. 2008). The percent mud and

percent gravel layers for the region were developed from more than 30 000 raw sediment sample datapoints compiled in *dbseabed* (Jenkins 2010), which were then imported into ArcGIS and interpolated using Inverse Distance Weighting. Trawl footprint data were provided by Fisheries New Zealand (FNZ) (Baird & Wood 2018), and trawl intensity calculated for each grid cell as the total cumulative area impacted by bottom trawling between 1 October 1989 and 30 September 2006 (i.e., all records up to the end of the last complete fishing year prior to the first of the camera surveys).

In total, 58 variables were considered, many of which were strongly correlated (particularly the terrain window-size variants) and all were of unknown ecological influence. Because of the wide range of taxa to be included in the models, each of which potentially responds to different characteristics of the physical environment at different scales, we reduced the number of variables by a conservative four-stage selection process. First, variables were grouped by four categories known to influence distributions of seabed fauna: Seafloor Characteristics; Water Chemistry; Water Physics, and Productivity. Second, each variable was examined visually (in GIS) and any with obvious processing artefacts were excluded. Third, correlations were calculated for all pairwise combinations of the remaining variables and graphical representations and cluster dendrograms were used to exclude the most highly correlated variables while also ensuring representation of each of the four high-level categories (i.e., seafloor characteristics, water chemistry, water physics, and productivity). Finally, the ecological influence of the environmental variables within each category was assessed through a set of initial exploratory BRT models for representative taxa (a combination of those most commonly recorded and those recorded to a high taxonomic resolution). This process resulted in a reduced set of 23 environmental variables.

Table 1: The thirty-nine environmental variables considered for community and habitat suitability models. Variables are grouped by four categories: Seafloor Characteristics; Water Chemistry; Water Physics, and Productivity. Seabed topography variables were each initially generated at a range of focal mean sizes (3 × 3 cells, 7 × 7 cells, and 15 × 15 cells), which expanded the total number of variables considered to 58.

Variable	Name	Units	Native Resolution	Reference
Seafloor Characteristics				
Depth[G]	*bathy*	meters	1 km^2	NIWA bathymetry
Percent gravel[G]	*grav*	%	–	NIWA
Percent mud[G]	*mud*	%	–	NIWA
Ruggedness [2G]	*Ruggedness*	–	–	Derived from bathymetry
Slope[G]	*slope*	degrees	–	Derived from bathymetry
Slope standard deviation[2G]	*slopeSD*	–	–	Derived from bathymetry
Aspect[G]	*aspect*	degrees	–	Derived from bathymetry
Depth range[2G]	*range*	m	–	Derived from bathymetry
Depth standard deviation[2G]	*std*	–	–	Derived from bathymetry
Profile curvature[G]	*profcurv*	–	–	Derived from bathymetry
Plan curvature[G]	*plancurv*	–	–	Derived from bathymetry
Curvature[G]	*curv*	–	–	Derived from bathymetry
Bathymetric Position Index – fine[G]	*bpi_fine*	–	–	Derived from bathymetry
Bathymetric Position Index – fine: standard deviation [G]	*bpi_fine_SD*	–	–	Derived from bathymetry
Bathymetric Position Index – broad[G]	*bpi_broad*	–	–	Derived from bathymetry
Bathymetric Position Index – broad: standard deviation[G]	*bpi_broad_SD*	–	–	Derived from bathymetry
Seamounts[G]	*seamounts*	–	–	Rowden et al. (2008); Yesson et al. (2011)
Trawl intensity	*trawl*	m^2	5 km^2	Baird & Wood 2018
Water Chemistry				
Apparent oxygen utilization[G]	*appox*	ml l^{-1}	1°	Garcia et al. (2014a)
Aragonite saturation state[G]	*arag*	-	0.5°	Bostock et al. (2013)

Variable	Name	Units	Native Resolution	Reference
Calcite saturation state[G]	*calcite*	-	0.5°	Bostock et al. (2013)
Dissolved oxygen[G]	*dissox*	ml l^{-1}	1°	Garcia et al. (2014a)
Nitrate[G]	*nitrate*	µmol l^{-1}	1°	Garcia et al. (2014b)
Percent oxygen saturation[G]	*percentox*	%	1°	Garcia et al. (2014a)
Phosphate[G]	*phosphate*	µmol l^{-1}	1°	Garcia et al. (2014b)
Silicate[G]	*silicate*	µmol l^{-1}	1°	Garcia et al. (2014b)
Salinity[G]	*salinity*	-	0.25°	Zweng et al. (2013)
Water Physics				
Sigma theta[G]	*sigma*	kg m^{-3}	0.25°	Derived from temperature and depth
Temperature[G]	*temp*	°C	0.25°	Locarnini et al. (2013)
Temperature residuals	*tempres*	°C	0.25°	Derived from temperature and depth
Dynamic topography	*dynoc*	m	0.25°	http://www.aviso.oceanobs.com
Tidal current speed	*tidalcurr*	ms^{-1}	1 km^2	NIWA
Sea surface temperature gradient	*sstgrad*	^oC km^{-1}	1 km^2	Uddstrom & Oien (1999)
Productivity				
Particulate organic carbon export[G]	*poc*	mg C m^{-2} d^{-1}	0.08°	Lutz et al. (2007)
Vertically Generalized Production Model[14G]	*vgpm*	mg C m^{-2} d^{-1}	0.167°	Oregon State University[3]
Eppley-VGPM[14G]	*epp*	mg C m^{-2} d^{-1}	0.167°	Oregon State University[3]
Carbon-Based Productivity Model-2[14G]	*cbpm*	mg C m^{-2} d^{-1}	0.167°	Oregon State University[3]
Dissolved organic matter	*dom*	*a*DOM (443) m^{-1}	1 km^2	NIWA

1-Surface data derived from MODIS –Aqua (NASA) as the mean, minimum, maximum, and standard deviation from mid-2002–2016.
2-Terrain metrics calculated using window sizes of 3, 5, 7, and 15 cells.
3-Data obtained from http://www.science.oregonstate.edu/ocean.productivity
4-Calculated as the mean, minimum, maximum, and standard deviation, for the period 2002 to 2016
G-Upscaled to 250 m bathymetry (Georgian et al. 2019)

These 23 variables were then offered as explanatory variables to an initial GF model. GF is robust to large sets of correlated explanatory variables but a smaller set of variables was required for RCP and the single-taxon RF and BRT models to avoid overfitting, especially with the relatively modest sample size (357 records). To achieve this reduction, firstly the ranked variable importance from the GF models was used to identify a sub-set of 18 variables on which to base the final GF models and as a starting point for the single-taxon models. Variables excluded in this process were either spatial scale variants (e.g., choice of the standard deviation of depth calculated using a 15 × 15 grid cell window rather than 3 × 3), one of a complementary pair (e.g., choice of percent gravel rather than percent mud), or strongly correlated with other more ecologically interpretable variables (e.g., choice of silicate rather than nitrate).

The 18 predictor variables used in the final GF model were then further reduced to a set of 12 on which to base the BRT and RF single-taxon models, by examining the R^2 weighted importance calculated for each variable in the final GF model and excluding the 6 least important. All 12 variables were offered to initial BRT and RF models for each taxon, and their ranked importance calculated. Only the 6 most important variables in each of these initial models were used in the final models for each taxon. Reducing the number of redundant or non-independent variables in the models increases the robustness of models and minimises the effects of multicollinearity that reduce their predictive power (Yoo et al. 2014). Although this procedure means that there is a different set of explanatory variables in each model, and variable influence cannot be consistently compared among all taxa for all variables, it ensures that the variables most relevant to each taxon were used in each model.

2.4 Selection of taxa

Bowden et al. (2019) condensed the 354 invertebrate taxa identified from the five photographic transect surveys into a set of 79 'aggregated' taxa. This set ranges in taxonomic resolution from species-level for distinctive taxa readily identified from imagery (e.g., *Metanephrops challengeri* and *Dermechinus horridus*), to family (e.g., Primnoidae and Stylasteridae), order (e.g., Ceriantharia and Brisingida), class (e.g., Asteroidea and Holothuroidea), or phylum (e.g., Brachiopoda). Some finer taxonomic detail is masked in this aggregation approach but it ensures that consistency of identifications is maintained across the entire data set and that distinctions likely to be relevant to management of benthic impacts, such as differentiation of brisingid seastars in the class Asteroidea and *Dermechinus horridus* in the class Echinoidea, are retained. For model development here, we excluded taxa that were present at fewer than 5 sites, resulting in a final set of 69 taxa available to model.

For single-taxon models, we prioritised the selection of taxa according to their relevance as indicators of a community/habitat/ecosystem that is sensitive or vulnerable to human-induced environmental impacts (e.g., fishing, seabed mining, climate change) as defined for New Zealand (MacDiarmid et al. 2013), the southwest Pacific (Parker et al. 2009), and the Antarctic (Agnew et al. 2009, Parker & Bowden 2010). The 20 taxa selected (Table 2, bold type) were present at between 57 and 302 of the 357 sample sites and ranged in taxonomic resolution from individual species (e.g., the branching coral *Goniocorella dumosa* and scampi, *Metanephrops challengeri*) to the Phylum level (e.g., Bryozoa). Notably, there were insufficient records to model three of the four reef-forming scleractinian corals found on the Chatham Rise, therefore observations of *Enallopsammia rostrata*, *Madrepora oculata*, and *Solenosmilia variabilis* were combined with those of *Goniocorella dumosa* to produce an overall model for "Coral Reef". Sea pens (Pennatulacea) were modelled as a group, combining all species except for *Kophobolemnon* sp., which is much smaller than most other species recorded in the group, can be readily distinguished from other genera and occurred in locally extremely high densities, which distorted the overall distribution for the group. Similarly, models for Asteroidea included all starfish taxa except for brisingids (Order Brisingida) as these are known to have different habits (obligate suspension-feeders) and are readily distinguished from other genera. Models for echinoids were separated into the Subclass Euechinoidea (all non-cidaroid regular echinoids) and the Order Spatangoida (burrowing heart urchins), as these are also readily distinguished. No further restrictions were imposed on the remaining combined groupings, and all taxa listed in Table 2 (except for Coral reef, as noted above) were considered for the community models.

Table 2: Taxa used in the models, membership status with respect to recognised lists of sensitive habitats (MacDiarmid et al. (2013), Vulnerable Marine Ecosystem (VME) indicator taxa (Agnew et al. 2009, Parker et al. 2009, Parker & Bowden 2010), and the number of Chatham Rise sites at which they were observed (non-zero records). Bold type indicates those taxa for which single-taxon habitat suitability models were built; all listed taxa (except for Coral reef, a combination of the four branching coral species listed separately) were considered for the community models. Code = abbreviations used in this study (based on the Fisheries New Zealand 3-letter taxon codes, where applicable).

Taxon	Common name	Code	Sensitive Habitat	VME indicator	Non-zero records
Goniocorella dumosa	Branching stony coral	GDU	Yes	yes	66
Coral Reef		REEF	Yes	yes	106
Pennatulacea	Sea pens	PTU	Yes	yes	163
Demospongiae	Common sponges	DEM	Yes	yes	238
Hexactinellida	Glass sponges	HEX	Yes	yes	104
Xenophyophoroidea	Giant forams	ZFR	Yes		62
Brachiopoda	Lamp shells	BPD	Yes	yes	69
Bryozoa	Lace corals	COZ	Yes	yes	207
Hydrozoa	Hydroids	HDR	Yes	yes	219
Stylasteridae	Hydrocorals	COR		yes	95
Metanephrops challengeri	Scampi	SCI			102
***Hyalinoecia* sp.**	Quill worms	HTU			134
Euechinoidea	Non-cidaroid echinoids	EUE			166
Spatangoida	Heart urchins	SPT			166

Taxon	Common name	Code	Sensitive Habitat	VME indicator	Non-zero records
Buccinidae	Whelks	BUCC			201
Volutidae	Volutes	VOL			151
Paguridae	Hermit crabs	PAG			302
Cidaroidea	Pencil urchins	CID		yes	197
Holothuroidea	Sea cucumbers	HTH			215
Asteroidea	Sea stars	ASR			335
Alcyonacea	Soft corals				73
Anemones					316
Anthomastus sp					108
Antipatharia	Black corals				42
Ascidiacea	Sea squirts				129
Barnacles					9
Bivalvia	Bivalves				29
Brachyura	True crabs				153
Brisingida	Brisingid sea stars			yes	100
Caridea	Caridean shrimps				255
Caryophylliidae	Cup corals				94
Ceriantharia sp	Tube anemone				188
Cladorhizidae	Carnivorous sponges				30
Corallimorpharia					36
Crinoidea (motile)	Feather stars			yes	73
Crinoidea (stalked)	Sea lilies			yes	10
Crustacean (lobster)	*Projasus parkeri*				11
Dermechinus horridus	Orange sea urchins				23
Echinothurioida	Leather urchins				146
Echiura	Spoon worms				13
Enallopsammia rostrata	Branching coral		yes	yes	7
Enypniastes eximia	Swimming holothurian				18
Epizoanthidae					30
Flabellum sp.					195
Galatheidae/Chirostylidae	Squat lobsters				231
Gastropoda	Sea snails				280
Gorgonacea	Gorgonian corals				100
Gorgonocephalidae	Basket stars				13
Hyalascus sp.	Quill worms		yes	yes	33
Isididae	Bamboo corals				41
Kophobelemnon sp			yes	yes	22
Lithodidae	Stone crabs				10
Madrepora oculata	Branching coral		yes	yes	8
Nudibranchia	Nudibranchs				29
Octopoda	Octopuses				67
Ophiuroidea	Brittle stars				166
Paragorgiidae	Bubblegum corals				7
Polychaeta					107
Primnoidae	Sea fans				57
Psolidae					27
Pycnogonida	Sea spiders				32
Radicipes sp					74
Scaphopoda	Tusk shells				27
Serolidae	*Brucerolis* sp.				84
Solenosmillia variabilis	Branching coral		yes	yes	9
Stephanocyathus sp	Cup coral				24
Taiaroa tauhou					101
Telesto sp					42
Worm (indet.)					67
Zoanthidea					43

2.5 Single-taxon models

Spatial autocorrelation

Before modelling, we calculated Moran's I index (via *spdep* in R) to assess spatial autocorrelation in the input presence-absence and abundance data. This index measures the correlation between observations as a function of the distance separating them; values can range from -1 (highly dispersed) to 1 (highly clustered), with a value of 0 indicating perfect spatial randomness. Where significant spatial autocorrelation exists, this can be accounted for by constructing an additional variable from the residuals of an initial model (Crase et al. 2012). The distance-based nearest neighbour analysis function *dnearneigh* was used to identify neighbouring data points for each record, setting the upper distance bound to a high level to avoid any no-neighbour entities. Moran's I test was then applied, using species presence values and residuals of the initial models, with weights calculated for the identified neighbours at each location.

Random Forest models

RF modelling is a non-parametric approach which builds classification or regression trees using random subsets of the input data (Breiman 2001). The RF models were built using *randomForest* in R. All models were tuned using the *train* function in the R package *caret* to select optimal values for complexity parameters *mtry* (the number of variables used in each tree node), *maxnodes* (the maximum number of terminal nodes in each trees), and *ntree* (the number of trees to grow). The RF approach to habitat suitability modelling has also been successfully applied in the past to benthic invertebrate data in the New Zealand region (Georgian et al. 2019, Rowden et al. 2017).

Boosted Regression Tree models

BRT modelling is an advanced form of additive regression based on decision trees, where the individual terms of the regression are simple trees, fitted in a stage-wise manner. Simple (short) trees are formed by relating a response to recursive binary splits of the data, then combined (boosted) to improve predictive power by focussing each successive tree on model residuals. Tree-based methods such as BRT and RF have the advantage over traditional methods that they can easily handle missing data, outliers, categorical as well as continuous variables, and automatically handle interactions between predictors (Elith et al. 2008). The BRT method has been widely used in ecological applications and has performed well in previous studies of deep-water invertebrate and fish distributions in New Zealand (e.g., Compton et al. 2013, Georgian et al. 2019, Leathwick et al. 2006, Rowden et al. 2017, Tracey et al. 2011).

The BRT models were run with the tree-complexity (number of splits) set to 5, thus allowing for a high level of variable interaction, and the learning rate (which determines the weight given to each successive tree in the model) adjusted so that the number of trees in the final models exceeded 1000, following guidelines in Elith et al. (2008). Stochasticity is incorporated into BRT models by selecting at random only a portion (the bag-fraction) of the data to use at each step in the model. We used the default value of 0.5 in all models. BRT models were built in the R statistical computing environment (R Core Team, 2018) using libraries (*gbm*) and functions described in Elith et al. (2008), Leathwick et al. (2006), and Elith & Leathwick (2011).

Hurdle models and uncertainty

The two components of the hurdle models were 1) a presence/absence model based on a binary logistic regression, which predicts probability of presence and 2) a regression model based only on the positive (i.e. non-zero) observations of species abundance, which predicts abundance at locations of species presence. For the regression model component, abundances were $\log_{10}$ transformed to provide a near-normal distribution of the response. Final estimates of abundance were made by multiplying the probabilities from the first component by the abundances from the second component.

To assess the relative confidence in predictions across the model extent, we used a bootstrap technique to produce spatially explicit uncertainty measures, after Anderson et al. (2016) and Georgian et al. (2019).

Random samples of the input data were drawn with replacement and sets of presence-absence, abundance, and hurdle models constructed using the same settings as the original. Predictions of abundance were then made for each cell of the model extent. This process was repeated 500 times for each model type (BRT and RF) resulting in 500 estimates of abundance for each taxon in each cell. Model uncertainties were then calculated as the coefficient of variation (CV) of the bootstrap output.

Model performance

Performance of the separate components of the hurdle models was assessed for each taxon by a process of cross-validation. The model input data was partitioned randomly to create 70% training 30% test data sets. Training data were used to construct a preliminary model to apply to test data to measure performance. For the presence/absence models, performance was evaluated using AUC (area under the Receiver Operating Characteristic Curve), defined in these models as the area under a plot of the fraction of true positives versus the fraction of true negatives. In general, AUC values over 0.5 indicate better than random performance, values over 0.7 indicate adequate performance, and values over 0.8 indicate excellent performance (Hosmer et al. 2013). Abundance model performance was evaluated as the correlation (R^2) between predicted and observed values for the test data. This process was repeated 10 times for each model type, and average AUC and R^2 values calculated to represent overall performance.

Overall performance of the hurdle models was also measured by cross-validation. Here the model input data was split into ten groups to create ten grids of predicted abundance from hurdle models trained on all but one group, in turn. The correlation between the observed and predicted abundance at the locations of each test group was then calculated and the mean of these ten values used to represent overall hurdle model performance.

Ensemble models

We produced an ensemble model for each taxon, incorporating the predictions and underlying assumptions and modelling strategies of both the BRT and RF hurdle models. This approach limits dependence on a single model type or structural assumption and enables a more robust characterization of the predicted spatial variation and uncertainties (Robert et al. 2016). Ensemble models were constructed by taking weighted averages of the predictions of the two hurdle models, using methods adapted from Oppel et al. (2012), Anderson et al. (2016), Rowden et al. (2017), and Georgian et al. (2019). This adapted procedure derives a two-part weighting for the BRT and RF components of the ensemble model, taking equal contributions from the overall model performance and the uncertainty measure (CV) in each cell, as follows,

$$W_{BRT1} = \frac{MPS_{BRT}}{MPS_{BRT}+MPS_{RF}} \text{ and } W_{RF1} = \frac{MPS_{RF}}{MPS_{BRT}+MPS_{RF}}$$

$$W_{BRT2} = 1 - \frac{CV_{BRT}}{CV_{BRT}+CV_{RF}} \text{ and } W_{RF2} = 1 - \frac{CV_{RF}}{CV_{BRT}+CV_{RF}}$$

$$W_{BRT} = \frac{W_{BRT1}+W_{BRT2}}{2} \text{ and } W_{RF} = \frac{W_{RF1}+W_{RF2}}{2}$$

$$X_{ENS} = X_{BRT} * W_{BRT} + X_{RF} * W_{RF}$$

$$CV_{ENS} = \sqrt{\frac{(CV_{BRT} * X_{BRT})^2 * W_{BRT}^2 + (CV_{RF} * X_{RF})^2 * W_{RF}^2}{X_{ENS}^2}}$$

where MPS_{BRT} and MPS_{RF} are the hurdle model performance statistics; X_{BRT} and X_{RF} are the model predictions; and CV_{BRT} and CV_{RF} are the bootstrap CVs; and X_{ENS} and CV_{ENS} are the weighted ensemble predictions and weighted CVs, respectively, from which maps of predicted species distribution and model uncertainty were produced.

Single-taxon model evaluation

For model validation, a set of independent taxon abundance data was compiled from the Fisheries New Zealand research trawl database *trawl*. The trawl database includes about 20 000 records of trawl catches from the Chatham Rise, although the number of specimens caught is not always recorded. These data are used with several caveats that impact on the recorded counts for each record: 1) the samples were collected using a variety of gear configurations, therefore catchability will vary to an unknown degree among records; 2) a count for colonial species such as bryozoans and *Goniocorella dumosa* is difficult to assign to a sample and may not match well to the counts from the image data; 3) some taxa are too rarely caught (e.g., buccinid whelks), or so fragile that they are nearly always destroyed on capture (e.g., xenophyophores) for sufficient material to be available for any comparison with the image data; and 3) whereas the models were built using biological records from no earlier than 2007, the research trawl data was compiled from all available records, going back to the 1960s, and therefore may be influenced by variable taxonomic resolution of recording and changes in faunal distributions resulting from population shifts or continued trawling disturbance (Bowden et al. 2015). For validation, predicted abundances from the ensemble models at sampled locations of each taxon in *trawl* were compared against the number of specimens recorded in *trawl*, using Spearman's rank-order correlation.

2.6 Community models

Regions of Common Profile

RCP is a multi-species, model-based approach to the delineation and mapping of species assemblages. A multivariate adaptation of a mixture-of-experts model is used to group sites based on their species profile (presence/absence or abundance) in relation to environmental conditions, thereby simultaneously grouping species and modelling the environmental variables which determine those groupings. These groupings can then be predicted at unsampled sites, based on the environmental conditions. The output of the model process does not produce a hard classification for the regions identified, instead providing the probability of each RCP occurring at a prediction location. The location can then be assigned to an RCP based on the RCP with the highest probability at that site. This approach has previously been used to classify assemblages of land-based vegetation types and marine fish (Foster et al. 2017, Hill et al. 2017) but application to marine benthic invertebrate communities is apparently yet to be attempted. This is partly because the RCP method is still in development and with existing code libraries some operations, such as extracting data about the characteristic fauna associated with each RCP, are not straightforward (Scott Foster, CSIRO, Hobart, pers. comm.).

The RCP model was based on abundance (numbers 1000 m^{-2}) of the 69-taxon data set and incorporated a negative binomial distribution to help compensate for overdispersion in the data, with a log-link function. Unlike GF, the RCP procedure is sensitive to overfitting. To avoid this issue the number of environmental predictors was limited to 9 by excluding the most correlated of those used for the single-taxon models. In addition, to counter the effect of correlation and assist with model convergence, each predictor was converted to an orthogonal polynomial.

The number of RCP groups must be specified when running the model. To determine the optimal number of groups, trial model runs were performed with numbers of groups ranging from 2 to 10. The model run with the lowest value of the Bayesian Information Criterion (BIC), after any "mis-fit" models based on a small number of sites were removed, was used as the basis for specifying the number of RCP groups. To avoid models based on local likelihood maxima, 500 model optimisations were performed, with random starting values. Predictions were made into unsampled space by applying the (transformed) grids of environmental variables to the RCP model, and a matrix of RCP-membership probabilities at the location of each grid cell was produced by running 500 Bayesian bootstraps. Each RCP can be examined separately, by plotting the gridded probabilities, but to produce a regional classification we assigned each grid cell to the RCP with the highest probability. By using this approach, a grid of model uncertainties was easily formed, empirically, from the estimated probabilities of the assigned RCP in each cell.

We considered the available data for validation of the RCP analysis, using methods described by Hill et al. (2017). To follow their approach would require an independent set of seafloor image data, collected and

analysed in a similar manner to that used for training the model. Unfortunately, such a dataset does not exist for the Chatham Rise. We considered using the data available from the trawl database, as used in the validation of the single-taxon models. However, these data are unsuitable because firstly, there are too few records of invertebrates with reliable density information (i.e., number caught), and secondly, the trawl catchability is likely to be highly variable across the 69 taxa used in the community models and would bias any comparison with the camera data.

Gradient Forests

GF is a method for modelling beta diversity (taxon turnover) based on relationships between sampled multi-species density data and environmental gradients (Ellis et al. 2012, Pitcher et al. 2011). GF builds an aggregation of RF models, each describing the environmental relationships of an individual taxon. The information from these individual models is then used to develop a set of transformations of the environmental layers, such that the correspondence between each layer and the faunal occurrence data is maximised (Compton et al. 2013, Pitcher et al. 2012, Stephenson et al. 2018). These transformed environmental layers can then be used to generate gridded maps of predicted taxon turnover across unsampled areas. Furthermore, the resulting maps can be used with statistical clustering techniques to define spatial classifications of the study area at a range of class levels defining areas likely to have similar community composition. In the context of planning for spatial management or conservation in general, and this study in particular, it is of note that GF differs from the other community modelling method used here, RCP, in that the optimal number of classes generated is not determined by a statistical goodness of fit test. Rather, the hierarchical classifications developed can be generated at any level of detail appropriate to the question being addressed. The drawback to this flexibility is that statistical uncertainty is not propagated through to the classification stage, so there is no formal test for the reliability of the resulting classifications.

GF is robust to the inclusion of correlated predictor variables (Ellis et al. 2012) and initial model runs to assess the effect of using different sets of environmental variables suggested that inclusion of correlated variables had little effect on model outcomes. However, because many correlated variables had no measurable effect on the results, a set of 18 variables (Table 3) was selected for inclusion in the final model runs, based on their ranked influence in the trial models and representation of the four categories of variables defined earlier (see Table 1). Trawl intensity was included because bottom trawling has been active over much of Chatham Rise for more than 30 years and thus is likely to have affected the observed distributions of some taxa. However, this layer differs from the others in that it represents an anthropogenic disturbance that is spatially correlated with seabed type, productivity, and potentially other parameters and can be highly variable among years and across a wide range of spatial scales (Baird & Wood 2018). The aim in this project is to generate the most accurate maps of benthic community distributions achievable. Because the trawl intensity layer made an apparently significant contribution to the GF model and because the methods used are correlative (i.e., with no assumption of causality), we decided to retain this variable in analyses but run two models in parallel: the first using the 18 base environmental layers including trawl intensity, and the second excluding trawl intensity.

GF models were run using function *gradientForest* in R, with subsequent classification steps following Stephenson et al. (2018). Input data consisted of the subset of the full taxon data set developed by Bowden et al. (2019), consisting of density measurements for 69 taxa at 358 sample sites across Chatham Rise (see Section 2.4), and the set of either 17 (excluding trawl history) or 18 (including trawl history) environmental predictor layers. A $\log_{10}(1+x)$ transformation was applied to the taxon density data to down-weight the influence of highly abundant taxa, enable a broader range of taxa to influence outcomes, and reduce the potential for artefacts arising from differences in density estimates derived from still image and video survey data. Models were run with 500 trees per taxon, the *compact* function set to *false*, and the correlation threshold for applying conditional permutation to allow for co-linear predictor variables set to 0.5. Model outputs include R^2 values for all taxa having correlations with environmental variables of greater than zero, ranking of predictor variables in terms of their contributions to both mean accuracy of the model and mean importance weighted by the taxon R^2 values, and plots showing: the density of RF kernel splits in relation to each of the environmental gradients; cumulative change in the abundances of individual taxa along each of the environmental gradients, and where changes in community composition occur along each of the environmental gradients. To visualise GF outputs in terms of taxon-turnover, principal components analysis (PCA) was used to summarise variations in the transformed environmental variables across the study area

at grid-cell resolution (1 × 1 km). Values from the first three dimensions of the PCA were used to define red, green, and blue colour values as input to a map representing generalised relationships between taxon turnover and environmental space.

Hard-boundary classifications were developed from the GF environmental transforms using methods developed for the MEC and BOMEC (Leathwick et al. 2012, Snelder et al. 2007), and most recently applied to a GF analysis of demersal fish species in the New Zealand EEZ (Stephenson et al. 2018). The full grid of transformed environmental predictor values (378 540 grid cells) was classified in two stages. First, non-hierarchical k-medoids clustering (using *clara* in R) was used to assign cells to 300 classes. Second, hierarchical agglomerative flexible UPGMA clustering with the Manhattan distance metric (using *agnes* in R) was used to summarise the 300 *clara* classes at 7, 15, 25, and 50-class levels, from which maps were developed in a geographic information system (QGIS). The 50-class level was chosen to approximate to the number of strata (n=36) used in the 2016 Chatham Rise research trawl survey (our mapped study domain extends beyond the limits of the trawl survey and the 50-class classification yields approximately 35 classes within the trawl survey strata domain), and the number of classes of the MEC and BOMEC classifications at 70-class level (see Snelder et al. 2007 for justification) that are represented in our study domain. The 7-class level was chosen for comparison with outputs from the RCP analysis (see below), and the two intermediate levels to assess how incremental increases in class-level affect class boundaries.

Community model evaluation

While there is apparently no robust way to evaluate the performance of the GF models at different class levels without an independent data set (Pitcher et al. 2012, Snelder et al. 2007, Stephenson et al. 2018), we used two approaches to compare classifications.

First, for the GF model only, we assessed the ability of transformed environmental variables to describe community composition at each classification level by comparing biological similarities among classes against environmental distances among classes in non-parametric RELATE matrix correlation tests (Clarke & Warwick 2001, Somerfield et al. 2002). Sample sites were overlaid on each GF classification and tagged with the corresponding class labels, enabling average density per taxon per class to be calculated for all classes in which there were at least three sample points. These data were $\log_{10}(1+x)$ transformed and used to calculate matrices of Bray-Curtis similarities among classes for each class-level. Environmental distance matrices were calculated using the Manhattan distance metric based on mean values of the GF-transformed variables for each class in the relevant classification. RELATE tests used weighted Spearman's rank correlation, with probability (p) computed by 999 permutations of the community data matrix.

Second, we assessed the degree to which different class levels and different classification methods separated the faunal data into distinct groupings, using ANOSIM (analysis of similarities, Clarke & Warwick 2001). One-way ANOSIM tests using Bray-Curtis dissimilarity and weighted Spearman rank correlations were run for each classification, with 'class' as the factor and taking the Global-R statistic as a measure of relative ability to group the faunal data. The R statistic ranges from 1, where all within-group similarities are greater than among-group similarities, to 0, where there is no difference between within-group and among-group similarities. Thus, a higher Global-R score indicates more effective separation of the faunal data by the classification boundaries. Because this test does not depend on the transformed environmental variables (which are different for each classification method), we were able to apply it not only to the two classifications developed here (RCP and GF) but also the MEC, the BOMEC, and the survey strata developed for the trawl survey strata.

3. Results

3.1 Environmental predictor variables

The 18 predictor variables used in the final GF model, as selected through analysis of correlation patterns, categorised-variable BRT models for key species, and initial GF model runs (Section 2.3), are shown in Table 3 along with the subset of 12 on which the BRT and RF single-taxon models were based. The 6 variables excluded (those with the lowest R^2 weighted importance in the final GF model (see Figure 30)) were *bpi_broad*, *grav*, *std15*, *silicate*, *dom*, and *poc*.

Table 3: **Reduced set of 18 environmental variables derived from elimination of correlated variables and assessment of relative influence in initial BRT and GF runs, showing which were used in each model type (see Table 1 for more detailed descriptions of the variables**).

Variable	Single-taxon models	Community models
Seafloor Characteristics		
bathy	y	y
profcurv	y	y
trawl	y	y
bpi_broad	n	y
grav	n	y
std15	n	y
Water Chemistry		
salinity	y	y
dissox	y	y
silicate	n	y
Water Physics		
tempres	y	y
dynoc	y	y
sstgrad	y	y
tidalcurr	y	y
Productivity		
epp_mean	y	y
epp_min	y	y
cbpm_mean	y	y
dom	n	y
poc	n	y

3.2 Single-taxon models

Tests for assessing spatial autocorrelation (Moran's I test) in the abundance data and on the residuals for each taxon typically produced near-zero values, indicating minimal or no clustering at the scale used for identification of nearest neighbours (0–150 km). Although a level of spatial autocorrelation is expected to be present in virtually all ecological data (Lennon 2000) the statistical modelling techniques we used can effectively account for some degree of spatial autocorrelation (Crase et al. 2012). In addition, sources of spatial autocorrelation are also likely to be partially explained by the explanatory variables, as they are not limited to endogenous factors such as dispersal limitations and breeding aggregations. The Moran's I tests showed that any remaining spatial autocorrelation in the model residuals was negligible, therefore they were deemed independent and identically distributed. This finding fulfils one of the key assumptions in statistical modelling (Dormann et al. 2007), the violation of which reduces the predictive power of the models and increases the chances of type I error in hypothesis testing (Lennon 2000, Doorman et al. 2007). For these reasons, we did not specifically include spatial autocorrelation in the modelling framework (e.g., by creating an additional variable to account for the spatial structure in the model residuals following Crase et al. 2012).

Variable selection and influence

The variables most frequently selected for the final 6-variable presence-absence models, for both BRT and RF, were *bathy* and *tidalcurr* (Appendix 1 - Table A-1, Table A-2). These variables were both selected in 15 of the 20 RF models as well as in 14 (*bathy*) and 12 (*tidalcurr*) of the BRT models. In 19 of the 40 models, combined, *bathy* was ranked either the first or second most important variable. Other variables frequently selected were *dynoc*, *dissox*, and *tempres* in the RF models, and *dissox*, *cbpm_mean*, and *epp_mean* in the BRT models.

The influence of *bathy* in the 6-variable models for abundance was less pronounced, present in 11 of the RF models and 10 of the BRT models. *dynoc* (15/20) was the most important variable overall in the RF models but less so in the BRT models (9/15). However, the most influential variable overall in the abundance models was *profcurv*, which was ranked as the first or second most important variable in 5 of the RF models and 6 of the BRT models. Other variables frequently selected included *tempres* in both models and *trawl* in the BRT models (see Table A-1, Table A-2).

The taxa examined each have their preferred depth range, which are expected to be wider for taxa comprising more species. Predictor influence plots (not shown) for the abundance and presence-absence models tend to reflect these ranges, showing distinct peaks at the most favoured depth for individual species such as *Goniocorella dumosa* and *Hyalinoecia* sp., and less defined depth ranges for e.g., Asteroidea and Demospongiae. Predicted abundance and presence tended to increase with increasing tidal current (*tidalcurr*) and higher values of dynamic topography (*dynoc*) for most species, although for some the pattern was less clear, reflecting the higher food supply associated with stronger tidal flows and ocean currents. Profile curvature (*profcurv*) of the seabed affects acceleration and deceleration of water flow and therefore food supply; profile curvature values were low at most sites but small increases tended to be associated with higher predicted abundance and presence. Values of dissolved oxygen (*dissox*) lower than 6.0 mg/l are considered sub-optimal (Garcia et al. 2014a); high abundance and presence values were also often associated with higher levels of dissolved oxygen, increasing strongly as levels approached 6.0 mg/l, a level not exceeded over much of the Chatham Rise. For most models in which trawl intensity (*trawl*) was selected as a predictor there were indications of increasing (e.g., Buccinidae, Paguridae, Volutidae, *Hyalinoecia* sp.) or decreasing (*Goniocorella dumosa*) abundance with increasing cumulative area trawled.

Model performance

Cross-validated performance metrics were similar for the Random Forest and Boosted Regression Tree presence/absence models, and generally indicated "adequate" to "excellent" fits to test data. Mean AUC values from the cross validation ranged from a low of 0.64–0.65 for Bryozoa to a high of 0.90–0.91 for Brachiopoda (Table 4). Performance metrics for the abundance models were also similar between the two methods, although correlation measures were higher for Random Forests than for Boosted Regression Trees for all but two taxa (Pennatulacea and Bryozoa). Mean correlations were variable among taxa, ranging from 0.31 (Holothuroidea) to 0.72 (Stylasteridae) for RF models to 0.29 (Volutidae) to 0.63 (*Hyalinoecia* sp.) for BRT models; and were 0.5 or greater for all but four taxa for the RF models, and all but 6 of the BRT models.

For the hurdle models, cross-validated correlation values (calculated in a slightly different way to those of the abundance models, see Section 2.5) were less similar between model types than those of the abundance models and overall a little less variable, particularly for the RF models. Performance statistics for the BRT hurdle models were lower overall than for the RF models, although for several taxa the values were quite similar and for *Goniocorella dumosa* and *Hyalinoecia* sp. the BRT model correlated slightly better with the test data than did the RF model. Overall, these values indicate a generally good level of agreement between the observed and predicted abundance at the independent test locations and allow a high level of confidence in the models.

The higher values of the performance statistics of the RF compared with the BRT models have the effect that (apart from *Goniocorella dumosa* and *Hyalinoecia* sp.) the RF models are more influential in the ensemble models, due to the higher weighting. The greatest differences in performance statistics are for Asteroidea and Holothuroidea where the RF models have about twice the weight of the BRT models in the final ensemble models; for other taxa, e.g., *Goniocorella dumosa* and scampi (*Metanephrops challengeri*), the contribution from each model type is close to equal.

Table 4: Model performance metrics for the presence/absence and abundance components of the BRT and RF habitat suitability hurdle models created for each taxon.

Taxon	Presence/absence (AUC)		Abundance (Correlation)		Hurdle (Correlation)	
	RF	BRT	RF	BRT	RF	BRT
Goniocorella dumosa	0.86	0.89	0.61	0.60	0.53	0.60
Coral Reef	0.84	0.83	0.52	0.50	0.65	0.53
Pennatulacea	0.76	0.78	0.53	0.56	0.59	0.40
Demospongiae	0.78	0.77	0.62	0.56	0.65	0.55
Hexactinellida	0.75	0.71	0.58	0.50	0.49	0.42
Xenophyophoroidea	0.83	0.84	0.50	0.35	0.54	0.34
Brachiopoda	0.90	0.91	0.63	0.61	0.59	0.47
Bryozoa	0.64	0.65	0.51	0.57	0.47	0.40
Hydrozoa	0.76	0.78	0.58	0.54	0.63	0.51
Stylasteridae	0.88	0.88	0.72	0.52	0.60	0.43
Metanephrops challengeri	0.85	0.88	0.50	0.46	0.66	0.59
Hyalinoecia sp.	0.78	0.77	0.65	0.63	0.60	0.67
Euechinoidea	0.76	0.78	0.65	0.60	0.68	0.52
Spatangoida	0.87	0.85	0.63	0.55	0.73	0.57
Buccinidae	0.71	0.73	0.65	0.55	0.62	0.53
Volutidae	0.79	0.80	0.39	0.29	0.63	0.38
Paguridae	0.76	0.76	0.61	0.59	0.75	0.57
Cidaroidea	0.79	0.78	0.34	0.30	0.61	0.40
Holothuroidea	0.81	0.81	0.31	0.30	0.66	0.33
Asteroidea	0.81	0.87	0.44	0.41	0.77	0.46

Model predictions

Predictions of abundance from the ensemble models were limited to the region from which the sample data was collected, i.e. the Chatham Rise and a small part of the adjacent coastlines of the North and South Islands. Predicted abundance from the models is presented in the same units as the input data, i.e., individuals 1000 m^{-2}.

Predictions from both the abundance and presence-absence components of the RF and BRT models were generally similar across the Chatham Rise region for most of the taxa modelled. A typical example is shown for the predatory gastropod mollusc family Volutidae in Figure 3. Both model types show regions of high abundance around the Chatham Islands, the shallow banks towards the west of the Rise, and some parts of the extreme west and southwest. Some differences can be seen however along the northern edge of the Rise where BRT tends to predict higher abundance. The presence-absence models are also in close agreement, with high probability of presence predicted for a large portion of the western end of the Rise and a strip along the southern flanks of the Rise. The areas with the lowest probability of presence, notably in deeper water in the south, central shallower regions, and the far east, are similar for both models. Not surprisingly then, the general patterns shown when the abundance and presence-absence models are combined into hurdle models are also similar between model types.

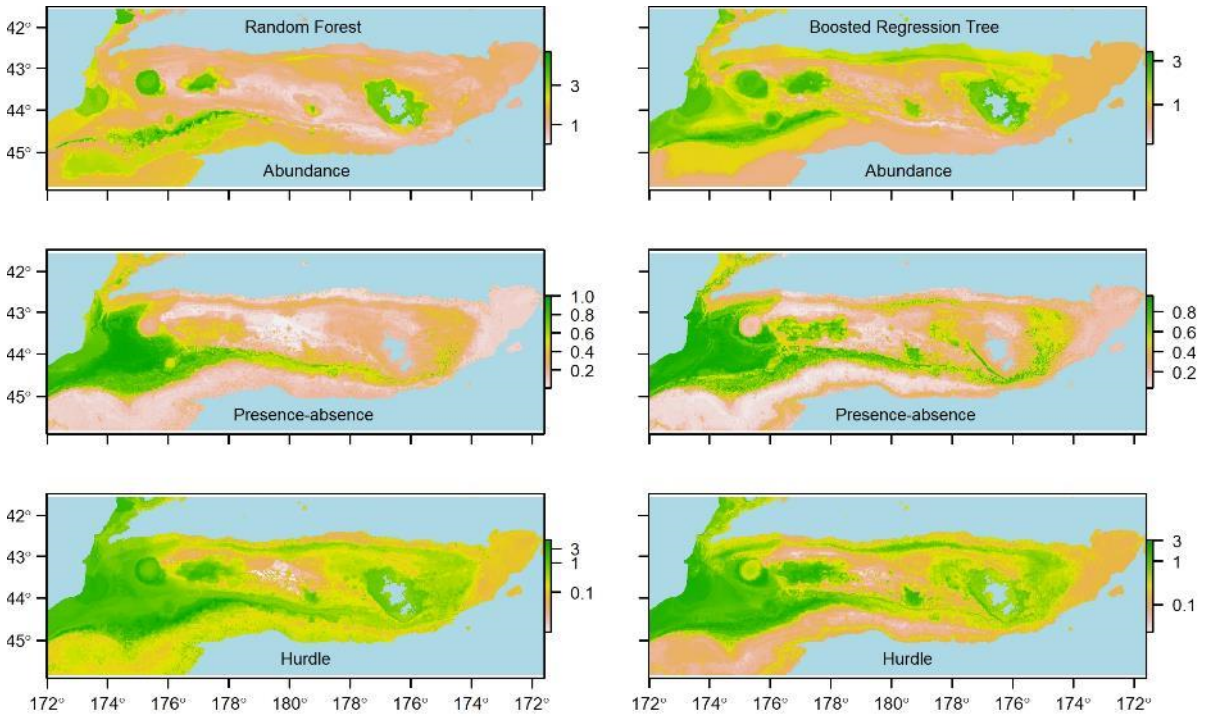

Figure 3: Volutidae. Predictions of abundance (individuals 1000 m^{-2}) from the separate components of the hurdle models using Random Forests (left) and Boosted Regression Trees (right). Top, abundance models; middle, presence-absence models; bottom, combined hurdle models. Note, the abundance models and hurdle models are plotted on a log scale to allow better discrimination of the variation in the predicted response.

Maps showing predicted and observed abundance from the ensemble models for each of the 20 taxa, along with estimated model precision, are shown in Figure 4 to Figure 23. Expanding circles are shown on the maps with areas proportional to observed abundance at the transect sample sites, with the scale set so that the maximum circle area in each plot is the same.

The 20 taxa show a high degree of variation in distributional patterns, with some showing a clear association with depth (e.g., Xenophyophoroidea in relatively deep water in all parts of the Rise (Figure 7), and Brachiopoda mostly in shallow water along the crest of the Rise (Figure 8)), and others showing a preference for certain regions of the Rise (e.g., *Hyalinoecia* sp. (Figure 12) and Buccinidae (Figure 14) in the southeast, Euechinoidea (Figure 13) along the south Rise, and Coral Reef mostly on the central crest of the Rise (Figure 19)). Visually, the agreement between predicted and observed abundance is excellent for most if not all taxa, although the relationship is less clear for some of the modelled taxa that are widespread or comprised of many species, such as Demospongiae and Cidaroida.

Transects from the Graveyard and Andes seamounts (TAN1503) often had high abundance values and dominated the abundance data for some taxa (e.g., Hexactinellidae (Figure 6) and Demospongiae (Figure 5) sponges, bryozoans (Figure 9), and stylasterid corals (Figure 11)) with conditions in these locations likely to have strongly influenced predictions in unsampled space.

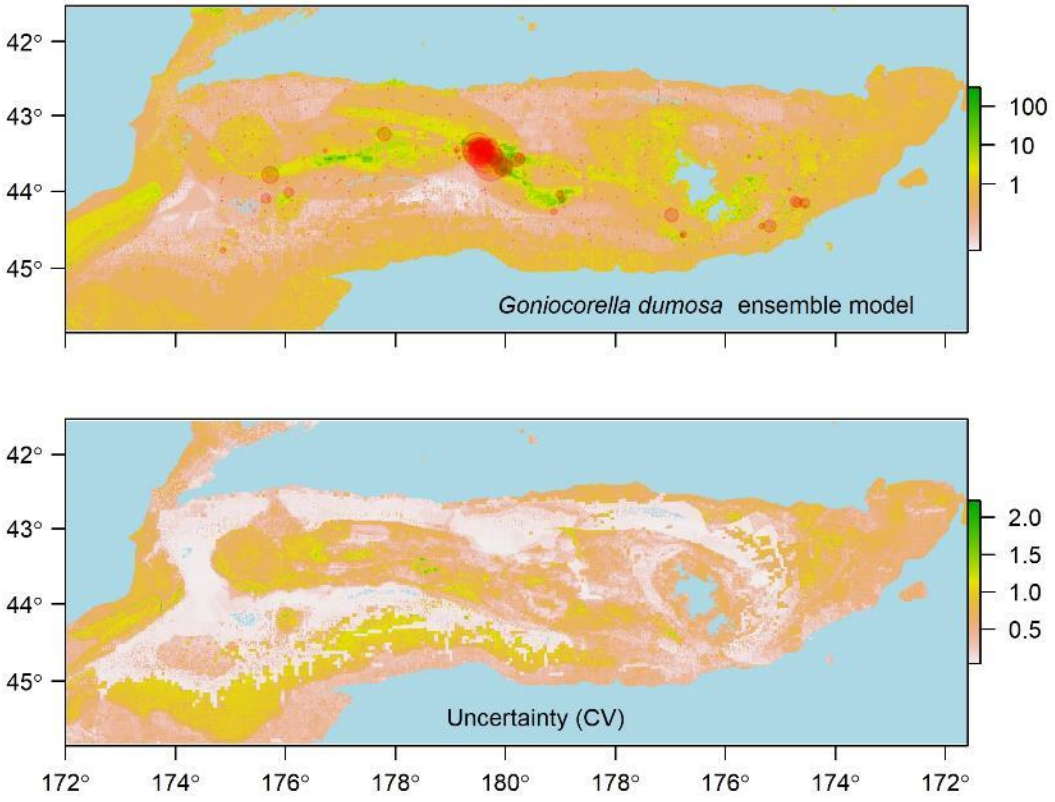

Figure 4: *Goniocorella dumosa.* **Ensemble model predictions of abundance (individuals 1000 m^{-2}) on a log scale (top), with observed abundance from the camera survey stations represented by red circles (scaled to have a constant maximum radius in this and each of the following plots), and estimated uncertainty (CV) (bottom) from bootstrapping.**

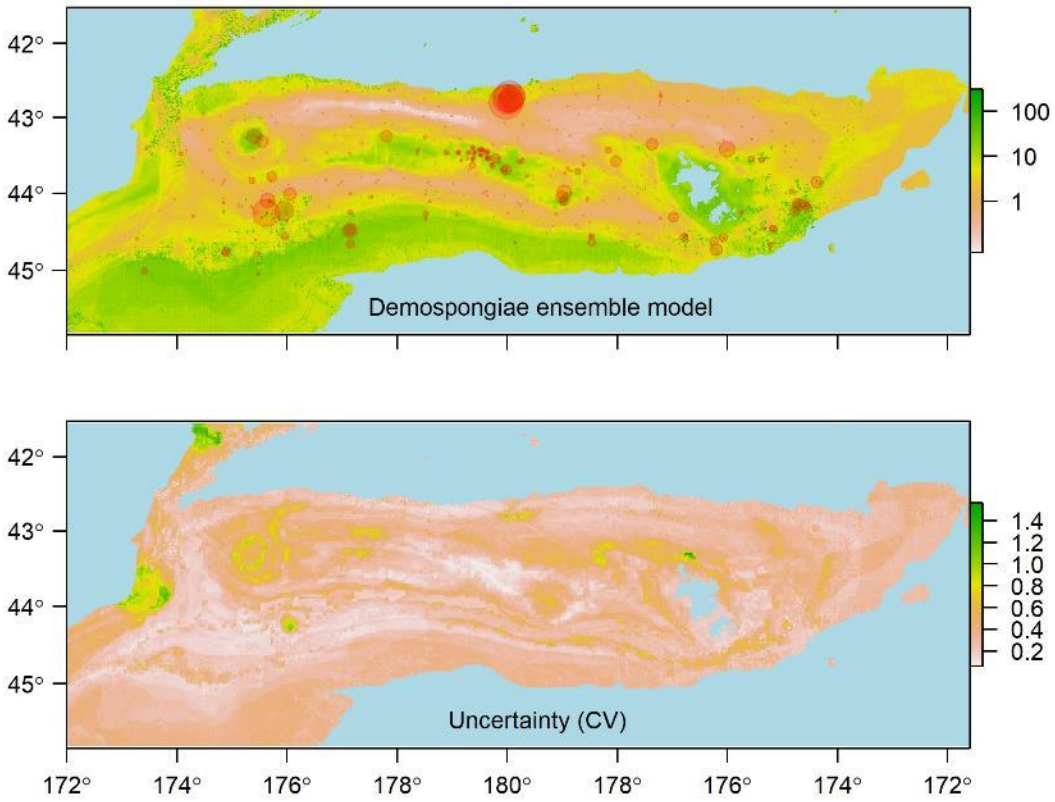

Figure 5: Demospongiae. See Figure 4 for details.

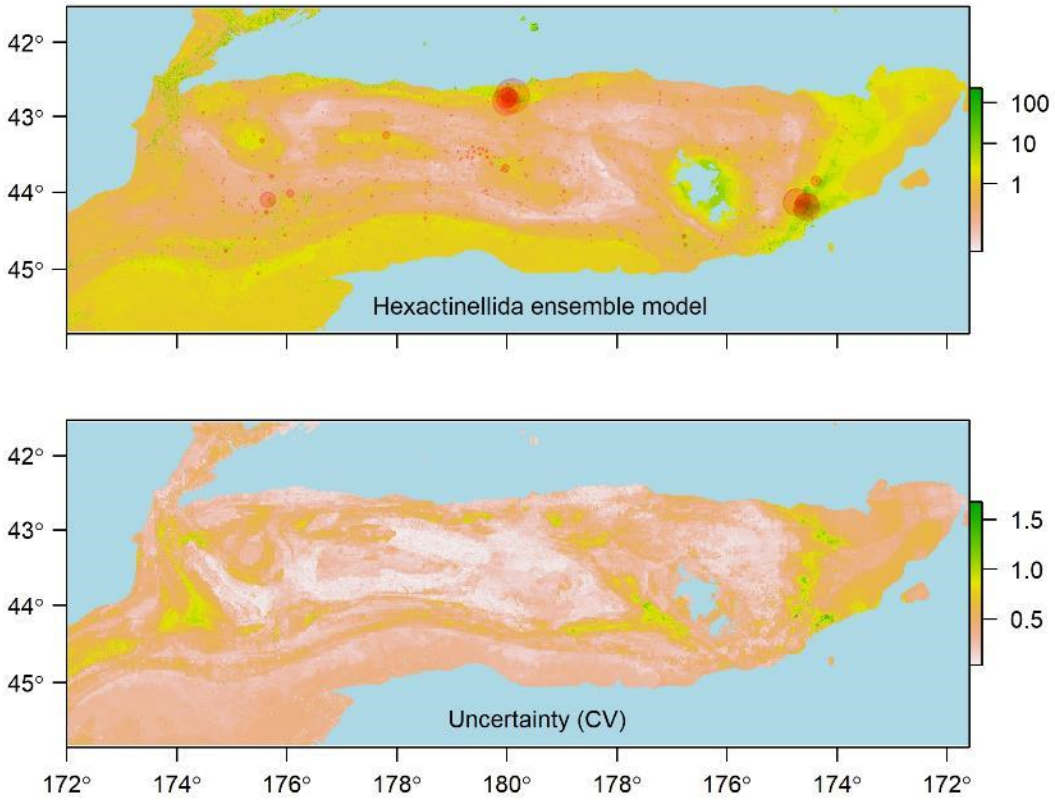

Figure 6: Hexactinellida. See Figure 4 for further details.

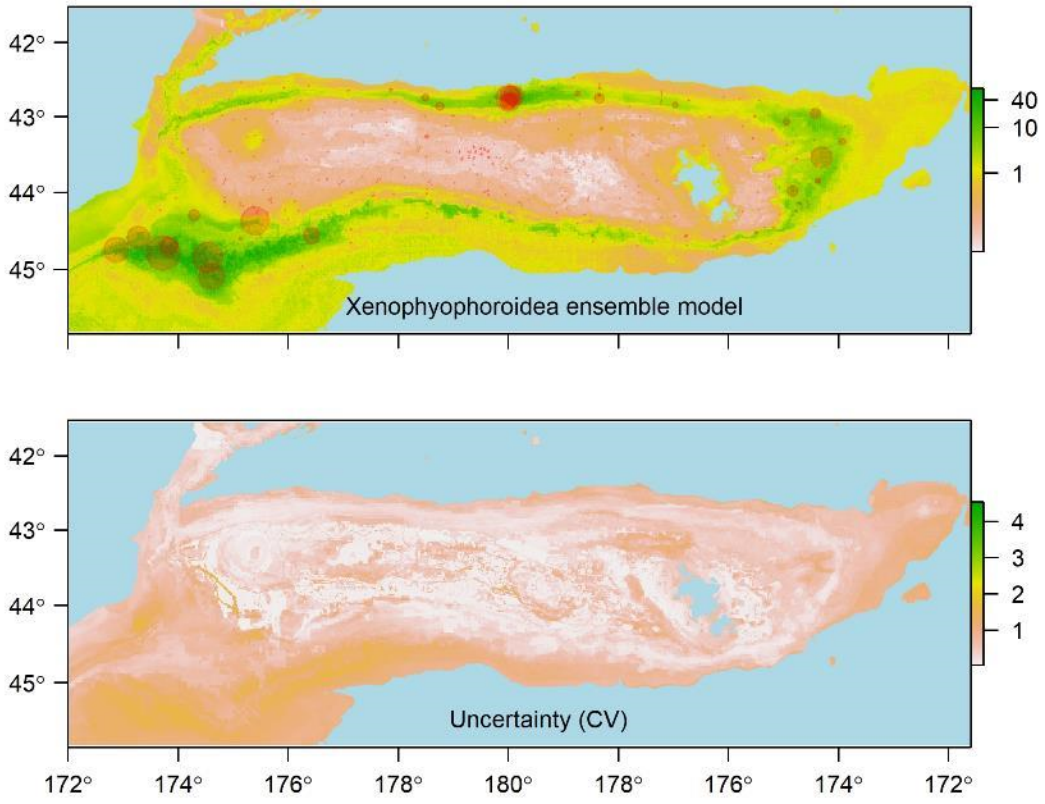

Figure 7: Xenophyophoroidea. See Figure 4 for details.

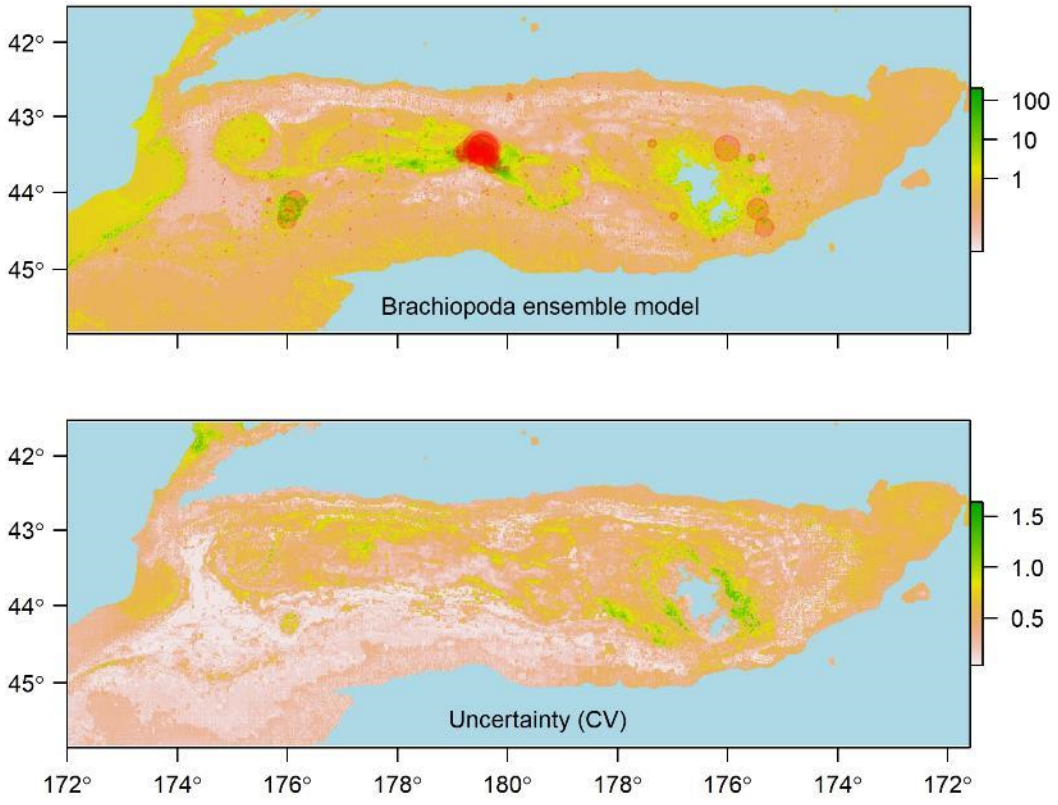

Figure 8: Brachiopoda. See Figure 4 for details.

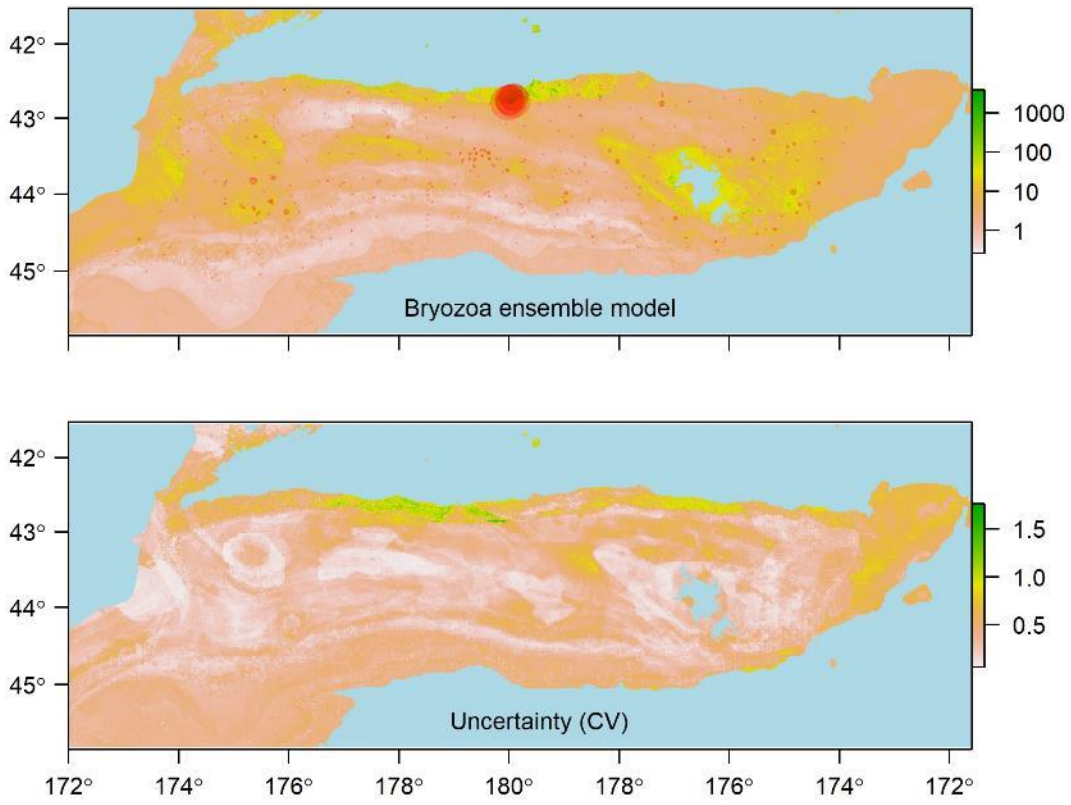

Figure 9: Bryozoa. See Figure 4 for details.

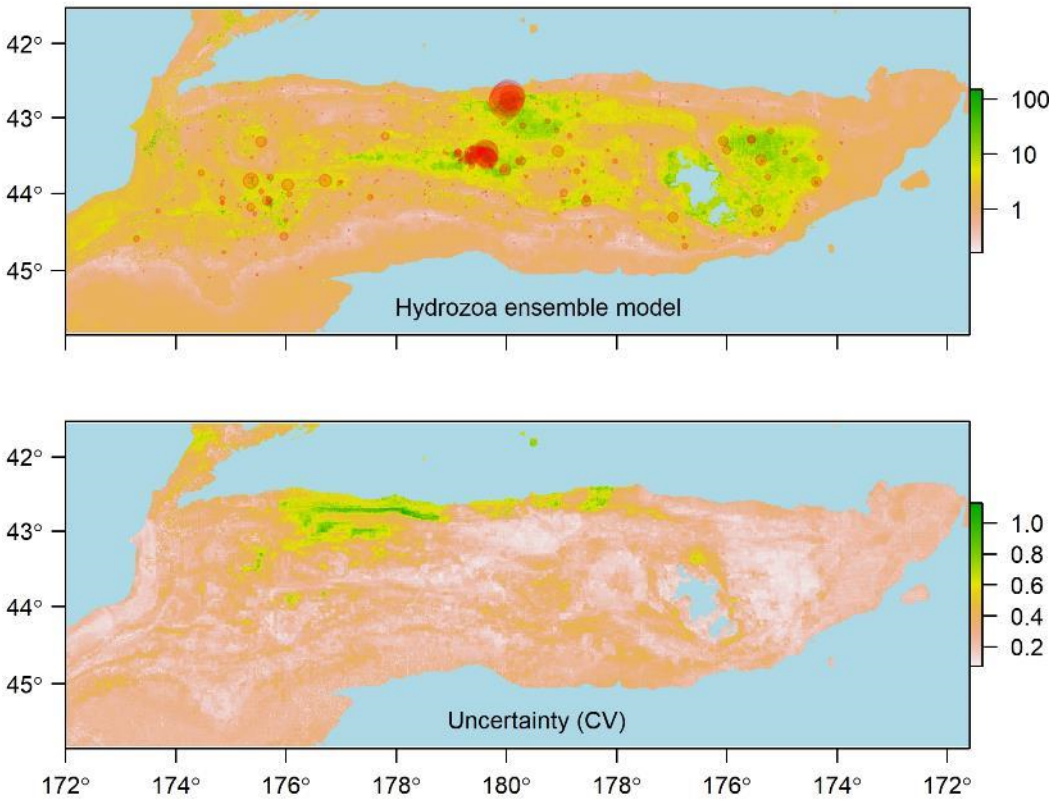

Figure 10: Hydrozoa. See Figure 4 for details.

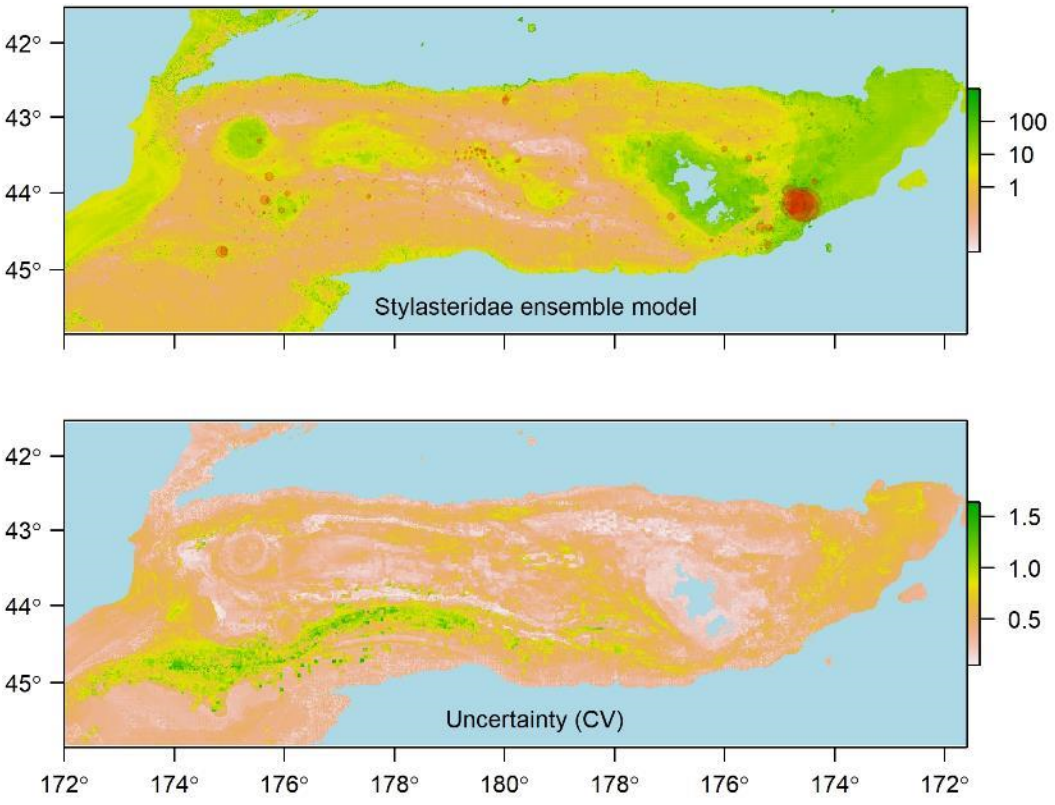

Figure 11: Stylasteridae. See Figure 4 for details.

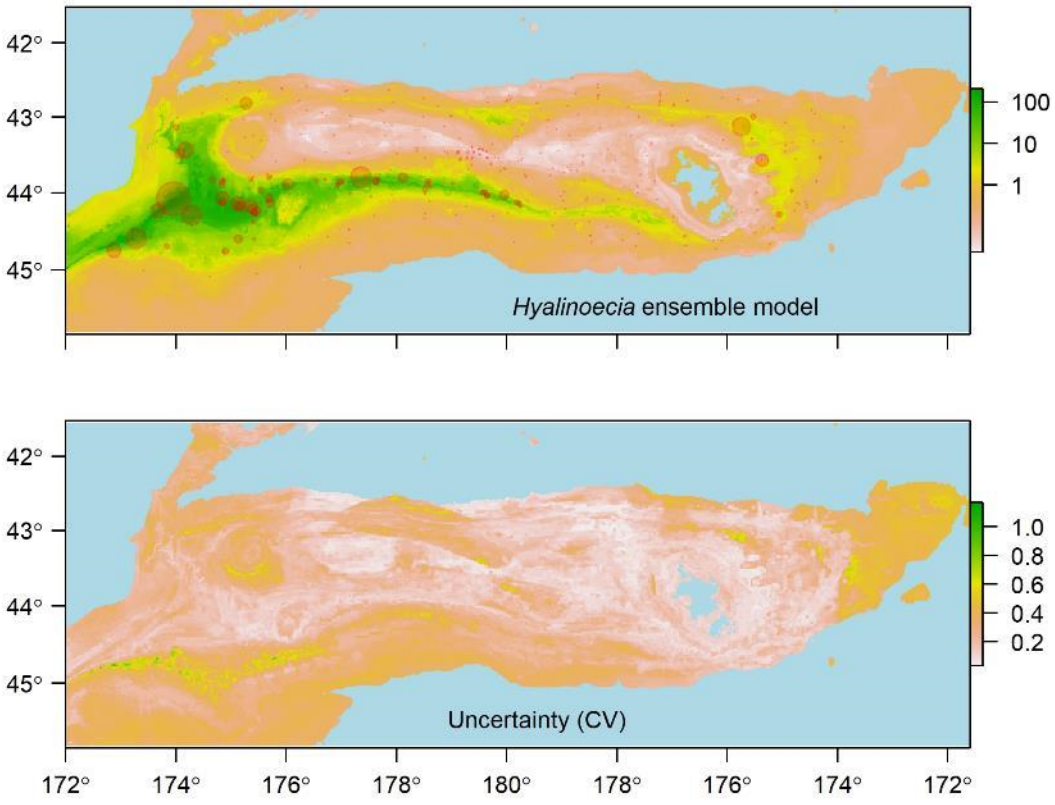

Figure 12: *Hyalinoecia* sp. See Figure 4 for details.

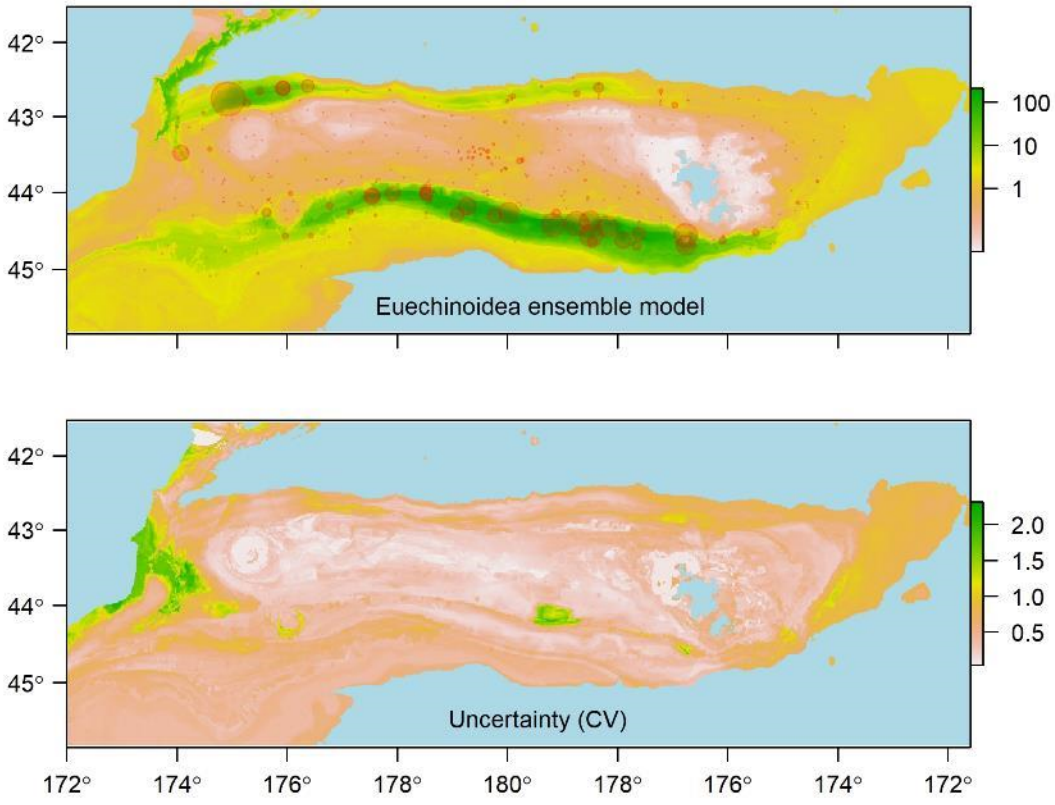

Figure 13: Euechinoidea. See Figure 4 for details.

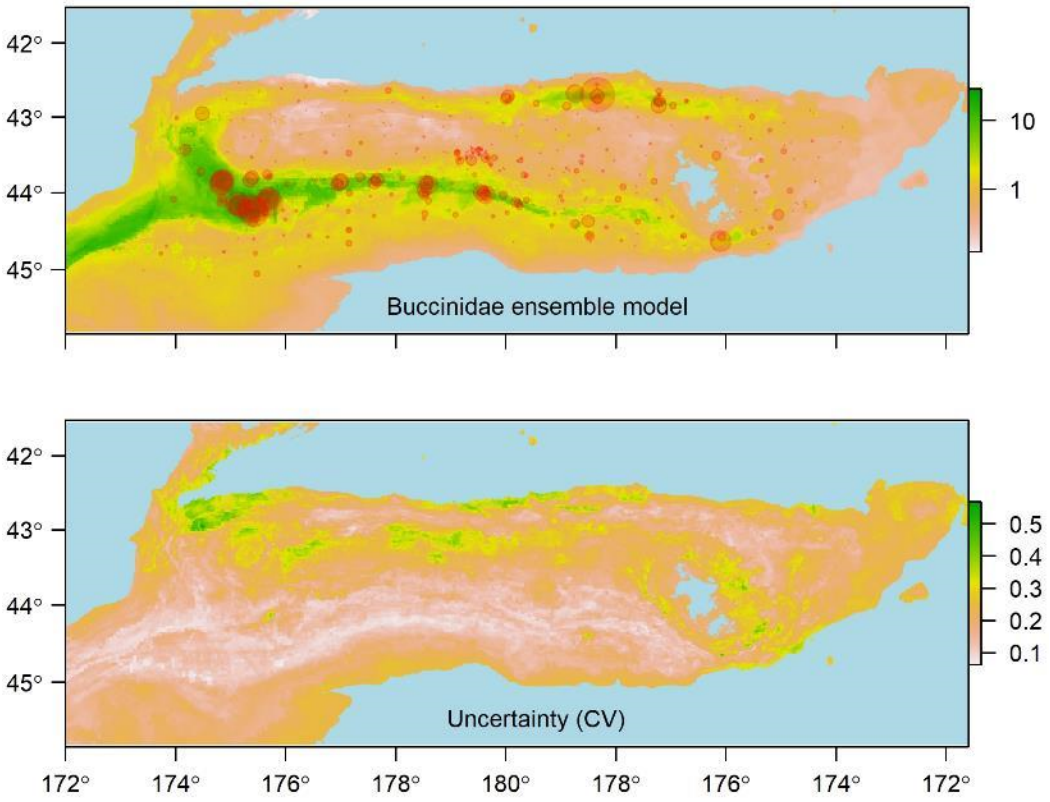

Figure 14: Buccinidae. See Figure 4 for details.

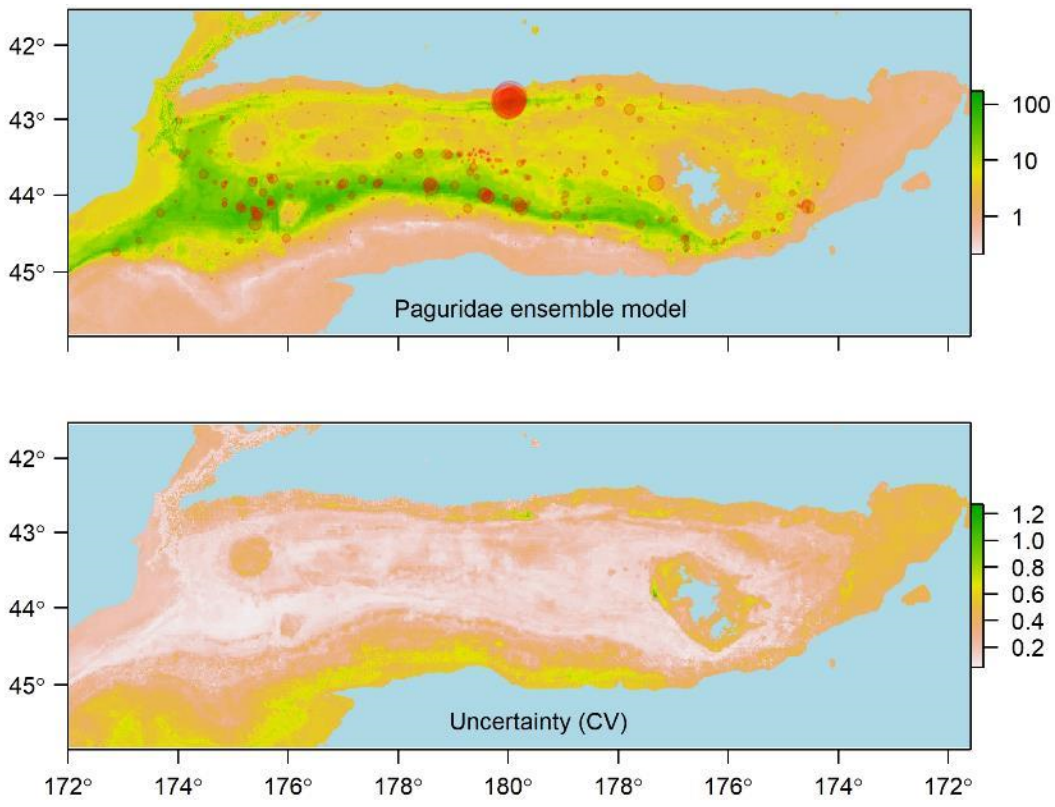

Figure 15: Paguridae. See Figure 4 for details.

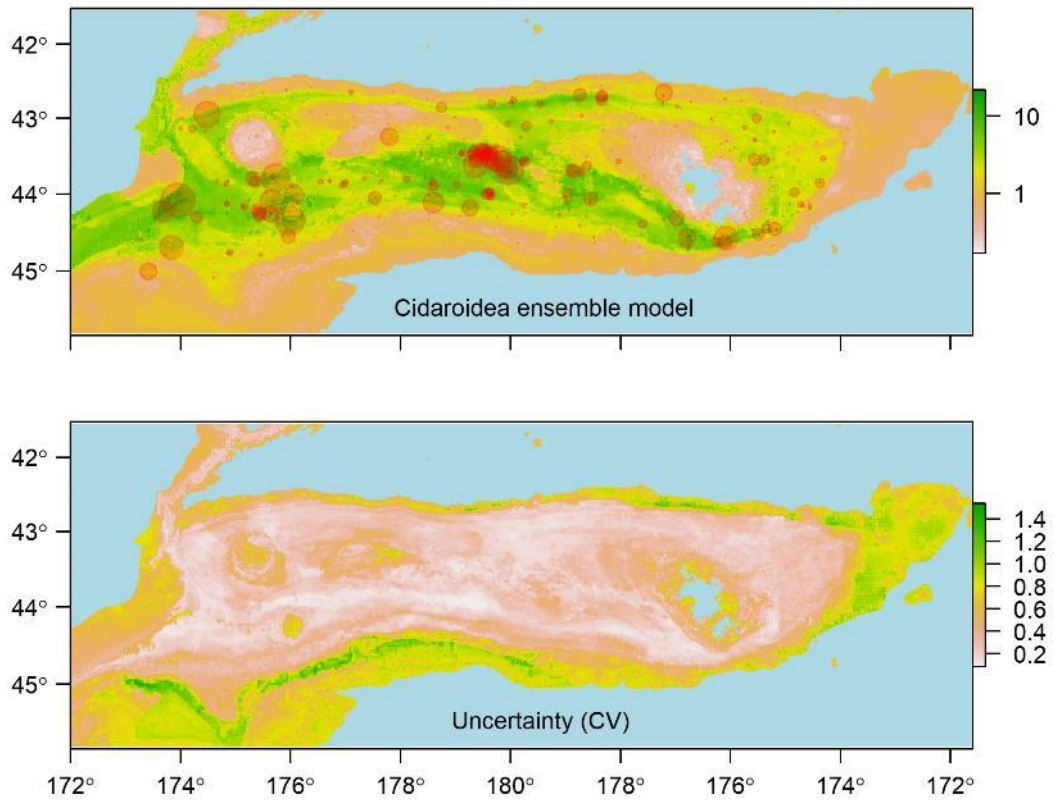

Figure 16: Cidaroidea. See Figure 4 for details.

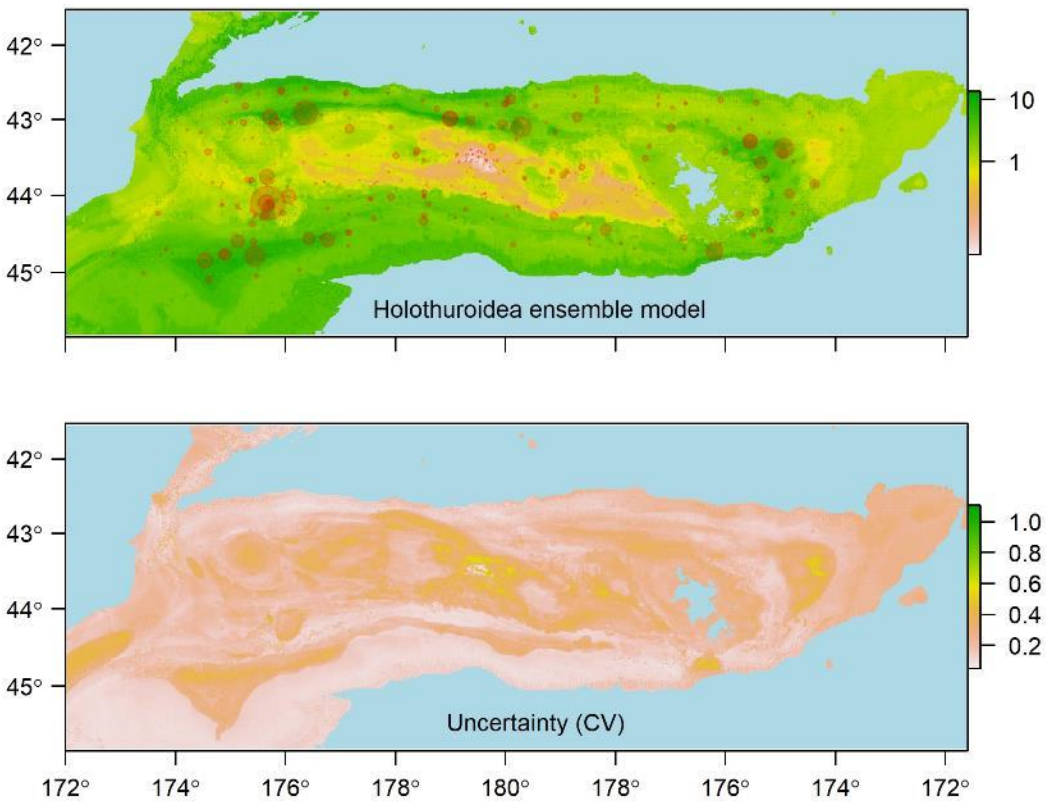

Figure 17: Holothuroidea. See Figure 4 for details.

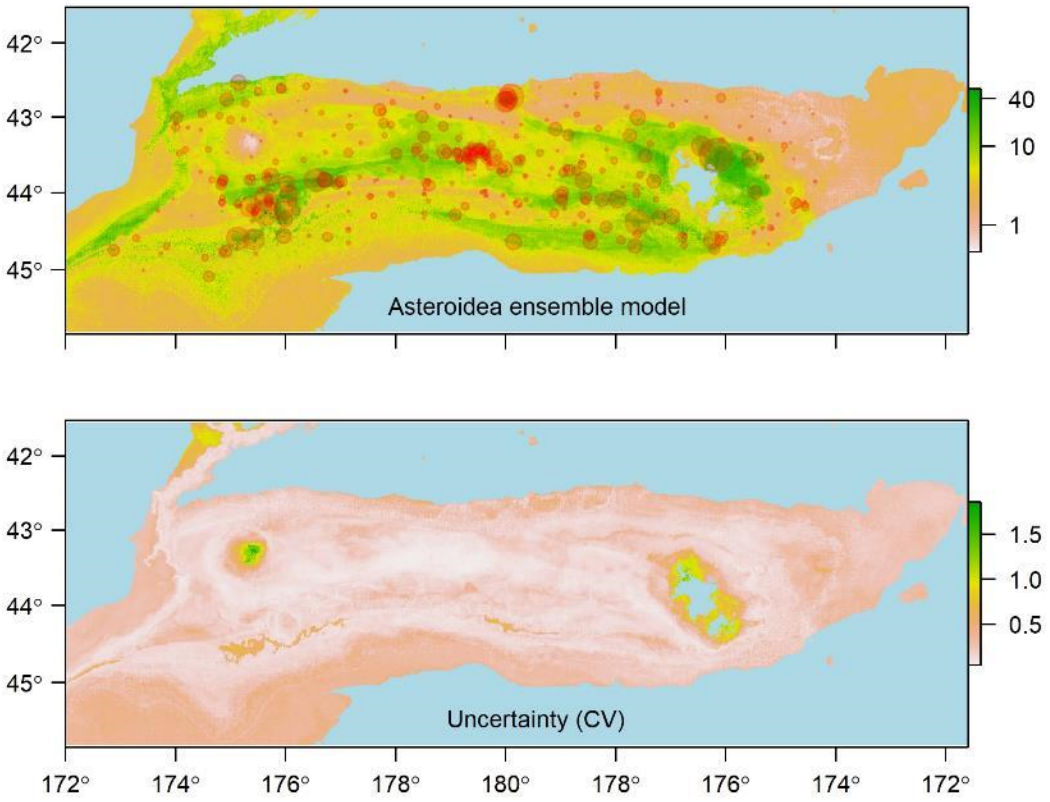

Figure 18: Asteroidea. See Figure 4 for details.

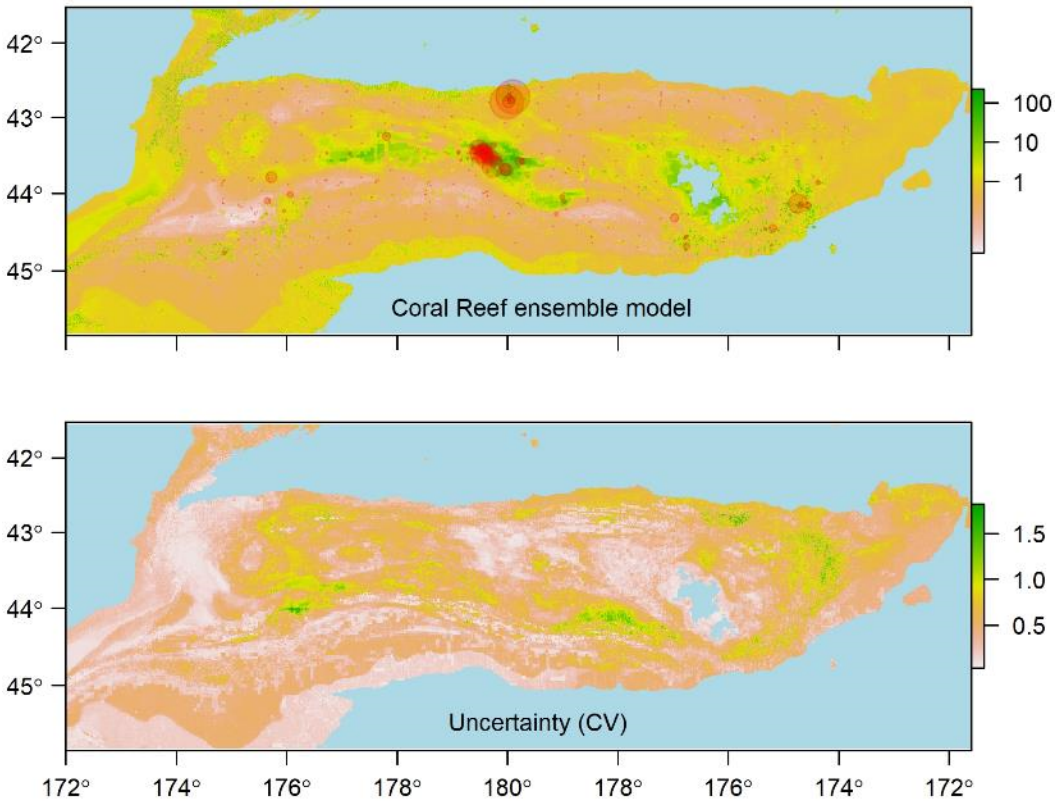

Figure 19: Coral Reef. See Figure 4 for details.

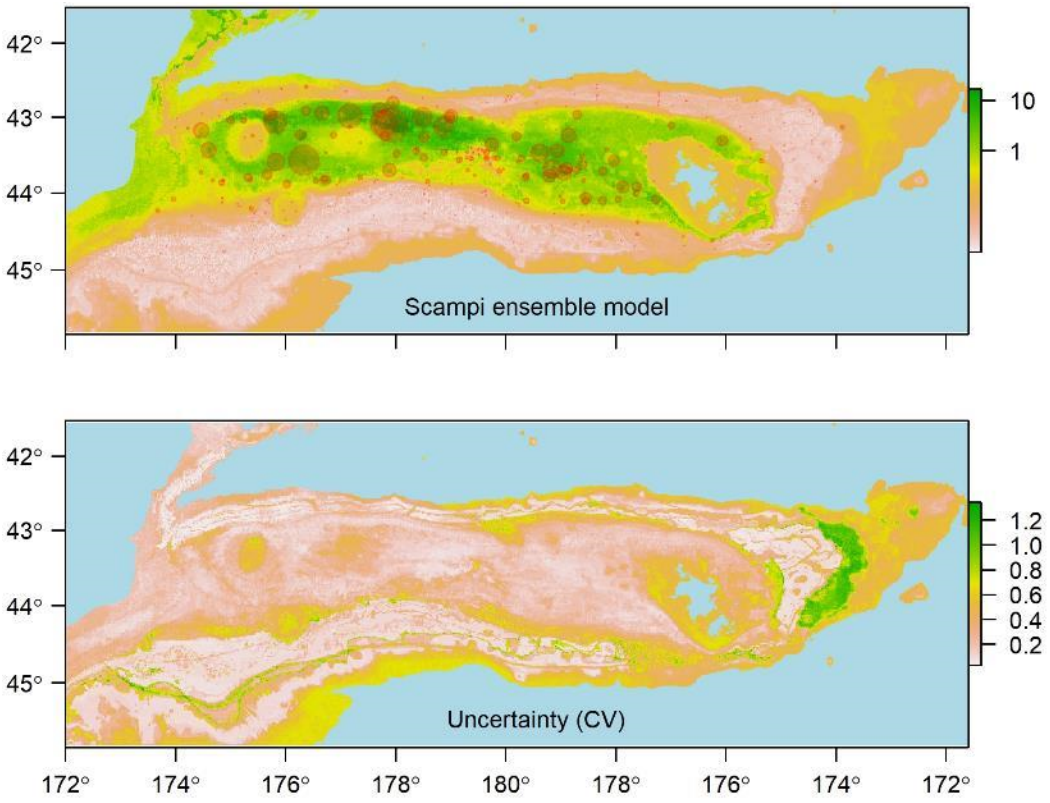

Figure 20: Scampi (*Metanephrops challengeri*). See Figure 4 for details.

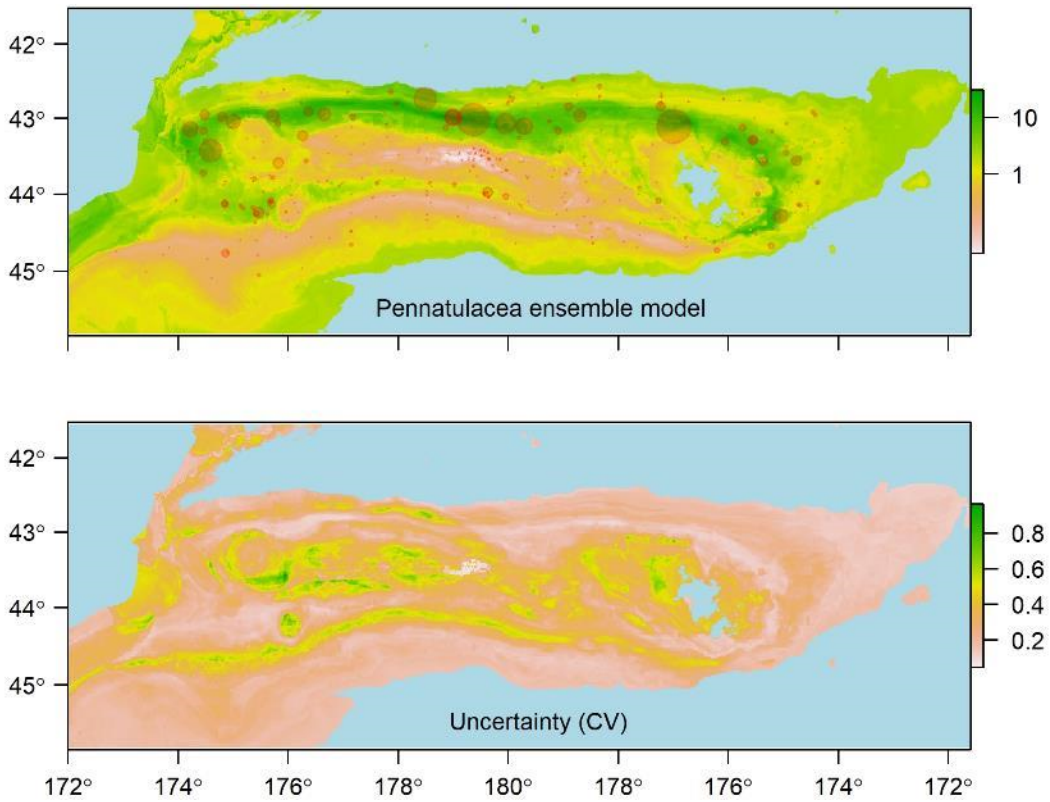

Figure 21: Pennatulacea. See Figure 4 for details.

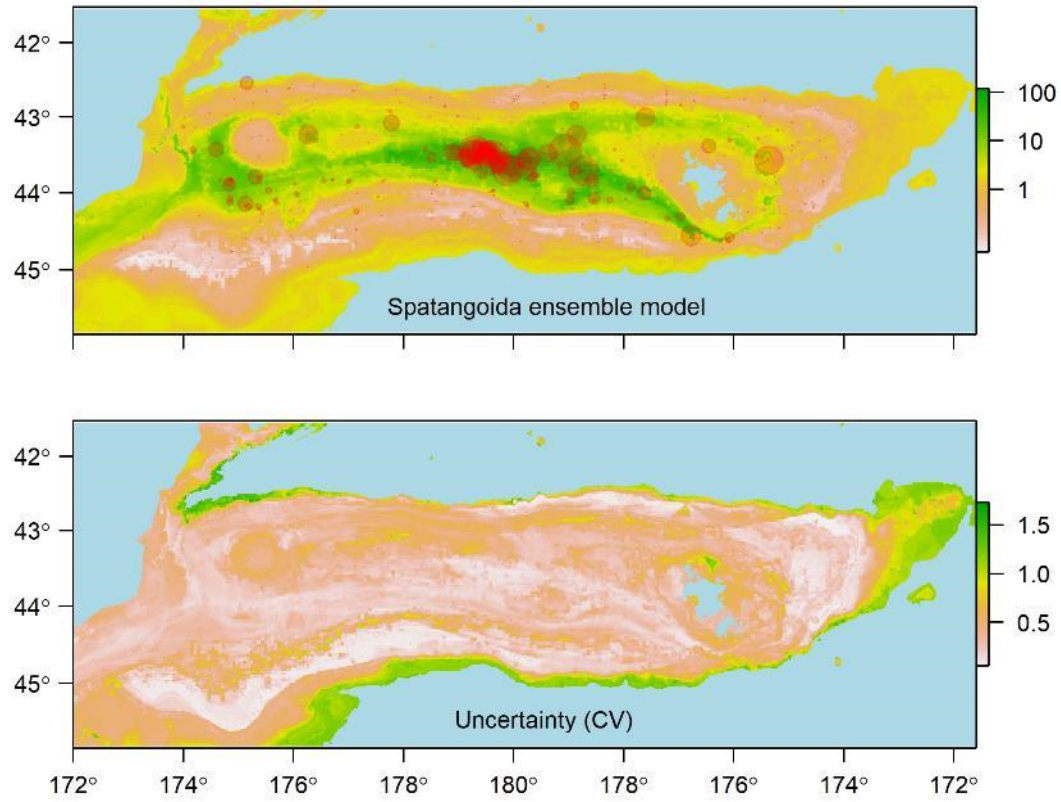

Figure 22: Spatangoida. See Figure 4 for details.

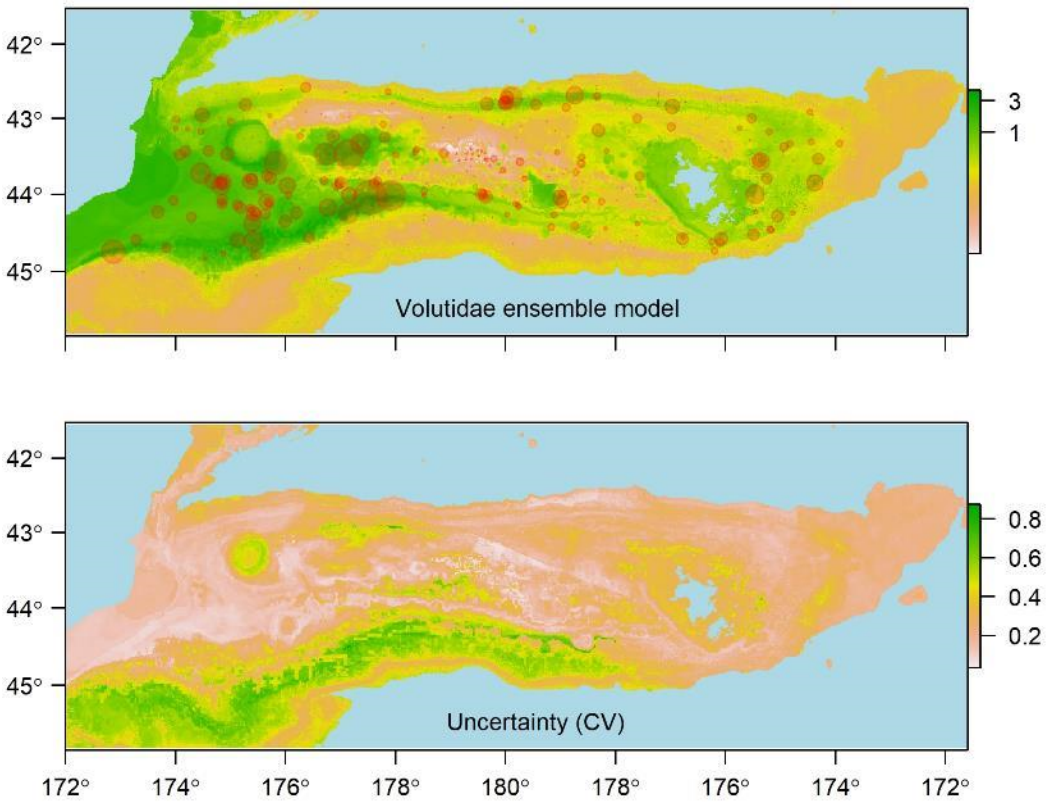

Figure 23: Volutidae. See Figure 4 for details.

3.3 Community models

Regions of Common Profile

To avoid potential over-fitting, a reduced set of 9 predictors, including the *trawl* layer, was chosen from the 12 used as a basis for the individual taxon models. Although showing moderate correlations with some of the other variables, *bathy* was retained due to its likely relationship with other, unavailable, environmental parameters that may have an influence on community composition, the relatively high confidence with which it is measured, and an expectation that its inclusion may help to more clearly delineate boundaries of predicted regions. However, the variable *tidalcurr* was excluded due to a high correlation with depth (89%); *cbpm_mean* was excluded due to high correlation (over 80%) with *dynoc*; and *epp_min* was excluded due to the combination of a high correlation with *epp_mean* and a lower rank in initial GF models.

The best model (taken to be the one with the lowest BIC value) classified the data into 7 RCP classes (Figure 24). Analysis of diagnostic plots describing normality and homogeneity of variance in model residuals revealed a small amount of deviation from normality at the extremes of the data but otherwise did not reveal any major inadequacies in the model.

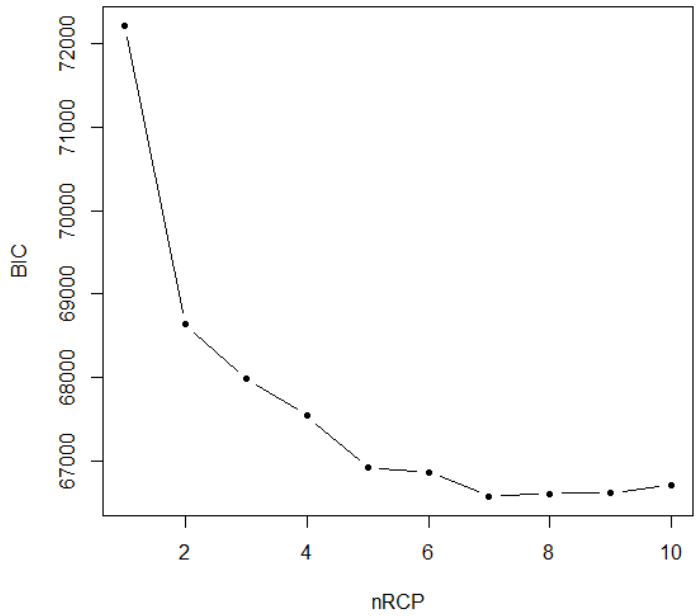

Figure 24. Bayesian Information Criterion (BIC) for the best model (from 500 model optimisations) for each trial number of RCP groups (nRCP).

The RCP classification showed some fragmentation into smaller, isolated, patches at fine spatial scales but differentiated northern and southern regions of the crest and shallow flanks of the Rise, the two shallowest regions (on Mernoo Bank and around the Chatham Islands), and the slope regions in depths of about 400–800 m on the western and southern slopes (Figure 25). In deeper depths, classes extended around most of the Rise, with no differentiation between northern, southern, and eastern flanks. RCP 1 is predicted to occur in middle depths on the western and southern flanks of the Rise, where the water is relatively cool for the depth and less saline (see APPENDIX 2 – Regions of Common Profile). RCP 4 and RCP 7 are located on the shallow crest of the Rise, with RCP 4 located on the central southern crest in relatively cool water and RCP 7 mostly northern and eastern in relatively warmer and more saline water. RCP 5 and RCP 6 lie in distinct bands that circle the Rise, RCP 5 centred around a depth of about 800–1100 m and RCP 6 mostly deeper than 1000 m. RCP 3 represents by far the smallest region and is restricted mainly to the Graveyard seamounts on the central north flank of the Rise. RCP 2 has an anomalous bimodal depth distribution, with predicted occurrence both in shallow waters around the Chatham Islands and the Mernoo Bank and in the deepest water on the eastern and southern flanks of the Rise.

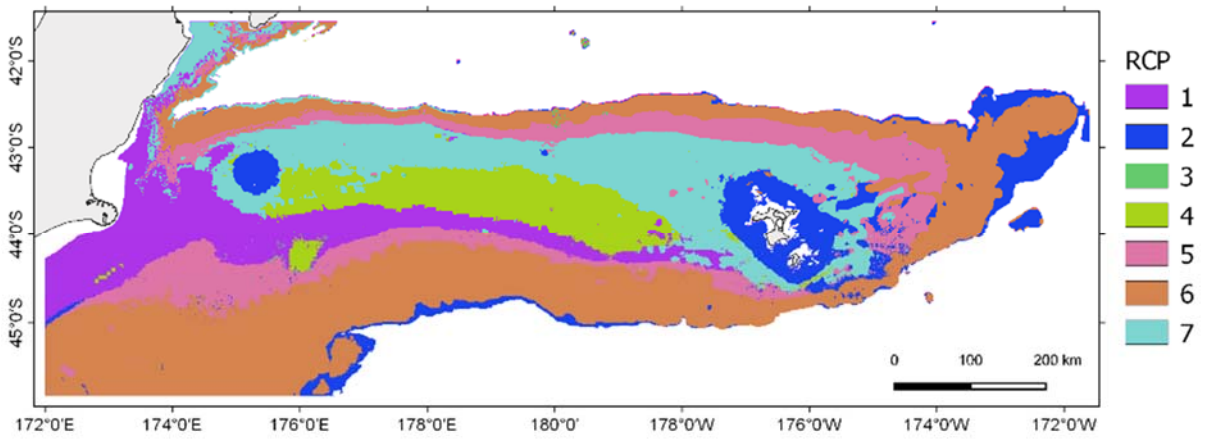

Figure 25: Regions of Common Profile (RCP). Spatial distribution of the seven RCP regions on Chatham Rise predicted to have similar seabed environments and fauna.

Model uncertainty was highly variable among the seven RCPs, with the probability associated with assigned RCPs in individual cells ranging from 0.22 (where several other RCPs were relatively likely) to 0.99 (where RCP membership is strongly supported). Overall, model uncertainty was greatest for RCP 3 (primarily on the Graveyard hills), and least for RCP 1 (in middle depths on the western and southern flanks of the Rise). RCP 2 had very low uncertainty in shallow depths on Mernoo Bank and around the Chatham Islands but high uncertainty in the apparently anomalous deeper areas in the eastern and southern Rise (Figure 26). Mapping the underlying probabilities for each RCP demonstrates the detail in the underlying model output and how this has been compressed to generate the 7-class, hard-boundary classification (Figure 27).

The RCP method is still in development (Scott Foster, CSIRO, Hobart, pers. comm.) and with existing code libraries it was not possible, within the resources of the current project, to extract detailed summaries of the taxa and environmental parameters characterising each RCP.

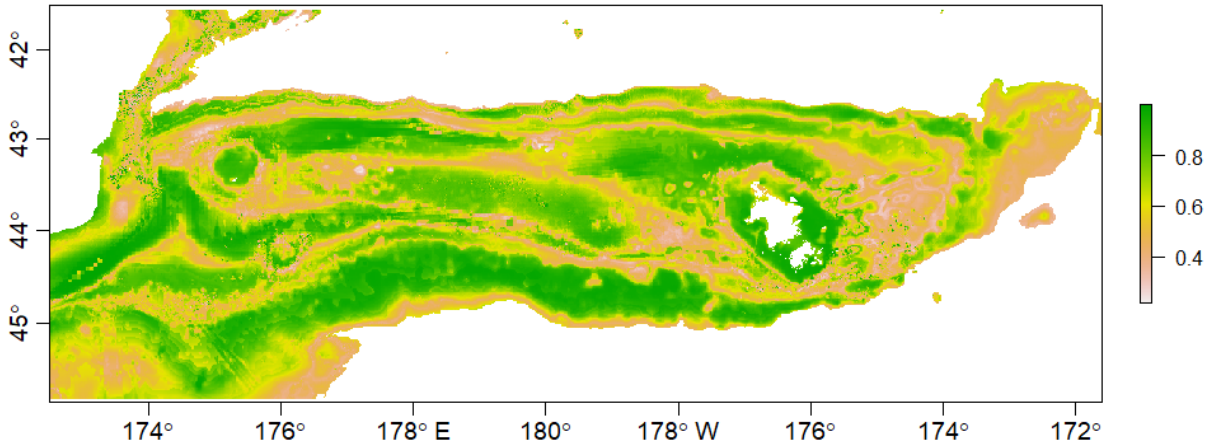

Figure 26: Regions of Common Profile (RCP) model certainty. For each cell, colour indicates the probability associated with the assigned RCP as plotted in Figure 25, based on 500 bootstrap samples.

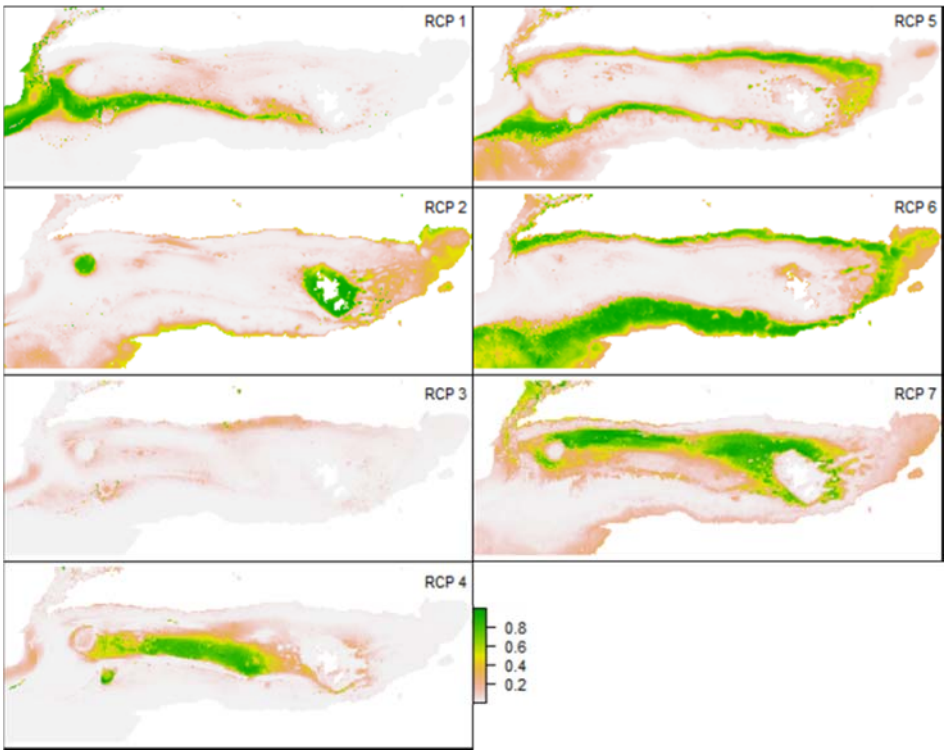

Figure 27: Regions of Common Profile (RCP). Mapped probabilities of occurrence for each of the seven RCP groupings defined by the model.

Gradient Forests

Of the 69 taxa available in the faunal data set, 54 were adequately represented in the GF models (R^2 greater than 0), with R^2 values per taxon ranging from 0.67 for squat lobsters (Galatheidae/Chirostylidae), to less than 0.01 for bamboo corals (Isididae), bivalve molluscs (Bivalvia), and the swimming holothuroid (*Enypniastes eximia*). Inclusion of trawl intensity as a predictive variable increased R^2 values for some taxa and reduced for others but had a minor effect overall, mean R^2 values across all modelled taxa being 0.361 and 0.359 for models excluding and including trawling, respectively (Figure 28). Diagnostic plots from GF (Figure 29 and Appendix 3), when viewed in the context of sampled distributions and the trawl intensity layer, indicated that the taxa with distributions inversely correlated with the occurrence of trawling were the stony coral *Goniocorella dumosa*, lamp shells (Brachiopoda), and burrowing urchins (Spatangoida), with positive correlations for a range of taxa including serolid isopods (Serolidae), hermit crabs (Paguridae), the small seapen *Kophobelemnon* sp., the solitary burrowing soft-coral *Taiaroa tauhou*, and the quill worm *Hyalinoecia* sp. In classifications, the main effect of including trawl intensity was to delineate small-scale classes associated with areas of particularly high cumulative trawl footprint at higher class-levels (Figure 33). Although the model excluding trawl intensity yielded a marginally higher mean taxon R^2 value, trawl intensity ranked as the second most influential variable in terms of both model accuracy and overall R^2 when included in the model (Figure 30 C). Because of this, we consider results both excluding and including the trawl intensity variable (Figure 31 and Figure 32).

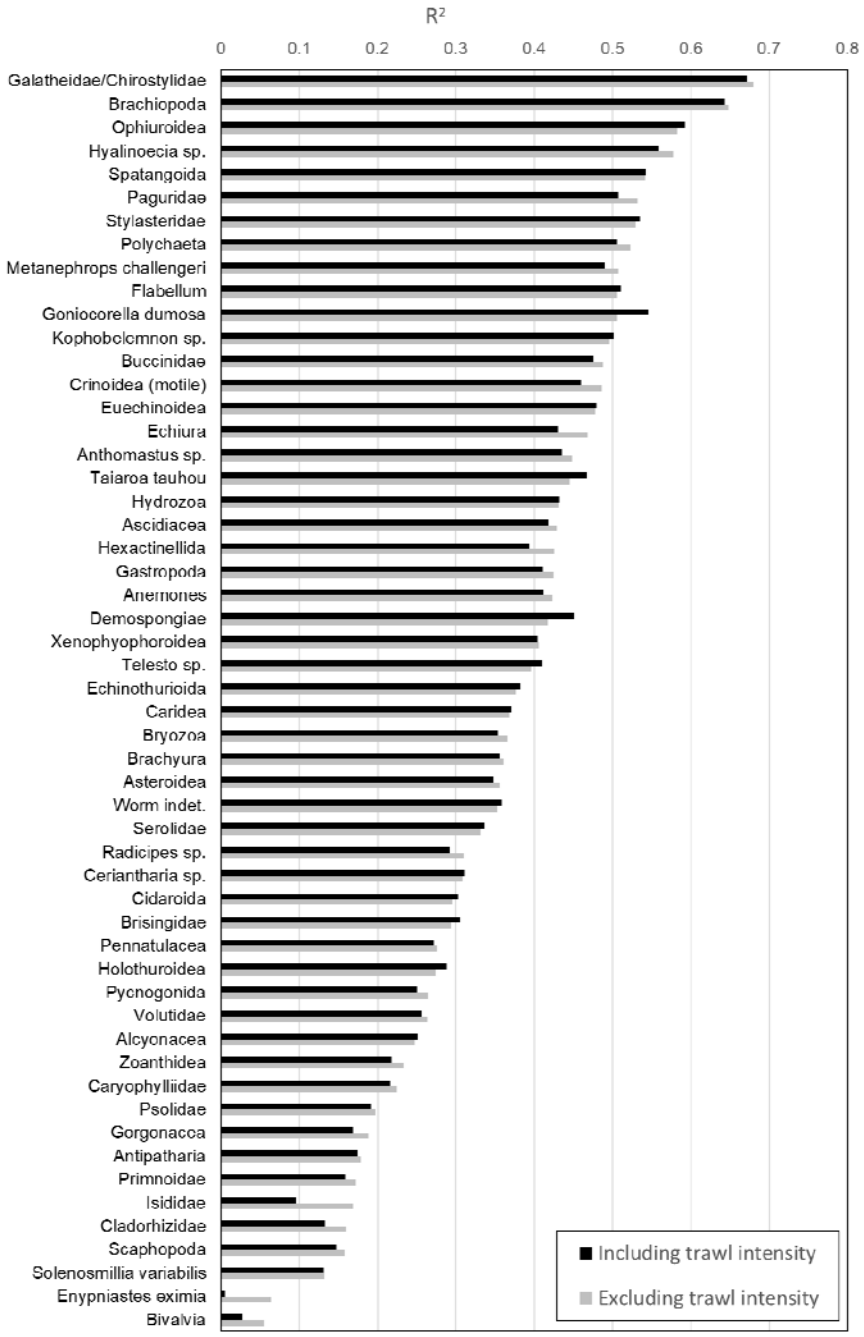

Figure 28: Gradient Forests. Correlations (R^2) between sampled distributions of individual taxa and the suite of transformed environmental variables, showing values including (black) and excluding (grey) trawl intensity as an environmental variable.

Predicted taxon turnover at base grid resolution (Figure 30 A) indicated well-defined gradients in community composition between the northern and southern flanks of the rise, and from Mernoo Gap (between Mernoo Bank and the South Island) in the west to beyond the Chatham Islands in the east. Sample coverage of the study area in relation to the range of the environmental predictor variables was good (Figure 30 B), suggesting that these predictions should be reliable, and classifications derived from the GF-transformed environmental variables had clear boundaries, without excessive fragmentation into small polygons or disparate instances of the same class, except at higher class-levels when trawl intensity was included, as noted above (Figure 31 and Figure 32). RELATE tests of correlations between matrices representing dissimilarities between GF classes in terms of transformed environmental space (average

values per class) and sampled faunal composition (average log-transformed densities of benthic taxa from sample sites within each class) were significant for all four class-levels examined (P<0.05) but varied widely in strength. Correlations were strongest for the 15-class (r=0.558) and 25-class (0.538) levels, lower for the 7-class level (0.321), and substantially lower for the 50-class level (0.020).

The taxa and environmental conditions associated with each of the GF classes in the 50-class classification excluding trawl intensity are listed in Tables A-3 and A-4, respectively (Appendix 3). By cross-referencing with class numbers labelled in the 50-class map in Figure 31 (top panel), the characteristic fauna associated with each class can be determined. For example, Class 30 to the southwest of Mernoo Bank is associated with quill worms (*Hyalinoecia* sp.), hermit crabs (Paguridae), polychaetes, *Flabellum* sp. solitary corals, bryozoans, *Anthomastus* sp. soft corals, predatory gastropods (Buccinidae), burrowing urchins (Spatangoida), the unitary burrowing soft coral *Taiaroa tauhou*, and others, while Class 2, extending northeast from Mernoo Bank, is associated with burrowing urchins (Spatangoida), seapens (Pennatulacea), holothuroids, spiral whip gorgonians (*Radicipes* sp.), *Munida gracilis* (Galatheidae/Chirostylidae), and prawns (Caridea). Of the other classes corresponding to areas of highest cumulative trawl intensity (Figure 33), Class 37 on the southern flank of the rise, east of Veryan Bank, was associated with high densities of *Taiaroa tauhou*, hermit crabs, the quill worm *Hyalinoecia* sp., anemones, the small seapen *Kophobelemnon* sp., and the galatheid crustacean *Munida gracilis* (Galatheidae/Chirostylidae), while Class 38 and Class 42 were dominated by high densities of *Hyalinoecia* sp. quill worms. On the central crest of the rise, encompassing much of the Mid-Chatham Rise Benthic Protection Area, Class 31 was associated with burrowing urchins, the stony coral *Goniocorella dumosa*, brachiopods, *Munida gracilis*, and other taxa.

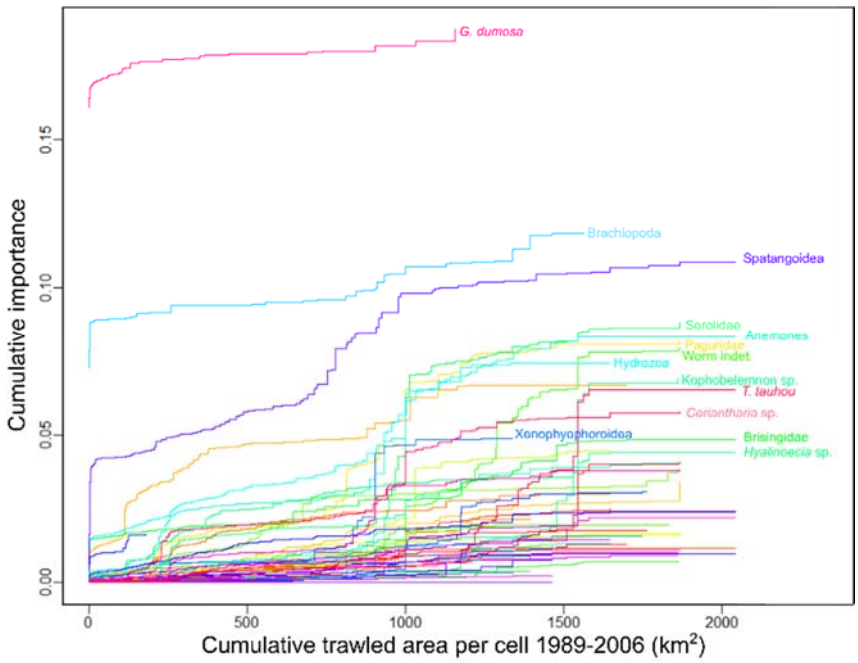

Figure 29: Importance of the trawl intensity variable (cumulative trawled area) in Gradient Forest functions (cumulative importance) predicting taxon occurrence on Chatham Rise. Labels identify taxa with the strongest correlations (positive or negative) with the trawl intensity.

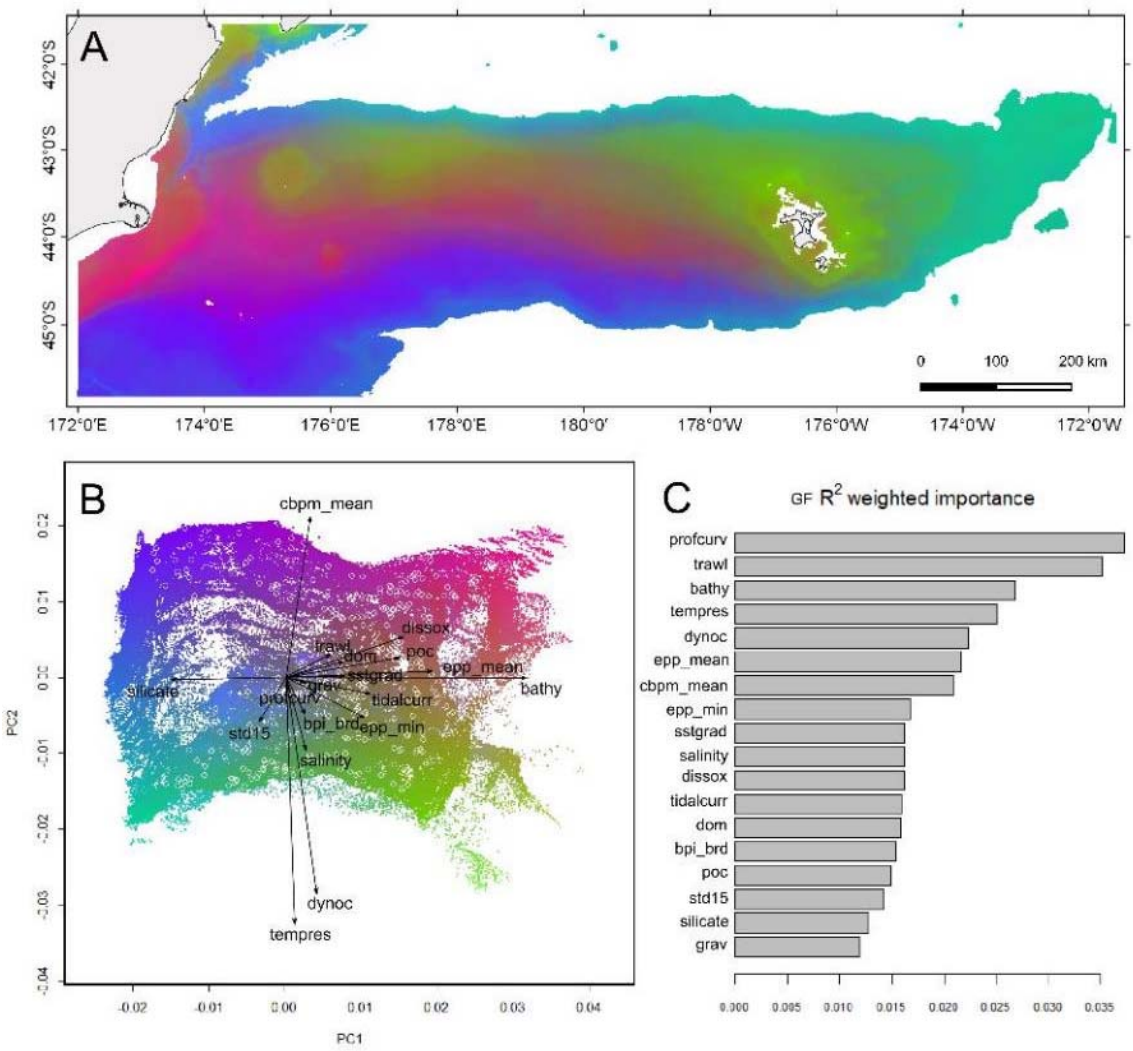

Figure 30: Gradient Forests. Map of benthic taxon turnover across Chatham Rise (A). Changes in community composition are represented by colour gradients (red, green, blue) based on scores from the first three axes from a Principal Components Analysis (B) of a suite of 18 environmental variables transformed to correlate with sampled taxon distributions. The relative importance (R^2) of each predictor variable in the full model is shown in (C). These results are from the model including trawl intensity as a predictor variable. White circles in (B) indicate the distribution of faunal sample sites in relation to the full range of environmental space across the study area.

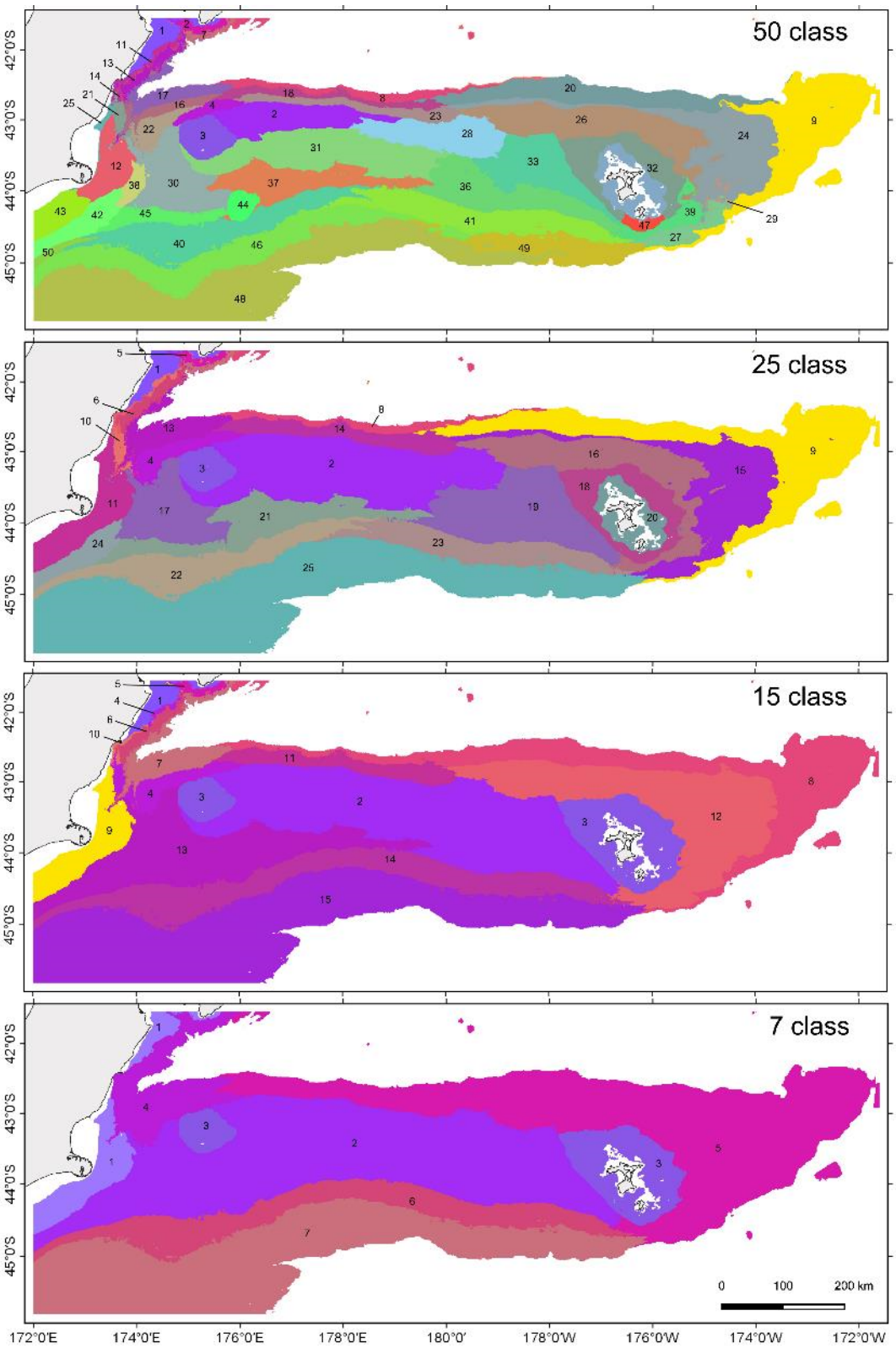

Figure 31: Gradient Forest. Classification of 17 transformed environmental variables, excluding trawl intensity, representing spatial areas predicted to differ in benthic community composition. Classification was via a two-stage procedure (non-hierarchical k-medoids 'clara' to yield 300 groups, then hierarchical 'agnes' to enable visualisation at multiple class levels). Plots show the hierarchical classification at 7, 15, 25, and 50 class levels. Classes in each level are labelled by number to enable reference to underlying data but both numbers and colours differentiate classes only within panels (class-levels) and have no relationship between panels.

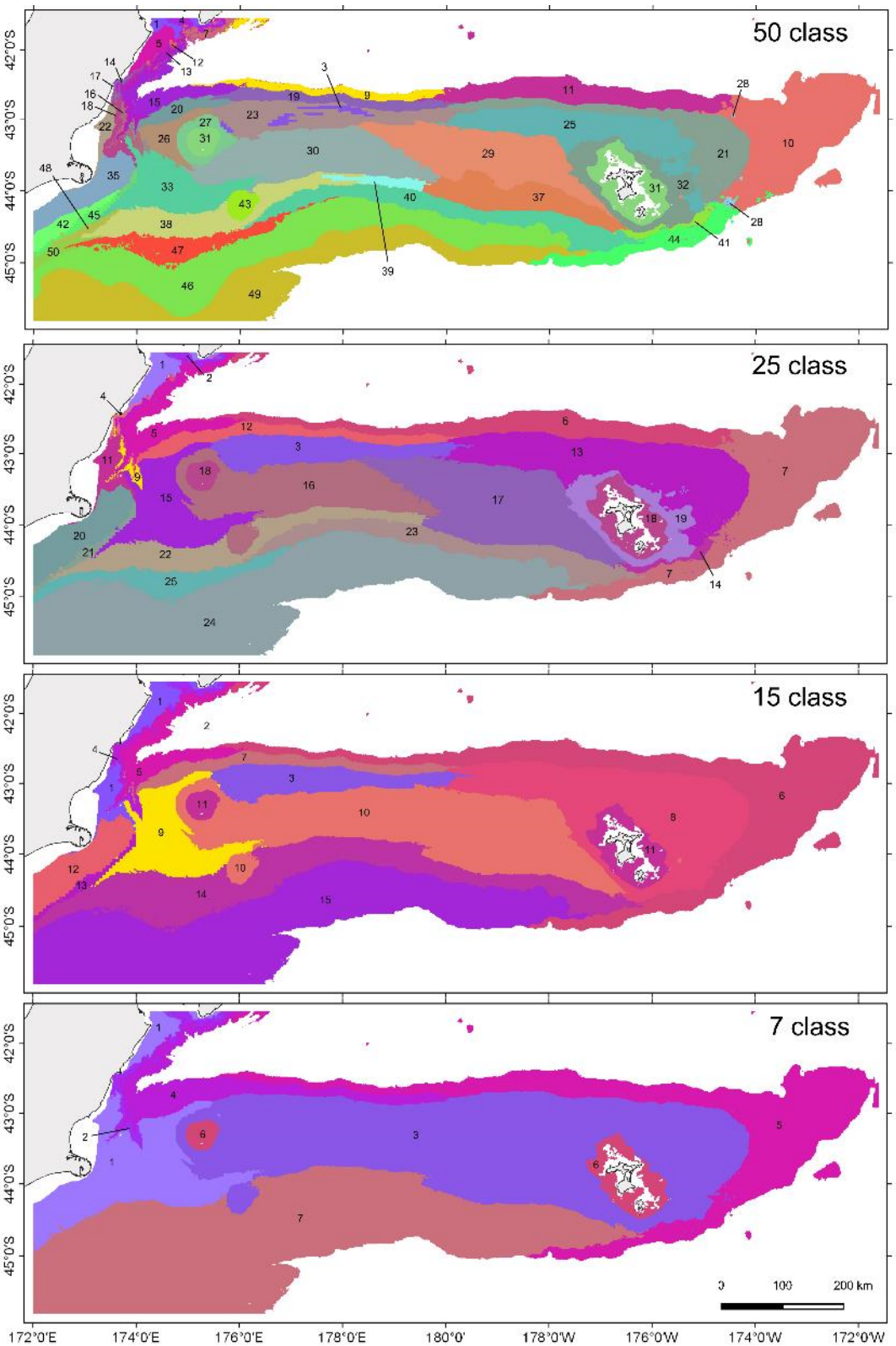

Figure 32: Gradient Forests. Classification of 18 transformed environmental variables, including trawl intensity as cumulative swept area for the period 1989 to 2006. Details as for preceding figure.

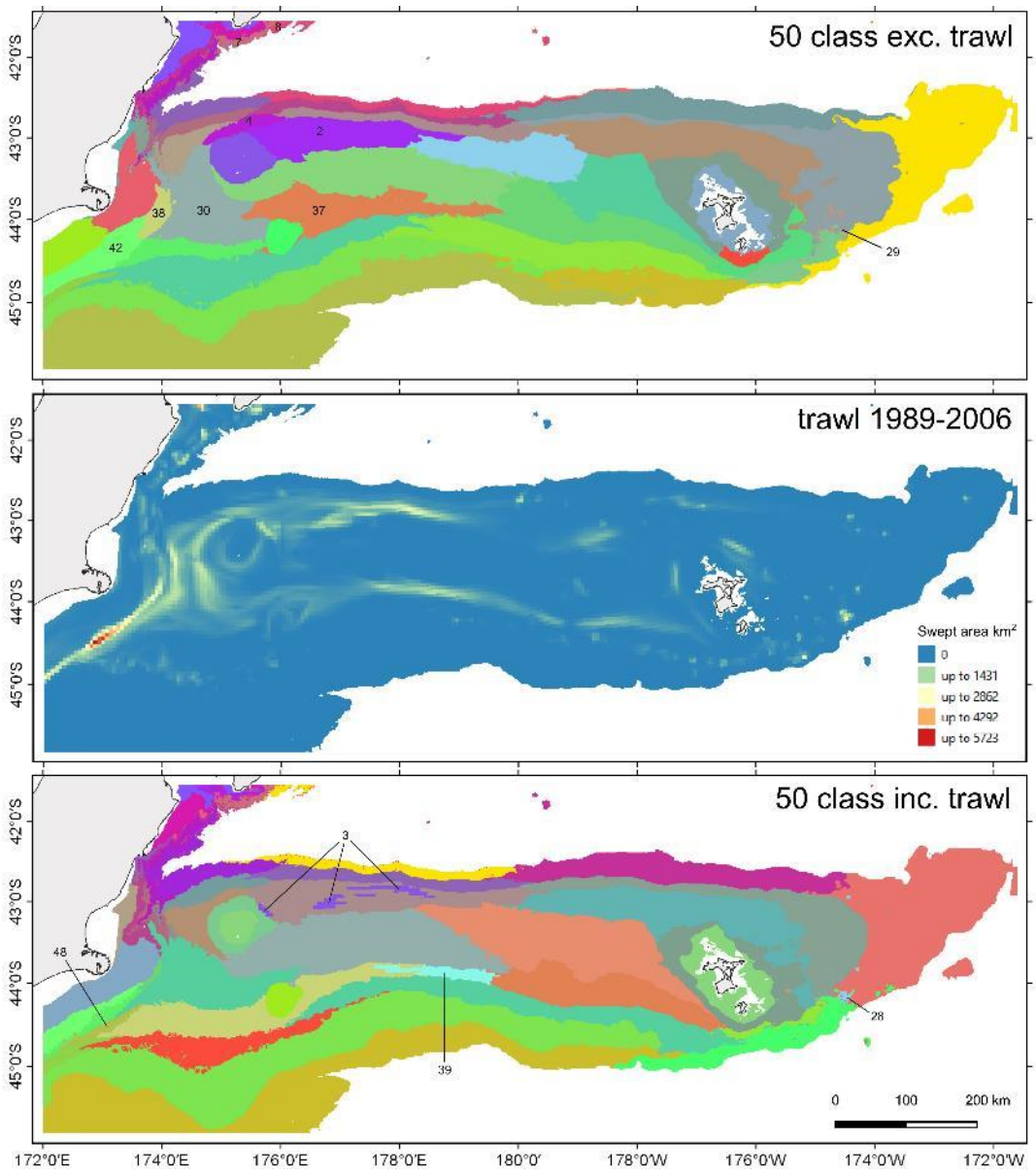

Figure 33: Effect of including trawl intensity as an environmental predictor in the Gradient Forests (GF) classification at 50-class level. GF classification excluding trawl intensity (top); trawl intensity as cumulative trawled seabed area per 5 × 5 km cell for the period 1989–2006 (middle); GF classification including trawl intensity (lower). Number labels indicate classes corresponding to areas of high cumulative trawl intensity.

Community model evaluation

Visual comparison of the RCP and GF outputs at 7-class level shows distinct differences between the two (Figure 34). While both classifications differentiate the shallow areas on Mernoo Bank and around the Chatham Islands, RCP resolves more class-structure on the crest of the rise and on the southern flank in middle depths, with Veryan Bank and the southern-central part of the crest separating out as a distinct class. At greater depths, by contrast, CR differentiates between the northern and southern flanks, whereas RCP shows continuous classes around the entire rise. Classifications at this class-level are necessarily simplification of reality but some aspects in both RCP and GF clearly do not match with what we know of taxon distributions from single-taxon models. For instance, RCP, as noted earlier, shows the same class occurring in the shallowest and deepest areas of the study area, while GF includes the whole of the crest, the southern flank to about 1000 m depth, Veryan Bank, and much of Mernoo Gap in a single class. Overall, however, the RCP appears to be a potentially more useful representation of benthic faunal distributions than GF at this class level because of its more nuanced representation of distributions in fishing depths.

This impression is supported by ANOSIM analyses (Table 5) quantifying the degree to which each classification divides the underlying faunal data into distinct groups; RCP scoring more highly than CR (R=0.524 and R=0.412, respectively). Extending the ANOSIM comparison to all available classifications (GF and RCP from this study, the MEC, the BOMEC, and the research trawl survey strata, see Figure 35) shows that GF at 50-classes scores highest (R=0.524) but that the RCP 7-class is comparable (0.524). R values for the MEC, BOMEC, and the two intermediate GF class levels (15 and 25 class) were all less than 0.4 but the survey strata developed for the research trawl time-series yielded the third highest value, at 0.498.

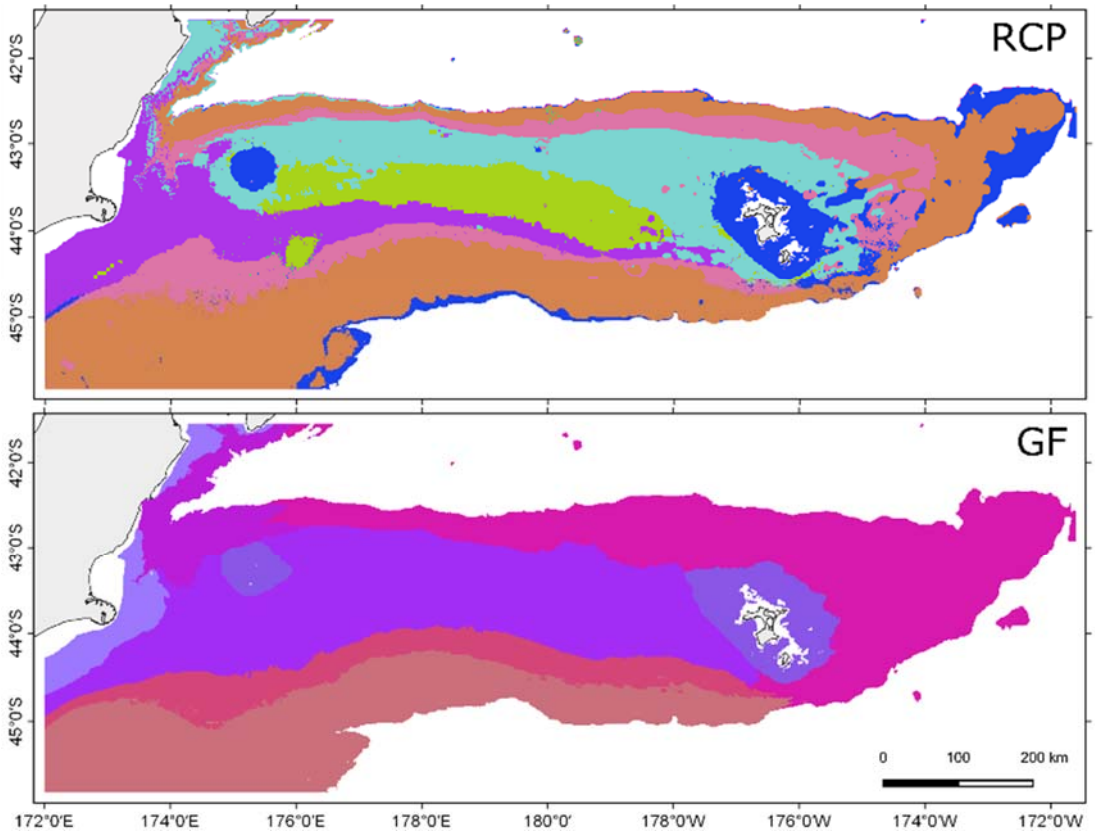

Figure 34. Comparison of RCP and GF classifications at 7-class level

Table 5. ANOSIM: results of analyses quantifying how well each classification separates the underlying fauna sample data into distinct groups. The R statistic ranges from 1, where all groups are distinct from each other, to 0, where there is no group structure. The table shows the classification name (see text for details), the total class-level (class-levels for MEC and BOMEC were selected to yield approximately 50 classes across the Chatham Rise study area), the number of classes useable in the analyses (classes containing at least three data points), and the ANOSIM Global R statistic. All analyses were significant at p<0.01.

Classification	Class-level	Classes used	Global R
GF	50	24	0.542
RCP	7	7	0.524
Trawl strata	36	33	0.498
GF	7	6	0.412
MEC	70	15	0.397
BOMEC	70	8	0.382
GF	15	10	0.375
GF	25	15	0.353

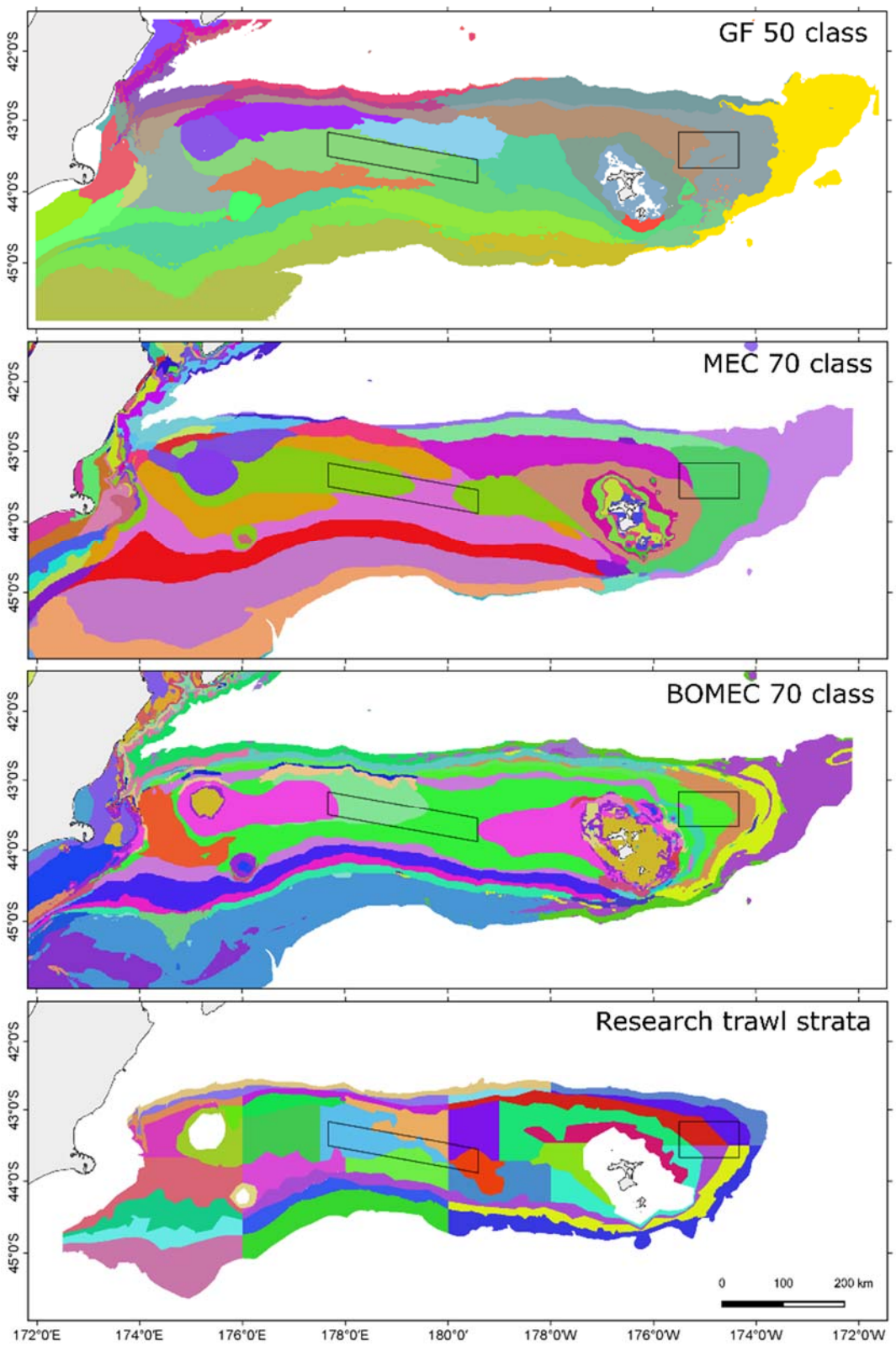

Figure 35: Environmental classifications for Chatham Rise: GF benthic classification developed in this study (GF 50-class): the New Zealand Marine Environment Classification (MEC) at 70-class level; the Benthic Optimised MEC (BOMEC) at 70-class level, and the survey strata used for routine research trawl surveys of Chatham Rise (2016 iteration). Colours are arbitrary, intended to clarify distinctions between classes, and are not comparable between panels. Black polygons show the two Benthic Protection Areas (BPAs) on Chatham Rise.

3.4 Assessing research trawl survey catch records as test-data

Validation of predictive models requires independent sample data and for quantitative, abundance-based models, the independent data also need to be abundance, rather than presence-absence (Anderson et al. 2019). For Chatham Rise, the research trawl survey time series (O'Driscoll et al. 2011) is an obvious candidate data set for testing predictions from models developed here. However, while many of the benthic invertebrate taxa in our study are frequently reported from research trawl catches, catchability of benthic taxa is unquantified and their abundance in catches is not recorded consistently, resulting in only a limited amount of relative abundance data available for comparison with model predictions. There is also an element of circularity in the use of these data to assess models developed from benthic survey data: the new, image-based, models were developed because of concerns about the level of uncertainty associated with earlier models based on physical catch records, so using data that went into the older models to assess the new ones is less than ideal.

The number of records in the trawl time series with abundance values ranged from 10 or less for *Goniocorella dumosa* and Coral Reef to over 100 for Asteroidea and *Metanephrops challengeri* (Table 6). Given the issues with catchability and inconsistency of abundance data, analysis here was limited to simple counts, rather than standardised densities per unit area, and to the single-taxon ensemble model outputs only. Correlations between ensemble model predictions of abundance and specimen counts recorded in the research *trawl* database were highly variable, ranging from -0.20 for Cidaroida to 0.80 for Demospongiae. Most comparisons showed a moderately positive correlation, however, with values below 0.20 for only 4 taxa, and correlations of about 0.5 or higher for 5 taxa.

Table 6: Calculated correlation (Spearman's rank-order correlation) between predicted abundance (numbers/1000 m^2) from ensemble models and numbers caught in research trawls at the same location (within the same grid cell).

		Trawl
Taxon	Correlation	Records
Goniocorella dumosa	0.36	8
Coral Reef	0.12	10
Pennatulacea	0.37	26
Demospongiae	0.80	13
Hexactinellida	0.39	12
Xenophyophoroidea		–
Brachiopoda		–
Bryozoa		–
Hydrozoa		–
Stylasteridae		–
Metanephrops challengeri	0.49	101
Hyalinoecia sp.	0.47	17
Euechinoidea	0.78	38
Spatangoida	0.13	27
Buccinidae		–
Volutidae		–
Paguridae	0.35	50
Cidaroidea	-0.20	31
Holothuroidea	0.47	91
Asteroidea	0.18	151

4. DISCUSSION

In this project (ZBD201611), we have advanced knowledge of benthic faunal distributions across Chatham Rise by: greatly expanding the seabed area surveyed using dedicated photographic surveys (Objective 1, Bowden et al. 2017); developing a spatially extensive and internally consistent quantitative dataset of benthic faunal distributions combining data from five previously disparate surveys (Objective 2, Bowden et al. 2019); and here generating new spatial predictions of habitat suitability for a wide range of individual benthic taxa and overall benthic taxon turnover, and developing new seabed faunal-habitat classification maps specific to Chatham Rise (Objective 4). Although formal validation of the distribution probabilities and spatial classifications generated here would require dedicated field sampling, which is beyond the scope of this project, internal model performance metrics, correspondence with research trawl bycatch data, and intuitive evaluation of predicted patterns and classes against the input dataset suggest that the outputs generated here are likely to be more reliable, and more consistent among taxa, than are those from earlier modelling initiatives (see Anderson et al. 2019).

The key high-level aim of the project was to reduce uncertainty in predictions of benthic distributions across Chatham Rise. To achieve this aim, we first used only data generated by consistent, auditable, photographic methods, rather than downloads from existing trawl bycatch or museum databases. While there are substantial quantities of potentially useful data available in such databases, their use in broad-scale biodiversity initiatives such as this can be problematic because there are intractable problems associated with inconsistencies in taxonomic identification level, sampling methods, spatial bias in the sampling locations, and the fact that only abundance is recorded (see e.g., Elith & Leathwick 2007, O'Driscoll et al. 2011). By using only photographic seabed surveys, by contrast, we were able to run spot audits of questionable identifications or counts in existing analysis data, and to quantify sampled seabed area, by direct reference to the original imagery. While there are almost certainly residual inconsistencies or biases in the final dataset, particularly due to the merging of abundance estimates generated from still images with those from video because of differences in the size of the sampling 'units' (Andrew & Mapstone 1987), these will be minor in comparison with existing data from bycatch and museum sources.

We also used techniques that enabled us to minimise the influence of biases associated with any one modelling method for single-taxon models. By using hurdle models, we minimised the potential for artefacts arising from zero-inflated, over-dispersed data, and by using two independent methods to model each taxon and combining their outputs in ensemble models, we ensured more conservative predictions and more robust characterisation of uncertainty. Furthermore, while all previous models predicting single-taxon distributions across Chatham Rise have been based on presence-absence or presence-background data, here we were able to use quantitative population density data, enabling more nuanced predictions. Spatial community classifications derived from habitat-suitability methods are more problematic to assess objectively but by using two entirely different contemporary approaches in parallel, we are at least able to comment on their similarities, and to demonstrate that while such classifications are necessarily simplifications of actual patterns, they may be useful as input to spatial planning initiatives.

It is difficult to quantitatively assess believability in single-taxon models without appropriate independent test data. The dataset used to build the current models was an ideal independent test set for assessing existing published models (Anderson et al. 2019) but available museum records and trawl survey bycatch records are less useful for testing the new models because their abundance information is inadequate and the catchability of benthic taxa by trawls is unquantified. The generally good agreement of the new model predictions with trawl survey data is encouraging, but for most taxa there were insufficient records with count data available to be able to derive meaningful results. Conventional, internally-generated, metrics of model performance are also not reliable for comparisons with existing models because model performance statistics are not calculated in a consistent manner across studies. There are also questions regarding the value of the commonly-used AUC statistic for comparing model performance between studies. In our study, AUC values were relatively low for many of the presence-absence models produced but this statistic has been shown to be inflated both by use of arbitrary background data to represent absences, rather than true absence data as used here, and by modelling larger spatial extents that encompass high proportions of clearly unsuitable habitat (Vierod et al. 2014). Thus, while two of the major steps taken to refine models here - the use of quantitative data with true absences and focussing at smaller spatial scales - are intuitively

logical ways to improve understanding of distributions, the resulting improvements may not be represented fully by simple, internally-referencing criteria such as AUC. Despite this, some general, qualitative comparisons can be made with the models presented here.

In their assessment of existing predictive distribution models on Chatham Rise using the faunal data set described here as independent test data, Anderson et al. (2019) identified the models of Compton et al. (2013) as the most reliable, which is perhaps unsurprising because these models were developed specifically for the Chatham Rise-Challenger Plateau region using photographic and physical sample data from voyage TAN0705. Compton et al. (2013) produced models for a range of benthic taxa, including scampi, *Hyalinoecia* sp., Paguridae, Spatangoida, and Volutidae, that can be compared directly with our results to illustrate how the additional data and refinements in method employed here change our perception of distribution probabilities. For instance: predictions of suitable habitat for scampi now extend further to the east on the shallow crest of the Rise; for Volutidae, a strong preference for suitable habitat to be on the south flank of the Rise is not as evident in the new model; for burrowing urchins (Spatangoida), predicted distribution is now strongly focussed on the shallow central and eastern areas of the Rise (an area that was largely unsampled by TAN0705 but targeted in CRP2012, TAN1306, and TAN1701 surveys); for hermit crabs (Paguridae) incorporation of abundance data here had a strong influence, with much higher suitability of habitat predicted in middle depths on the southern flank of the Rise, and for quill worms (*Hyalinoecia* sp.) high suitability on a large section of the shallow central crest of the Rise in the earlier model is no longer supported.

Coral taxa are of particular interest for issues associated with the conservation and management of sensitive marine habitats, with *Goniocorella dumosa* being of particular interest in relation to crestal areas of Chatham Rise (EPA 2015, Rowden et al. 2014), and other thicket-forming stony corals, including *Solenosmilia variabilis, Enallopsammia rostrata*, and *Madrepora oculata*, in relation to the effects of trawl fisheries on seamounts in the region (Clark et al. 2016, Clark et al. 2019, Williams et al. 2010). Habitat suitability models for *G. dumosa* tend to be broadly similar across existing studies (Anderson et al. 2016, Anderson et al. 2015, Anderson et al. 2014, Georgian et al. 2019) in that they show highest probabilities of suitable habitat across central crestal areas of the Rise extending from Mernoo Bank in the west, to the Chatham Islands in the east. Our predictions indicate a more constrained distribution, with well-defined areas of high probability occurring patchily from the area between Mernoo and Veryan Banks in the west, to the Andes seamounts in the east (Figure 4).

An apparent anomaly in predictions of *G. dumosa* habitat occurs in a fine-scale model of the central crest area of the Rise produced by Rowden et al. (2014), which predicted that an area of high habitat-suitability north of the western end of the mid-Chatham Rise BPA, centred between 178° E and 179° E at approximately 43° S. This prediction is not well-supported by other existing models but in our ensemble model here there is a band of relatively high predicted occurrence that corresponds closely with that in the Rowden et al. (2014) model, albeit with much lower strength of prediction (Figure 4). Examination of the environmental predictor layers used suggests that this prediction is driven primarily by correlation between *G. dumosa* presence sites and areas where there are steep gradients in the sea-surface temperature layer (*sstgrad,* an indicator of oceanic frontal features). Rowden et al. (2014) used camera data from three of the five surveys used for the current models (TAN0705, CRP2012, and TAN1306), and a similar set of environmental layers, so similarity with our model is to be expected, but it is likely that the restricted spatial extent of the model domain used by Rowden et al. (2014), with consequently smaller ranges for environmental gradients and numbers of sampled sites, will have contributed to exaggerating predictions in this area. It is also of note here that *G. dumosa* was not recorded at any sites in the combined dataset used here that fall within the band of higher predicted habitat suitability identified in the Rowden et al. (2014) model and here.

For thicket-forming stony corals, a category that combines *S. variabilis*, *E. rostrata*, *M. oculata*, and *G. dumosa*, spatial predictions tend to be dominated by *G. dumosa* records. This situation is because occurrence of the other three taxa is highly concentrated on a relatively few seamount features (predominantly the Graveyard and Andes hills) and thus yield few presence sites, with consequently low influence in correlative models. When compared with existing models, our predictions for the occurrence of thicket-forming corals show distributions that are similar to those of Baird et al. (2013) and Anderson et

al. (2015) but, as with the *G. dumosa* model, areas of high predicted occurrence are more spatially constrained, particularly along the northeastern and southern flanks of the Rise. Given the relatively small number of presence records for thicket forming corals other than *G. dumosa* here, it would be interesting to see if predictions of coral presence would expand if faunal data were available from more seamount sites. In addition to features in the Graveyard and Andes complexes, our current image-based dataset includes sites on 'Smith City' seamount at the northeastern extremity of the Rise and a number of smaller features on the southeastern flanks. However, hill features on the southwestern flanks, where our models also indicate relatively high probability of occurrence, have not been sampled using dedicated benthic gear and might serve as useful model validation sites in future surveys.

Anderson et al. (2016) and Georgian et al. (2019) also produced habitat suitability models for four other taxa modelled here: Stylasteridae; Hexactinellida; Demospongiae, and Pennatulacea, using a similar approach but covering different spatial extents and not incorporating density data. Models for Stylasteridae agree with ours, showing highest habitat suitability on the southeastern flank of the Rise, encompassing the Andes seamounts. The agreement between these models is interesting because these earlier studies did not have access to data from the 2015 photographic survey of the Andes (TAN1503), which recorded very high densities of stylasterid corals on some features, yet still predicted correctly to the area. Models for the broad taxonomic grouping Demospongiae also match moderately well with our predictions, but our model for Pennatulacea (seapens) differs strongly, with much higher densities predicted along the northern flanks than the southern. This contrast in predicted occurrences highlights the value of being able to include reliable population density data in models. Seapens occur in a high proportion of seabed transects all over the Rise but the pattern of higher densities along the northern flank that is clear in seabed imagery and is captured by the abundance models here, is not evident in presence-absence models of occurrence probability.

This study was not designed to assess the influence of trawl disturbance on benthic communities and incorporation of the full range of seabed habitats in the study area complicates any attempts to draw conclusions from the model outputs because seabed type is confounded with trawl effort. However, correlations between trawl disturbance and faunal distributions here align with findings from previous studies in New Zealand (Bowden & Leduc 2017, Lundquist et al. 2018) and other parts of the world (Clark et al. 2016, Collie et al. 2000, de Juan et al. 2007, Kenchington et al. 2007) into the effects of disturbance from bottom trawling on different functional groups of the benthos. Abundances of small mobile predators and scavengers, primarily whelks (Buccinidae and Volutidae), hermit crabs (Paguridae), and quill worms (*Hyalinoecia* sp.) were highest in areas greater trawl disturbance, whereas emergent sessile filter and suspension-feeding taxa, including sponges (Demospongiae and Hexactinellidae) and corals (*G. dumosa* and the REEF grouping) were at lower abundances or absent in the most trawled areas. Given these patterns, the data set assembled under the present project, and model predictions developed from it here, might usefully be used in a more focussed study to extend the single-habitat analyses of Bowden & Leduc (2017) into the effects of trawl disturbance.

In contrast to the two single-taxon modelling methods used here (BRT and RF), which both yielded similar results, the two community modelling approaches, RCP and GF, yielded somewhat different spatial classifications. While RCP is considered to be the more statistically rigorous method of the two, the small number of RCPs or classes indicated (seven) and some aspects of their spatial boundaries (fragmentation of classes and the bimodal depth distribution of RCP2) raise questions about the utility of the resulting classification by comparison with the various class-level outputs that can be produced from the GF model. The RCP classification does, however, capture some aspects of benthic community distributions across the Rise that are apparent from the underlying data and the single-taxon models. RCP1, in particular, matches with the modelled distributions of quill worms (*Hyalinoecia* sp.), whelks (Buccinidae), and hermit crabs (Paguridae). When compared to the GF classification at the same class-level (Figure 34), there are obvious differences in the spatial distribution of classes, with the GF classification showing stronger differentiation between northern and southern flanks of the Rise at depth but capturing none of the variability on the crest and western flanks that is evident in the single-taxon models and the RCP classification. At the 50-class level, by contrast, the GF model of taxon turnover summarises many of the major spatial changes in faunal composition apparent in the underlying faunal dataset and the single-taxon models. This 50-level class

output shows clear differentiation between the west and east sectors and the north and south flanks of the rise, with finer-scale differentiation primarily representing changes in depth. Whether the trawl intensity variable was included or not in this model, two areas associated with high trawl intensity are delineated in the classification: on the northwest flank east of Mernoo Bank in approximately 400–800 m depth, and on the southwest flank north and east of Veryan Bank in the same depth range.

The difference in outputs between RCP and GF in our study might be related to the state of development of each method and the level of experience we have with each. GF has been used in several New Zealand studies to date, and methods for classifying and interpreting the output data have been refined, primarily by John Leathwick and colleagues, since their early use for the original MEC. RCP, by contrast, is less well-understood and in recent communications with the author of RCP (Scott Foster at CSIRO) about our results it became clear that the RCP code currently available is still in development and that use of the BIC criterion for selection of the optimal class level is not necessarily the most effective or useful way of interpreting the model results for management applications. Given this, it might be instructive in future to use the model probabilities from the RCP analysis to generate output classifications over a much wider range of class-levels than was attempted here and, thus, be able to compare directly with GF outputs at higher class-levels.

The issue of how to assess classifications objectively, whether in terms of deciding between classification types, or selecting an optimal class-level of a given model, is highlighted by the apparently contradictory results of the Mantel tests and ANOSIM R analyses, here. For the GF classification, RELATE tests indicated that correlation strength between the transformed environmental variables and the faunal distributions was strongest at the 15 to 25 class level, suggesting that this level of detail may be more appropriate than the 50-class, whereas ANOSIM R values were highest for the 50-class interpretation, suggesting that the faunal data are better predicted at this level. While the indication of lower class-level for the GF is more in line with the 7-class indication from the RCP analysis, the ANOSIM approach is, arguably, the more useful of the two evaluation methods here: firstly because it provides a direct measure of how effectively a classification partitions the underlying faunal data that we are interested in and, secondly, it can be used to compare among classifications rather than just among class-levels of a single classification. This is because it does not reference the transformed variables generated by the modelling process and thus can be applied to any classification.

The ANOSIM analysis indicated that the 50-class GF classification and the RCP 7-class classification developed here are the most useful summaries of benthic distributions across Chatham Rise (highest Global R value), both classifications scoring considerably higher than the MEC and BOMEC. It is particularly interesting that the RCP scored this highly, given the relatively low class-level, the reduced number of environmental variables used, and the relative lack of development of the method, suggesting that this approach is worthy of further investigation. Gauged only against the MEC and BOMEC, the higher scoring of the GF and RCP models might be attributed to their being tested here against the data that was used to build them. The performance of the trawl survey strata renders this unlikely, however, because this schema was developed from entirely independent trawl catch records yet still scored substantially more highly than did the two older classifications.

Indeed, similarities of pattern between the new classifications informed by benthic imagery and the research trawl survey strata (if allowance is made for the hard meridional boundaries of the trawl strata) adds confidence to the new predictions because it demonstrates convergence on common ecological boundaries via two completely independent data sets, both based on knowledge of the ecosystem accumulated over many years. Similarly, while it scored less highly in tests against the image data, the original MEC, when viewed at class-levels appropriate to the region of interest, can be seen to be a useful summary of the spatial distribution of seabed habitats and fauna. This observation is encouraging for future initiatives based on these modelling approaches because the MEC was developed using remarkably little benthic faunal data, and at the spatial scale of the entire New Zealand EEZ rather than a single, well-sampled, target region as here. Overall, the broad similarity amongst classification schemes developed under initiatives over recent years suggests that we are converging on a more convincing description of benthic faunal distributions on Chatham Rise, which might be used with greater confidence to address questions associated with spatial management of seabed habitats and resources.

Future directions

Although the models developed here are the best-informed and thus likely to be the most reliable representations of benthic faunal distributions across Chatham Rise to date, there are clearly areas in which improvements might be made in future. The accuracy, consistency, and spatial resolution of environmental predictor layers are the most obvious areas in which such improvements might be made. Perhaps the most pressing of these in relation to mapping seabed habitats and fauna is the lack of consistent fine-scale information about the physical composition and topography of the seabed. Distributions of benthic fauna are highly patchy at scales from centimetres to kilometres and much of this patchiness is driven by availability of habitat at fine spatial scales, whether it be soft sediments for mobile burrowing and deposit feeding taxa or hard substrata for sessile fauna, including the corals, sponges, and other habitat-forming fauna that are commonly associated with sensitive seabed habitats.

The faunal occurrence data derived from seabed video and still imagery here was recorded natively at scales of less than 1 m, potentially enabling characterisation of patch structure at very fine spatial scales. For models at the scale of Chatham Rise, however, we are constrained to working at a grid size of 1 × 1 km because environmental variables, including seabed topography metrics, are not yet available at finer resolution. Multibeam echosounder (MBES) data can resolve seabed topography at scales of 25 × 25 m but the resolution varies with depth, and survey coverage for most regions of the New Zealand Exclusive Economic Zone (EEZ), including Chatham Rise, is patchy and incomplete. Similarly, while sediment core samples can provide fine-scale information on sediment composition, they result in point-sampled data with incomplete spatial coverage, strong bias towards soft-sediment seabed (because corers do not work on hard substrata), and highly skewed distributions (e.g., Bostock et al. 2019, Jenkins 2010). Thus, such data have inherently the same properties as the faunal datasets we are trying to predict from and are only coerced into continuous gridded data layers by spatial interpolation, which introduces artefacts and unquantified uncertainties. As such, these substrate data layers are, at best, not yet informative enough to be useful for inclusion in predictive models of benthic faunal distributions (e.g., Anderson et al. 2016). Oceanographic variables are derived either from algorithms applied to satellite image data, or from bio-physical circulation models, or combinations of these. With on-going refinements of satellite imaging technology and understanding of oceanographic processes, it is likely that the spatial resolution and accuracy of such predictor layers will continue to increase, and this is perhaps the most likely short-term route by which models such as those developed here will be improved.

Another aspect of these analyses that may have an influence on the reliability of the resulting predictions is the implicit assumption that the distributions of benthic fauna do not change appreciably over time. This assumption is introduced because, to generate sufficient density of data to enable effective predictions, we have merged data from surveys that collectively span a decade. While this assumption is unlikely to be wholly true at smaller scales and for more ephemeral taxa, there is some evidence to support it for sessile and common motile fauna. Such evidence includes the similarity between the outputs of habitat suitability models built by different studies using disparate data sources, as detailed above and, within the dataset developed here, from strong community similarity between neighbouring sites that were sampled independently on two or more of the surveys but separated by up to 10 years (site similarity cluster data, not shown here). For the Graveyard seamounts, Clark et al. (2019) use data from repeat photographic surveys to demonstrate that there has been no quantifiable shift in benthic community structure over a period of 15 years.

The essence of the correlative modelling techniques used here is to be able to predict distributions into unsampled space reliably. Thus, while a near-perfect 'model' of seabed distributions within a restricted area might be generated by exhaustive sampling of the target area, the real value of these methods lies in being able to predict distributions in un-surveyed areas with some level of confidence. An obvious next stage for exploring the potential of the models developed here will be to predict to neighbouring seabed regions; most obviously Challenger Plateau and Campbell Plateau but potentially to the entire New Zealand EEZ. Such expansion of the modelled predictions would depend on the availability of the same environmental predictor layers at appropriate resolution and would come with the caveat that predictions into regions where environmental conditions are outside of the range sampled on the Rise are likely to be less reliable. In addition, for modelled taxa that represent multiple species (e.g., Asteroidea and Holothuroidea) the reliability of predictions may be affected by changes in taxonomic composition of these

groups with increasing distance away from Chatham Rise. Models developed using data from Chatham Rise may have potential to yield useful predictions more broadly across New Zealand regional seas, however, because the Rise coincides with, and partially constrains, the intersection between the two major oceanic realms that influence New Zealand's seabed: Sub-Tropical and Sub-Antarctic (Nodder et al. 2012). This situation means that our models encompass a broader range of environmental conditions than would have been the case with similar models based on other areas of the EEZ. The range of environments and associated fauna is evident in model results here, which show distinct differences between faunal distributions on the northern and southern slopes of the Rise, with the documented change from warmer sub-tropical waters to cooler sub-Antarctic waters (Chiswell 2002, McKnight & Probert 1997, Nodder et al. 2003), and from west to east with gradients of decreasing primary production (Nodder et al. 2007).

Conclusions

In conclusion, through this project (ZBD201611) we have advanced knowledge of the seabed distributions of invertebrate fauna on Chatham Rise by developing a new dataset of photographic survey data and then using a variety of contemporary modelling methods to develop new predictions of how individual taxa and overall community composition vary spatially across the Rise. These predictions are the best-informed representations of seabed distributions in the New Zealand region at these scales and provide a resource that will have applications in marine environmental management and ecosystem research. Potential applications include quantification of benthic impacts from bottom-contact fishing gear and other anthropogenic agencies, informing spatial management of biodiversity through the design of marine protected areas, and informing research into ecosystem linkages between water-column and seabed processes. A further obvious application will be to use the modelled relationships with environmental gradients developed here to predict distributions beyond Chatham Rise. However, although these are currently the best available representations of seabed distributions, like all model outputs they have limitations and will inevitably incorporate some degree of inaccuracy. Thus, as new sample data and improved predictor variable layers become available, it will be important to review the process undertaken in this project; using new sample data, potentially from other parts of the EEZ, to test the validity of the most recent predictions, then refining the models by incorporating the new data.

5. Acknowledgments

This study was commissioned and funded by the New Zealand Ministry for Primary Industries (MPI, project ZBD2016-11), with additional support during post-voyage objectives through the NIWA core-funded programme *Ecosystem Structure and Function* (COES1801). We thank Mary Livingston for project governance and review of the draft report at Fisheries New Zealand, Wendy Nelson for internal review of the draft report at NIWA, and all at NIWA and NIWA Vessels who contributed to earlier stages of the project.

6. REFERENCES

Agnew, D.; Jones, C.; Lockhart, S.J.; Martin-Smith, K.; O'Brian, P.; Parker, S.J.; Ramm, D.; Reid, K.; Rogers, A.D.; Sharp, B.; Watters, G.M. (2009). Report of the workshop on vulnerable marine ecosystems - La Jolla, CA, USA, 3 to 7 August 2009. 17 p.

Anderson, O.F.; Bowden, D.A.; Rowden, A.A.; Clark, M.R. (2019). Quantifying benthic biodiversity: assessing the utility of existing models of benthic fauna distributions on Chatham Rise. *No. 3249*. 34 p.

Anderson, O.F.; Guinotte, J.M.; Rowden, A.A.; Tracey, D.M.; Mackay, K.A.; Clark, M.R. (2016). Habitat suitability models for predicting the occurrence of vulnerable marine ecosystems in the seas around New Zealand. *Deep-Sea Research Part I-Oceanographic Research Papers 115*: 265–292. <http://dx.doi.org/10.1016/j.dsr.2016.07.006>

Anderson, O.F.; Mikaloff Fletcher, S.E.; Bostock, H.C. (2015). Development of models for predicting future distributinos of protected coral species in the the New Zealand region. NIWA Client Report to Department of Conservation No. WLG2015-65. 28 p.

Anderson, O.F.; Tracey, D.M.; Bostock, H.C.; Williams, M.; Clark, M.R. (2014). Refined habitat suitability modelling for protected coral species in the New Zealand EEZ. National Institute of Water and Atmsopheric Research, Report No. WLG2014-69. 46 p.

Andrew, N.L.; Mapstone, B.D. (1987). Sampling and the description of spatial pattern in marine ecology. *Oceanography and Marine Biology 25*: 39–90.

Araujo, M.B.; Guisan, A. (2006). Five (or so) challenges for species distribution modelling. *Journal of Biogeography 33(10)*: 1677–1688. <http://dx.doi.org/10.1111/j.1365-2699.2006.01584.x>

Baird, S.; Tracey, D.M.; Mormede, S.; Clark, M. (2013). The distribution of protected corals in New Zealand waters. NIWA Client Report WLG2012-43 to the Department of Conservation. 96 p.

Baird, S.J.; Wood, B.A. (2018). Extent of bottom contact by New Zealand commercial trawl fishing for deepwater Tier 1 and Tier 2 target fishstocks, 1989–90 to 2015–16. *New Zealand Aquatic Environment and Biodiversity Report 193*.

Baird, S.J.; Wood, B.A.; Bagley, N.W. (2011). Nature and extent of commercial fishing effort on or near the seafloor within the New Zealand 200 n. mile Exclusive Economic Zone, 1989–90 to 2004–05. *New Zealand Aquatic Environment and Biodiversity Report No. 73*. 143 p.

Black, J.; Tilney, R. (2015). Monitoring New Zealand's trawl footprint for deepwater fisheries: 1989–90 to 2010–11. *New Zealand Aquatic Environment and Biodiversity Report No. 176.* 60 p.

Black, J.; Wood, R.; Berthelsen, T.; Tilney, R. (2013). Monitoring New Zealand's trawl footprint for deepwater fisheries: 1989–90 to 2009–10. *New Zealand Aquatic Environment and Biodiversity Report No. 110*.

Bostock, H.C.; Jenkins, C.; Mackay, K.; Carter, L.; Nodder, S.; Orpin, A.; Pallentin, A.; Wysoczanski, R. (2019). Distribution of surficial sediments in the ocean around New Zealand/Aotearoa. Part A: continental slope and deep ocean. *New Zealand Journal of Geology and Geophysics 62(1)*: 1–23.

Bostock, H.C.; Mikaloff Fletcher, S.E.; Williams, J.M. (2013). Estimating carbonate parameters from hydrographic data for the intermediate and deep waters of the Southern Hemisphere oceans. Biogeosciences 10: 6199-6213.

Bowden, D.A.; Clark, M.R.; Hewitt, J.; Rowden, A.; Leduc, D.; Baird, S. (2015). Designing a programme to monitor trends in deep-water benthic communities. *New Zealand Aquatic Environment and Biodiversity Report No. 143*. 151 p.

Bowden, D.A.; Davey, N.; Fenwick, M.; George, S.; Macpherson, D.; Ray, C.; Stewart, R.; Christensen-Field, C.; Gibson, K. (2017). Quantifying Benthic Biodiversity: A factual voyage report from RV *Tangaroa* voyage TAN1701 to Chatham Rise, 4 January - 2 February 2017. *New Zealand Aquatic Environment and Biodiversity Report No. 185*. 194 p.

Bowden, D.A.; Leduc, D. (2017). Ocean Survey 20/20, Chatham Rise Benthos: effects of seabed trawling on benthic communities. *New Zealand Aquatic Environment and Biodiversity Report No. 183*. 67 p.

Bowden, D.A.; Rowden, A.A.; Anderson, O.F.; Clark, M.R.; Hart, A.; Davey, N.; Carter, M.; Chin, C. (2019). Quantifying Benthic Biodiversity: developing a dataset of benthic invertebrate faunal distributions from seabed photographic surveys of Chatham Rise. *New Zealand Aquatic Environment and Biodiversity Report No.* 221. 35 p.

Breiman, L. (2001). Random forests. *Machine Learning 45(1)*: 5–32. <http://dx.doi.org/10.1023/a:1010933404324>

Chiswell, S.M. (2001). Eddy energetics in the Subtropical Front over the Chatham Rise, New Zealand. *New Zealand Journal of Marine and Freshwater Research 35(1)*: 1–15.

Chiswell, S.M. (2002). Temperature and salinity mean and variability within the Subtropical Front over the Chatham Rise, New Zealand. *New Zealand Journal of Marine and Freshwater Research 36(2)*: 281–298.

Clark, M.R. (2010). Effects of Trawling on Seamounts. *Oceanography 23(1)*: 132–133.

Clark, M.R.; Althaus, F.; Schlacher, T.A.; Williams, A.; Bowden, D.A.; Rowden, A.A. (2016). The impacts of deep-sea fisheries on benthic communities: a review. *ICES Journal of Marine Science 73*: 51–69. <http://dx.doi.org/10.1093/icesjms/fsv123>

Clark, M.R.; Anderson, O.F.; Francis, R.; Tracey, D.M. (2000). The effects of commercial exploitation on orange roughy (*Hoplostethus atlanticus*) from the continental slope of the Chatham Rise, New Zealand, from 1979 to 1997. *Fisheries Research 45(3)*: 217–238.

Clark, M.R.; Bowden, D.A.; Rowden, A.A.; Stewart, R. (2019). Little Evidence of Benthic Community Resilience to Bottom Trawling on Seamounts After 15 Years. *Frontiers in Marine Science 6(63)*. <http://dx.doi.org/10.3389/fmars.2019.00063>

Clark, M.R.; Dunn, M.R. (2012). Spatial management of deep-sea seamount fisheries: balancing sustainable exploitation and habitat conservation. *Environmental Conservation 39(3)*: 204–214. <http://dx.doi.org/10.1017/s0376892912000021>

Clarke, K.R.; Warwick, R.M. (2001). Change in marine communities: an approach to statistical analysis. 2nd. PRIMER-E Ltd., Plymouth, U.K. 172 p.

Collie, J.S.; Escanero, G.A.; Valentine, P.C. (2000). Photographic evaluation of the impacts of bottom fishing on benthic epifauna. *ICES Journal of Marine Science 57(4)*: 987–1001.

Compton, T.J.; Bowden, D.A.; Pitcher, R.C.; Hewitt, J.E.; Ellis, N. (2013). Biophysical patterns in benthic assemblage composition across contrasting continental margins off New Zealand. *Journal of Biogeography 40(1)*: 75–89. <http://dx.doi.org/10.1111/j.1365-2699.2012.02761.x>

Cragg, J.G. (1971). Some statistical models for limited dependent variables with application to demand for durable goods. *Econometrica 39(5)*: 829–844. <http://dx.doi.org/10.2307/1909582>

Crase, B.; Leidloff, A.; Wintle, B. (2012). A new method for dealing with residual spatial autocorrelation in species distribution models. *Ecography 35*: 879–888. <http://dx.doi.org/10.1111/j.1600-0587.2011.07138.x>

Davies, A.J.; Guinotte, J.M. (2011). Global Habitat Suitability for Framework-Forming Cold-Water Corals. *PLoS ONE 6(4)*. <http://dx.doi.org/e1848310.1371/journal.pone.0018483>

De'ath, G. (2007). Boosted trees for ecological modeling and prediction. *Ecology 88(1)*: 243–251.

de Juan, S.; Thrush, S.F.; Demestre, M. (2007). Functional changes as indicators of trawling disturbance on a benthic community located in a fishing ground (NW Mediterranean Sea). *Marine Ecology-Progress Series 334*: 117–129.

Dormann, C.F.; McPherson, J.M.; Araujo, M.B.; Bivand, R.; Bolliger, J.; Carl, G.; Davies, R.G.; Hirzel, A.; Jetz, W.; Kissling, W.D.; Kuhn, I.; Ohlemuller, R.; Peres-Neto, P.R.; Reineking, B.; Schroder, B.; Schurr, F.M.; Wilson, R. (2007). Methods to account for spatial autocorrelation in the analysis of species distributional data: a review. *Ecography 30(5)*: 609–628. <http://dx.doi.org/10.1111/j.2007.0906-7590.05171.x>

Elith, J.; Leathwick, J. (2007). Predicting species distributions from museum and herbarium records using multiresponse models fitted with multivariate adaptive regression splines. *Diversity and Distributions 13(3)*: 265–275.

Elith, J.; Leathwick, J. (2011). Boosted reression trees for ecological modelling. *r-project.org*. <http://dx.doi.org/http://cran.r-project.org/web/packages/dismo/vignettes/brt.pdf. 22 p>

Elith, J.; Leathwick, J.R.; Hastie, T. (2008). A working guide to boosted regression trees. *Journal of Animal Ecology 77(4)*: 802–813. <http://dx.doi.org/10.1111/j.1365-2656.2008.01390.x>

Elith, J.; Phillips, S.J.; Hastie, T.; Dudík, M.; Chee, Y.E.; Yates, C.J. (2011). A statistical explanation of MaxEnt for ecologists. *Diversity and Distributions 17(1)*: 43–57. <http://dx.doi.org/10.1111/j.1472-4642.2010.00725.x>

Ellis, N.; Smith, S.J.; Pitcher, C.R. (2012). Gradient forests: calculating importance gradients on physical predictors. *Ecology 93(1)*: 156–168. <http://dx.doi.org/10.1890/11-0252.1>

EPA (2015). Decision on marine consent application by Chatham Rock Phosphate Ltd to mine phosphorite nodules on the Chatham Rise. *No. EEZ000006*. 299 p.

Ferrier, S.; Manion, G.; Elith, J.; Richardson, K. (2007). Using generalized dissimilarity modelling to analyse and predict patterns of beta diversity in regional biodiversity assessment. *Diversity and Distributions 13(3)*: 252–264.

Foster, S.D.; Givens, G.H.; Dornan, G.J.; Dunstan, P.K.; Darnell, R. (2013). Modelling biological regions from multi-species and environmental data. *Environmetrics 24(7)*: 489–499. <http://dx.doi.org/10.1002/env.2245>

Foster, S.D.; Hill, N.A.; Lyons, M. (2017). Ecological grouping of survey sites when sampling artefacts are present. *Journal of the Royal Statistical Society Series C-Applied Statistics 66(5)*: 1031–1047. <http://dx.doi.org/10.1111/rssc.12211>

Garcia, H.E.; Locarnini, R.A.; Boyer, T.P.; Antonov, J.I.; Baranova, O.K.; Zweng, M.M.; Reagan, J.R.; Johnson, D.R. (2014a). Volume 3: Dissolved Oxygen, Apparent Oxygen Utilization, and Oxygen Saturation. NOAA Atlas NESDIS 75, World Ocean Atlas 2013. 27 p.

Garcia, H.E.; Locarnini, R.A.; Boyer, T.P.; Antonov, J.I.; Baranova, O.K.; Zweng, M.M.; Reagan, J.R.; Johnson, D.R. (2014b). Volume 4: Dissolved Inorganic Nutrients (phosphate, nitrate, silicate). *World Ocean Atlas 2013*. NOAA Atlas NESDIS 76, 25 p.

Georgian, S.E.; Anderson, O.F.; Rowden, A.A. (2019). Ensemble habitat suitability modeling of vulnerable marine ecosystem indicator taxa to inform deep-sea fisheries management in the South Pacific Ocean. *Fisheries Research 211*: 256–274. <http://dx.doi.org/10.1016/j.fishres.2018.11.020>

Helson, J.; Leslie, S.; Clement, G.; Wells, R.; Wood, R. (2010). Private rights, public benefits: Industry-driven seabed protection. *Marine Policy 34(3)*: 557–566. <http://dx.doi.org/10.1016/j.marpol.2009.11.002>

Hill, P. (2009). Designing a deep-towed camera vehicle using single conductor cable. Sea Technology 50(12): 49-51.

Hill, N.A.; Foster, S.D.; Duhamel, G.; Welsford, D.; Koubbi, P.; Johnson, C.R. (2017). Model-based mapping of assemblages for ecology and conservation management: A case study of demersal fish on the Kerguelen Plateau. *Diversity and Distributions 23(10)*: 1216–1230. <http://dx.doi.org/10.1111/ddi.12613>

Hosmer, D.W.J.; Lemeshow, S.; Sturdivant, R.X. (2013). Applied Logistic Regression, Third Edition. John Wiley and Sons, 528 p.

Jenkins, C.J. (2010). Seafloor Substrates. INSTAAR. University of Colorado. p.

Kaiser, M.J.; Clarke, K.R.; Hinz, H.; Austen, M.C.V.; Somerfield, P.J.; Karakassis, I. (2006). Global analysis of response and recovery of benthic biota to fishing. *Marine Ecology-Progress Series 311*: 1–14.

Kenchington, E.L.; Kenchington, T.J.; Henry, L.A.; Fuller, S.; Gonzalez, P. (2007). Multi-decadal changes in the megabenthos of the Bay of Fundy: The effects of fishing. *Journal of Sea Research 58(3)*: 220–240. <http://dx.doi.org/10.1016/j.seares.2007.04.001>

Leathwick, J.; Rowden, A.; Nodder, S.D.; Gorman, A.R.; Bardsley, S.; Pinkerton, M.; Baird, S.J.; Hadfield, M.; Currie, D.J.; Goh, A. (2012). A Benthic-Optimised Marine Environment Classification (BOMEC) for New Zealand waters. *New Zealand Aquatic Environment and Biodiversity Report No. 88*. 54 p.

Leathwick, J.R.; Elith, J.; Francis, M.P.; Hastie, T.; Taylor, P. (2006). Variation in demersal fish species richness in the oceans surrounding New Zealand: an analysis using boosted regression trees. *Marine Ecology-Progress Series 321*: 267–281.

Lennon, J.J. (2000). Red-shifts and red herrings in geographical ecology. *Ecography 23(1)*: 101–113. <http://dx.doi.org/10.1034/j.1600-0587.2000.230111.x>

Locarnini, R.A.; Mishonov, A.V.; Antonov, J.I.; Boyer, T.P.; Garcia, H.E.; Baranova, O.K.; Zweng, M.M.; Paver, C.R.; Reagan, J.R.; Johnson, D.R.; Hamilton, M.; Seidov, D. (2013). Volume 1: Temperature. *World Ocean Atlas 2013*. NOAA Atlas NESDIS 73. 40 p.

Lundquist, C.J.; Bowden, D.; Cartner, K.; Stephenson, F.; Tuck, I.; Hewitt, J.E. (2018). Assessing Benthic Responses to Fishing Disturbance Over Broad Spatial Scales That Incorporate High Environmental Variation. *Frontiers in Marine Science 5(405)*. <http://dx.doi.org/10.3389/fmars.2018.00405>

MacDiarmid, A.; Bowden, D.; Cummings, V.; Morrison, M.; Jones, E.; Kelly, M.; Neil, H.; Nelson, W.; Rowden, A. (2013). Sensitive Marine Benthic Habitats Defined. NIWA Client Report to the Ministry for Environment No. WLG2013-18. 72 p.

Marchal, P.; Francis, C.; Lallemand, P.; Lehuta, S.; Mahevas, S.; Stokes, K.; Vermard, Y. (2009). Catch-quota balancing in mixed-fisheries: a bio-economic modelling approach applied to the New Zealand hoki (Macruronus novaezelandiae) fishery. *Aquatic Living Resources 22(4)*: 483–498. <http://dx.doi.org/10.1051/alr/2009033>

Martinez-Rincon, R.O.; Ortega-Garcia, S.; Vaca-Rodriguez, J.G. (2012). Comparative performance of generalized additive models and boosted regression trees for statistical modeling of incidental catch of wahoo (*Acanthocybium solandri*) in the Mexican tuna purse-seine fishery. *Ecological Modelling 233*: 20–25. <http://dx.doi.org/10.1016/j.ecolmodel.2012.03.006>

McClatchie, S.; Millar, R.B.; Webster, F.; Lester, P.J.; Hurst, R.; Bagley, N. (1997). Demersal fish community diversity off New Zealand: Is it related to depth, latitude and regional surface phytoplankton? *Deep-Sea Research Part I-Oceanographic Research Papers 44(4)*: 647–667. <http://dx.doi.org/10.1016/s0967-0637(96)00096-9>

McKnight, D.G.; Probert, P.K. (1997). Epibenthic communities on the Chatham Rise, New Zealand. *New Zealand Journal of Marine and Freshwater Research 31(4)*: 505–513. <http://dx.doi.org/10.1080/00288330.1997.9516784>

Nodder, S.D.; Bowden, D.A.; Pallentin, A.; Mackay, K.A. (2012). Seafloor Habitats and Benthos of a Continental Ridge: Chatham Rise, New Zealand. *In*: Harris, P.T. (ed.). Seafloor Geomorphology as Benthic Habitat, pp. 763–776. Elsevier Inc.,

Nodder, S.D.; Duineveld, G.C.A.; Pilditch, C.A.; Sutton, P.J.; Probert, P.K.; Lavaleye, M.S.S.; Witbaard, R.; Chang, F.H.; Hall, J.A.; Richardson, K.M. (2007). Focusing of phytodetritus deposition beneath a deep-ocean front, Chatham Rise, New Zealand. *Limnology and Oceanography 52(1)*: 299–314.

Nodder, S.D.; Pilditch, C.A.; Probert, P.K.; Hall, J.A. (2003). Variability in benthic biomass and activity beneath the subtropical front, Chatham Rise, SW Pacific Ocean. *Deep-Sea Research Part I-Oceanographic Research Papers 50(8)*: 959–985.

O'Driscoll, R.L.; MacGibbon, D.; Fu, D.; Lyon, W.; Stevens, D. (2011). A review of hoki and middle-depths trawl surveys of the Chatham Rise, January 1992-2010. *New Zealand Fisheries Assessment Report 2011/47*. 72 p.

Oppel, S.; Meirinho, A.; Ramirez, I.; Gardner, B.; O'Connell, A.F.; Miller, P.I.; Louzao, M. (2012). Comparison of five modelling techniques to predict the spatial distribution and abundance of seabirds. *Biological Conservation 156*: 94–104. <http://dx.doi.org/10.1016/j.biocon.2011.11.013>

Parker, S.J.; Bowden, D.A. (2010). Identifying taxonomic groups vulnerable to bottom longline fishing gear in the Ross Sea region. *CCAMLR Science 17*: 105–127.

Parker, S.J.; Penney, A.J.; Clark, M.R. (2009). Detection criteria for managing trawl impacts on vulnerable marine ecosystems in high seas fisheries of the South Pacific Ocean. *Marine Ecology-Progress Series 397*: 309–317. <http://dx.doi.org/10.3354/meps08115>

Pitcher, C.R.; Ellis, N.; Smith, S.J. (2011). Example analysis of biodiversity survey data with R package gradientForest. 16 p. Retrieved, from http://gradientforest.r-forge.r-project.org/biodiversity-survey.pdf.

Pitcher, C.R.; Lawton, P.; Ellis, N.; Smith, S.J.; Incze, L.S.; Wei, C.L.; Greenlaw, M.E.; Wolff, N.H.; Sameoto, J.A.; Snelgrove, P.V.R. (2012). Exploring the role of environmental variables in shaping patterns of seabed biodiversity composition in regional-scale ecosystems. *Journal of Applied Ecology 49(3)*: 670-679. <http://dx.doi.org/10.1111/j.1365-2664.2012.02148.x>

Potts, J.M.; Elith, J. (2006). Comparing species abundance models. *Ecological Modelling 199(2)*: 153–163.

R Core Team (2018). R: A language and environment for statistical computing. R Foundation for Statistical Computing, Vienna, Austria.

Reiss, H.; Birchenough, S.; Borja, A.; Buhl-Mortensen, L.; Craeymeersch, J.; Dannheim, J.; Darr, A.; Galparsoro, I.; Gogina, M.; Neumann, H.; Populus, J.; Rengstorf, A.M.; Valle, M.; van Hoey, G.; Zettler, M.L.; Degraer, S. (2015). Benthos distribution modelling and its relevance for marine ecosystem management. *ICES Journal of Marine Science 72(2)*: 297–315. <http://dx.doi.org/10.1093/icesjms/fsu107>

Robert, K.; Jones, D.O.B.; Roberts, J.M.; Huvenne, V.A.I. (2016). Improving predictive mapping of deep-water habitats: Considering multiple model outputs and ensemble techniques. *Deep-Sea Research Part I-Oceanographic Research Papers 113*: 80–89. <http://dx.doi.org/10.1016/j.dsr.2016.04.008>

Robinson, N.M.; Nelson, W.A.; Costello, M.J.; Sutherland, J.E.; Lundquist, C.J. (2017). A Systematic Review of Marine-Based Species Distribution Models (SDMs) with Recommendations for Best Practice. *Frontiers in Marine Science 4*. <http://dx.doi.org/10.3389/fmars.2017.00421>

Rowden, A.; Leduc, D.; Torres, L.; Bowden, D.; Hart, A.; Chin, C.; Davey, N.; Nodder, S.D.; Pallentin, A.; Mackay, K.A.; Northcote, L.; Sturman, J. (2014). Benthic epifauna communities of the central Chatham Rise crest. NIWA Client Report to Chatham Rock Phosphate Ltd. No. WLG2014-9. 116 p.

Rowden, A.; Oliver, M.; Clark, M.R.; Mackay, K. (2008). New Zealand's 'SEAMOUNT' database: recent updates and its potential use for ecological risk assessment. *New Zealand Aquatic Environment and Biodiversity Report 27*.

Rowden, A.A.; Anderson, O.F.; Georgian, S.E.; Bowden, D.A.; Clark, M.R.; Pallentin, A.; Miller, A. (2017). High-Resolution Habitat Suitability Models for the Conservation and Management of Vulnerable Marine Ecosystems on the Louisville Seamount Chain, South Pacific Ocean. *Frontiers in Marine Science 4(335)*. <http://dx.doi.org/10.3389/fmars.2017.00335>

Rowden, A.A.; Leduc, D.; Torres, L.; Bowden, D.A.; et al. (2013). Benthic communities of MPL area 50270 on the Chatham Rise. NIWA Client Report No. WLG2012-25. 103 p.

Snelder, T.H.; Leathwick, J.R.; Dey, K.L.; Rowden, A.A.; Weatherhead, M.A.; Fenwick, G.D.; Francis, M.P.; Gorman, R.M.; Grieve, J.M.; Hadfield, M.G.; Hewitt, J.E.; Richardson, K.M.; Uddstrom, M.J.; Zeldis, J.R. (2007). Development of an ecologic marine classification in the New Zealand region. *Environmental Management 39(1)*: 12–29.

Somerfield, P.J.; Clarke, K.R.; Olsgard, F. (2002). A comparison of the power of categorical and correlational tests applied to community ecology data from gradient studies. *Journal of Animal Ecology 71(4)*: 581–593.

Stephenson, F.; Leathwick, J.R.; Geange, S.W.; Bulmer, R.H.; Hewitt, J.E.; Anderson, O.F.; Rowden, A.A.; Lundquist, C.J. (2018). Using Gradient Forests to summarize patterns in species turnover across large spatial scales and inform conservation planning. *Diversity and Distributions 24(11)*: 1641–1656. <http://dx.doi.org/10.1111/ddi.12787>

Tracey, D.M.; Rowden, A.A.; Mackay, K.A.; Compton, T. (2011). Habitat-forming cold-water corals show affinity for seamounts in the New Zealand region. *Marine Ecology-Progress Series 430*: 1-U59. <http://dx.doi.org/10.3354/meps09164>

Uddstrom, M.J.; Oien, N.A. (1999). On the use of high-resolution satellite data to describe the spatial and temporal variability of sea surface temperatures in the New Zealand region. *Journal of Geophysical Research-Oceans 104(C9)*: 20729–20751. <http://dx.doi.org/10.1029/1999jc900167>

Valle, M.; van Katwijk, M.M.; de Jong, D.J.; Bouma, T.J.; Schipper, A.M.; Chust, G.; Benito, B.M.; Garmendia, J.M.; Borja, A. (2013). Comparing the performance of species distribution models of Zostera marina: Implications for conservation. *Journal of Sea Research 83*: 56–64. <http://dx.doi.org/10.1016/j.seares.2013.03.002>

Vierod, A.D.T.; Guinotte, J.M.; Davies, A.J. (2014). Predicting the distribution of vulnerable marine ecosystems in the deep sea using presence-background models. *Deep-Sea Research Part II - Topical Studies in Oceanography 99*: 6–18. <http://dx.doi.org/10.1016/j.dsr2.2013.06.010>

Williams, A.; Schlacher, T.A.; Rowden, A.A.; Althaus, F.; Clark, M.R.; Bowden, D.A.; Stewart, R.; Bax, N.J.; Consalvey, M.; Kloser, R.J. (2010). Seamount megabenthic assemblages fail to recover from trawling impacts. *Marine Ecology 31*: 183–199. <http://dx.doi.org/10.1111/j.1439-0485.2010.00385.x>

Yesson, C.Y.C.; Clark, M.R.; Taylor, M.L.; Rogers, A.D. (2011). The global distribution of seamounts based on 30 arc seconds bathymetry data. *Deep-Sea Research Part I-Oceanographic Research Papers 58(4)*: 442–453. <http://dx.doi.org/10.1016/j.dsr.2011.02.004>

Yoo, W.; Mayberry, R.; Bae, S.; Singh, K.; Peter He, Q.; Lillard, J.W., Jr. (2014). A Study of Effects of MultiCollinearity in the Multivariable Analysis. *International Journal of Applied Science and Technology 4(5)*: 9–19.

Zweng, M.M.; Reagan, J.R.; Antonov, J.I.; Locarnini, R.A.; Mishonov, A.V.; Boyer, T.P.; Garcia, H.E.; Baranova, O.K.; Johnson, D.R.; Seidov, D.; Biddle, M.M. (2013). World Ocean Atlas 2013. *In*: Levitus, S. (ed.). pp. 39. NOAA Atlas NESDIS 74.

7. APPENDIX 1 – Single-taxon models

Table A-1: Random Forest models for individual taxa. Variable contribution ranks for presence/absence and abundance models. Numbers below each taxon code (see Table 2 for scientific names) indicate the relative rank-importance of the six variables selected for each model. Count = number of models in which the variable is used; Average = the average variable rank, when used. Variables are ordered by Count, then Average.

Presence/absence models

Variable	ASR	BPD	BUCC	CID	COR	COZ	DEM	EUE	GDU	HDR	HEX	HTH	HTU	PAG	PTU	REEF	SCI	SPT	VOL	ZFR	Count	Average
bathy	1	1	–	3	2	–	–	2	2	2	–	1	–	1	1	4	1	2	4	3	15	2.0
tidalcurr	4	2	–	2	3	–	–	4	3	5	2	2	–	4	2	5	2	3	–	2	15	3.0
dynoc	2	–	4	–	5	–	2	–	6	–	6	4	5	–	3	3	5	4	2	6	14	4.1
dissox	3	–	–	6	–	3	–	6	–	4	–	3	–	3	4	–	4	1	3	1	12	3.4
tempres	5	–	1	4	–	6	1	3	–	3	–	6	6	–	5	–	–	6	–	–	11	4.2
cbpm_mean	6	5	3	–	6	5	–	–	4	–	4	5	1	–	–	–	3	–	–	5	11	4.3
salinity	–	4	2	1	–	4	4	1	–	1	–	–	–	–	–	–	6	–	5	4	10	3.2
profcurv	–	6	–	–	1	1	5	–	5	–	1	–	–	–	–	1	–	–	6	–	8	3.3
sstgrad	–	–	–	5	–	–	6	5	–	–	5	–	3	6	–	6	–	5	–	–	8	5.1
trawl	–	3	–	–	4	–	3	–	1	6	–	–	4	–	–	2	–	–	–	–	7	3.3
epp_mean	–	–	6	–	–	–	–	–	–	–	3	–	2	2	6	–	–	–	1	–	6	3.3
epp_min	–	–	5	–	–	2	–	–	–	–	–	–	–	5	–	–	–	–	–	–	3	4.0

Abundance models

Variable	ASR	BPD	BUCC	CID	COR	COZ	DEM	EUE	GDU	HDR	HEX	HTH	HTU	PAG	PTU	REEF	SCI	SPT	VOL	ZFR	Count	Average
dynoc	3	–	–	–	4	2	5	1	5	1	3	4	5	–	–	3	3	2	3	1	15	3.0
profcurv	6	4	–	4	6	6	1	–	3	2	1	1	–	–	–	2	–	–	–	5	12	3.4
bathy	2	5	–	1	–	–	4	2	–	–	–	–	4	3	3	–	6	5	2	–	11	3.4
tempres	4	–	–	5	2	4	–	5	–	–	–	6	–	4	1	–	4	4	–	6	11	4.1
tidalcurr	–	3	–	6	–	–	6	6	4	4	–	5	–	–	5	5	–	6	5	–	11	5.0
salinity	1	–	–	–	–	–	–	3	2	–	–	3	2	2	4	–	1	1	1	–	10	2.0
sstgrad	–	2	3	2	5	–	2	–	1	–	–	2	–	–	2	6	–	–	–	4	10	2.9
dissox	–	–	4	3	3	3	–	–	–	–	5	–	3	5	–	–	2	–	–	3	9	3.4
epp_mean	5	–	2	–	–	5	–	4	6	3	–	–	–	6	–	4	5	–	–	–	9	4.4
cbpm_mean	–	6	5	–	1	–	–	–	–	–	4	–	1	–	–	1	–	–	4	2	8	3.0
trawl	–	–	1	–	–	–	3	–	–	6	2	–	6	1	–	–	–	3	6	–	8	3.5
epp_min	–	1	6	–	–	1	–	–	–	5	6	–	–	–	6	–	–	–	–	–	6	4.2

Table A-2: Boosted Regression Tree models for individual taxa. Variable contribution ranks for presence/absence and abundance models. Numbers below each species code (see Table 2 for the taxa represented) indicate the relative importance of the six variables selected for each model. Count = number of models in which the variable is used; Average = the average variable rank, when used. Variables are ordered by Count, then Average.

Presence/absence models

Variable	ASR	BPD	BUCC	CID	COR	COZ	DEM	EUE	GDU	HDR	HEX	HTH	HTU	PAG	PTU	REEF	SCI	SPT	VOL	ZFR	Count	Average
Bathy	4	1	–	2	2	–	–	5	2	3	–	1	6	1	1	6	1	2	4	3	16	2.8
Tidal-Curr	–	2	5	5	3	4	–	3	4	–	2	3	–	–	2	–	3	6	–	1	13	3.3
Salinity	6	–	4	1	–	3	4	1	–	2	–	–	–	3	5	–	–	–	2	–	10	3.1
Dissox	1	–	–	3	–	5	6	–	–	5	–	2	–	–	4	5	–	1	3	2	11	3.4
CBPM-mean	–	5	2	–	5	6	–	–	–	1	5	–	1	–	–	–	2	–	–	4	9	3.4
EPP-mean	–	6	3	–	–	–	–	6	–	–	3	4	4	2	–	–	6	–	1	–	9	3.9
Tempres	2	–	1	–	–	–	1	2	–	–	–	6	2	–	–	–	–	5	5	–	8	3.0
Prof-curv	–	4	–	6	1	2	3	–	3	–	1	–	–	6	–	2	–	–	6	–	10	3.4
Footprint	–	3	–	–	4	–	2	–	1	4	6	–	3	–	–	1	–	–	–	6	9	3.3
Dynamic-topog	3	–	6	–	–	–	5	–	–	–	–	5	–	–	3	3	–	3	–	5	8	4.1
EPP-min	5	–	–	4	6	1	–	–	6	6	–	–	–	4	–		5	–	–	–	8	4.6
SST-Grad	–	–	–	–	–	–	–	4	5	–	4	–	5	5	6	4	4	4	–	–	9	4.6

Abundance models

Variable	ASR	BPD	BUCC	CID	COR	COZ	DEM	EUE	GDU	HDR	HEX	HTH	HTU	PAG	PTU	REEF	SCI	SPT	VOL	ZFR	Count	Average
Prof-curv	6	1	–	5	1	1	1	–	2	2	1	5	–	6	–	1	4	–	–	5	14	2.9
Footprint	–	6	1	4	6	–	2	–	–	6	3	–	6	4	–	–	5	1	–	1	12	3.8
Bathy	1	–	–	1	–	–	4	2	–	–	–	4	4	1	2	–	–	3	5	–	10	2.7
Tempres	5	–	–	3	2	6	–	4	3	–	–	–	5	3	1	6	6	4	–	–	12	4.0
SST-Grad	–	–	6	2	3	5	3	–	1	–	5	3	–	–	3	–	–	5	–	4	11	3.6
Salinity	–	–	3	–	–	–	–	3	4	–	–	1	2	5	5	–	2	2	–	6	10	3.3
Dynamic-topog	2	–	–	–	5	3	5	1	–	3	4	2	–	–	–	–	–	–	6	–	9	3.4
EPP-min	4	4	4	6	–	2	–	–	6	1	–	–	–	2	6	3	–	–	–	–	10	3.8
Dissox	–	5	5	–	4	–	–	–	–	–	6	–	3	–	–	–	1	–	3	3	8	3.8
EPP-mean	3	–	2	–	–	–	–	5	–	–	2	–	–	–	–	5	3	6	4	–	8	3.8
Tidal-Curr	–	4	–	–	–	4	–	6	5	4	–	6	–	–	4	4	–	–	1	–	9	4.2
CBPM-mean	–	2	–	–	–	–	6	–	–	5	–	–	1	–	–	2	–	–	2	2	7	2.9

8. APPENDIX 2 – Regions of Common Profile

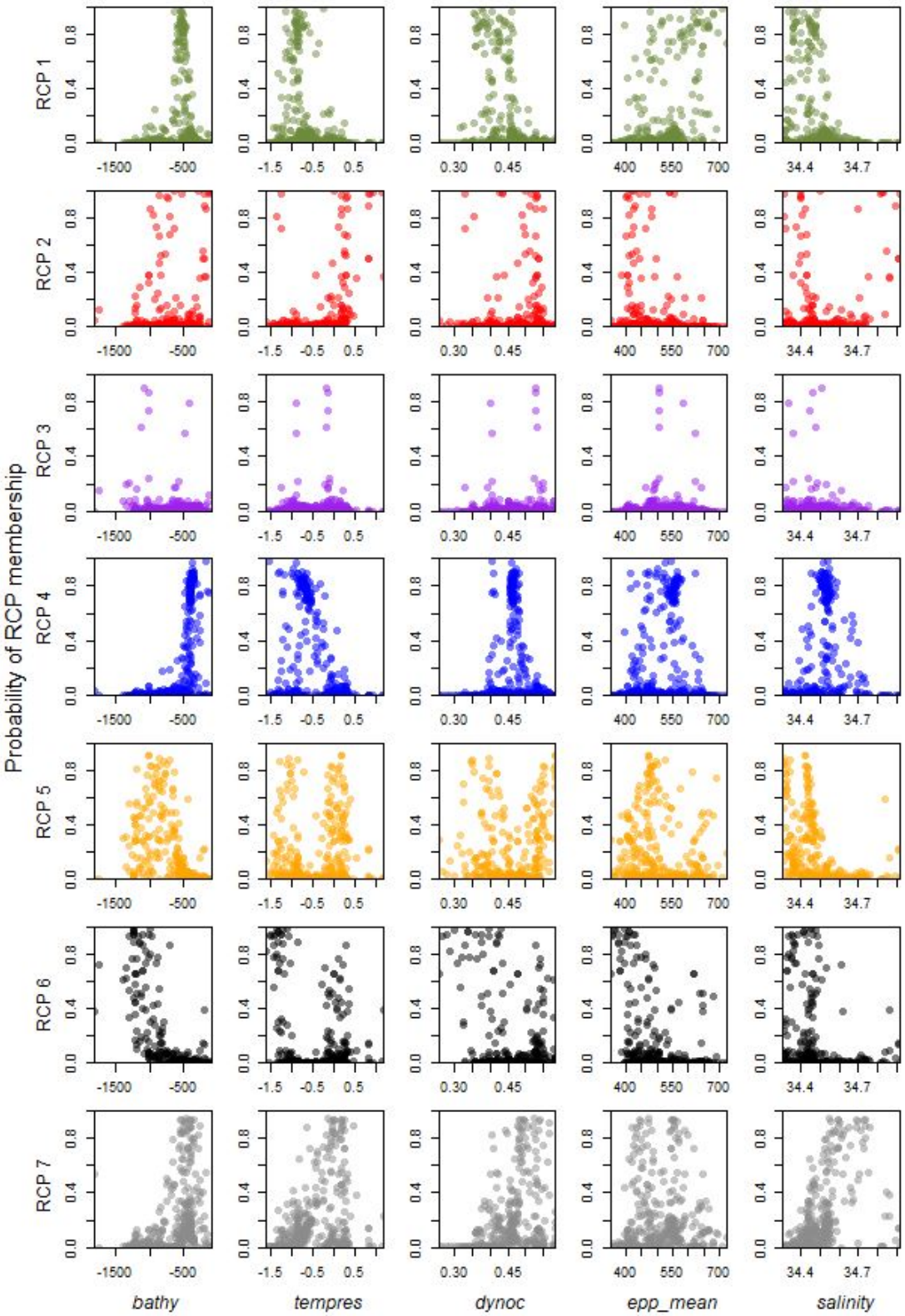

Figure A-1. Response of each RCP to the environmental predictors *bathy*, *tempres*, *dynoc*, *epp_mean*, and *salinity*, based on predicting RCP membership for each site based only on the environmental covariates.

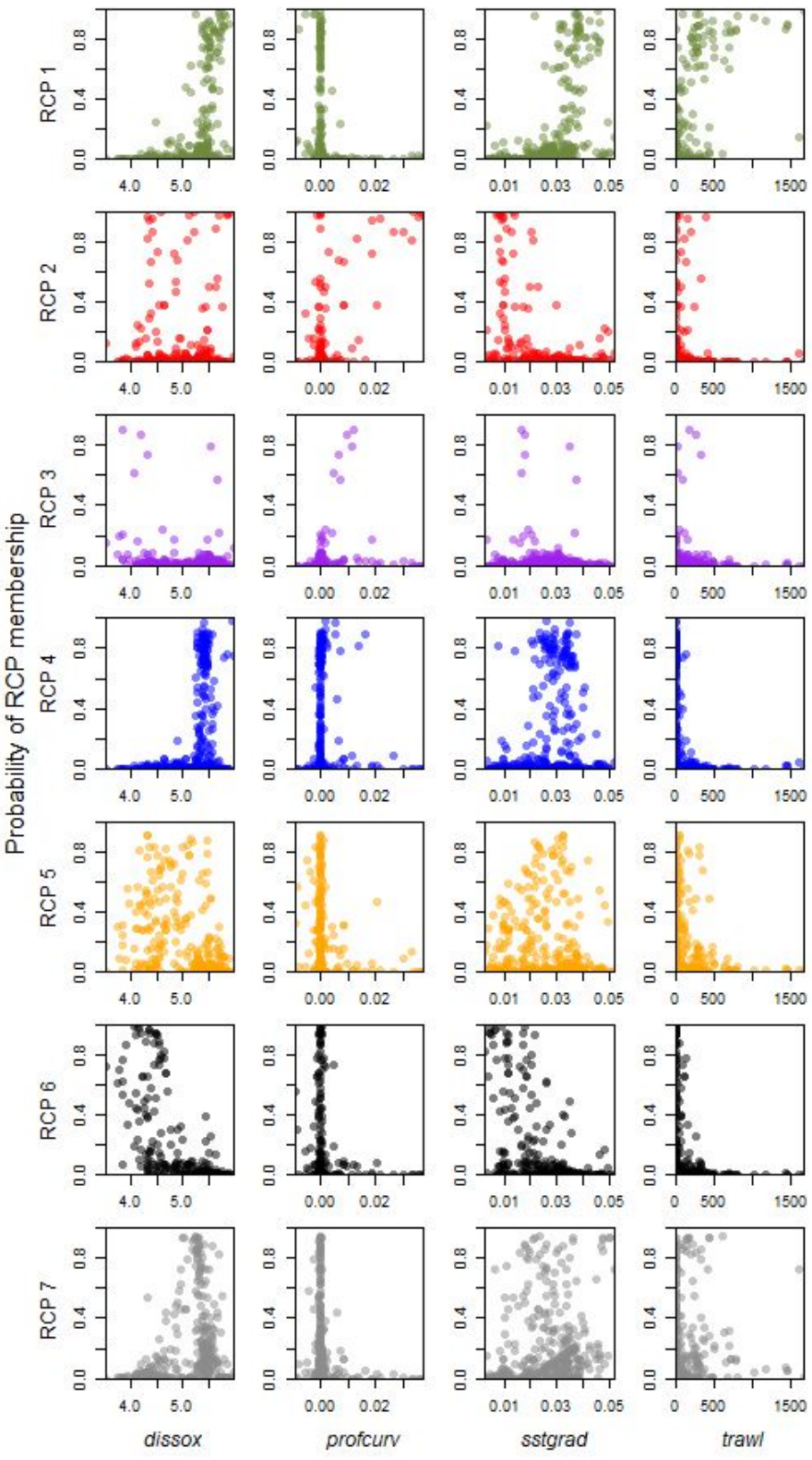

Figure A-2. Response of each RCP to the environmental predictors *dissox*, *profcurv*, *sstgrad*, and *trawl*, based on predicting RCP membership for each site based only on the environmental covariates.

9. APPENDIX 3 – Gradient Forests

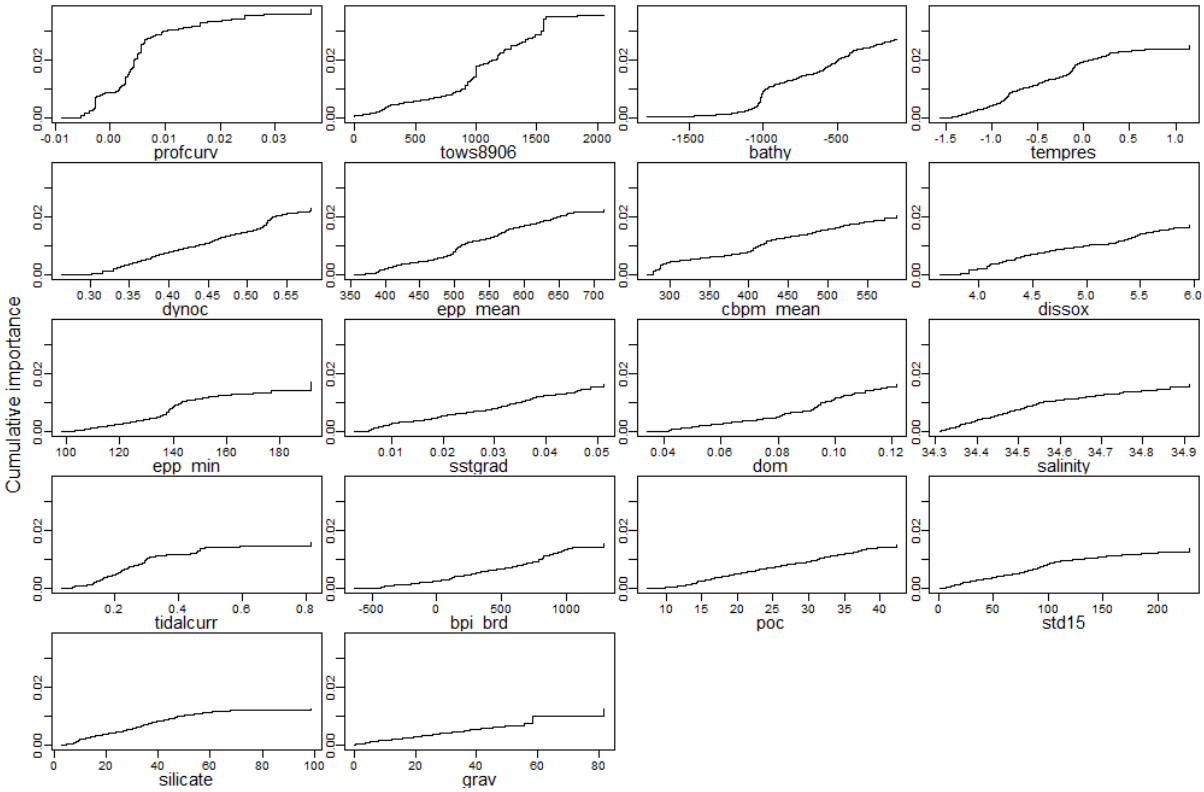

Figure A-3: Summary plots of functions fitted by the final Gradient Forest model, including trawl history, indicating the relative rate of taxon turnover along each of the 18 environmental gradients used as predictors; steeper curves represent greater taxon turnover. Cumulative importance measured as R^2.

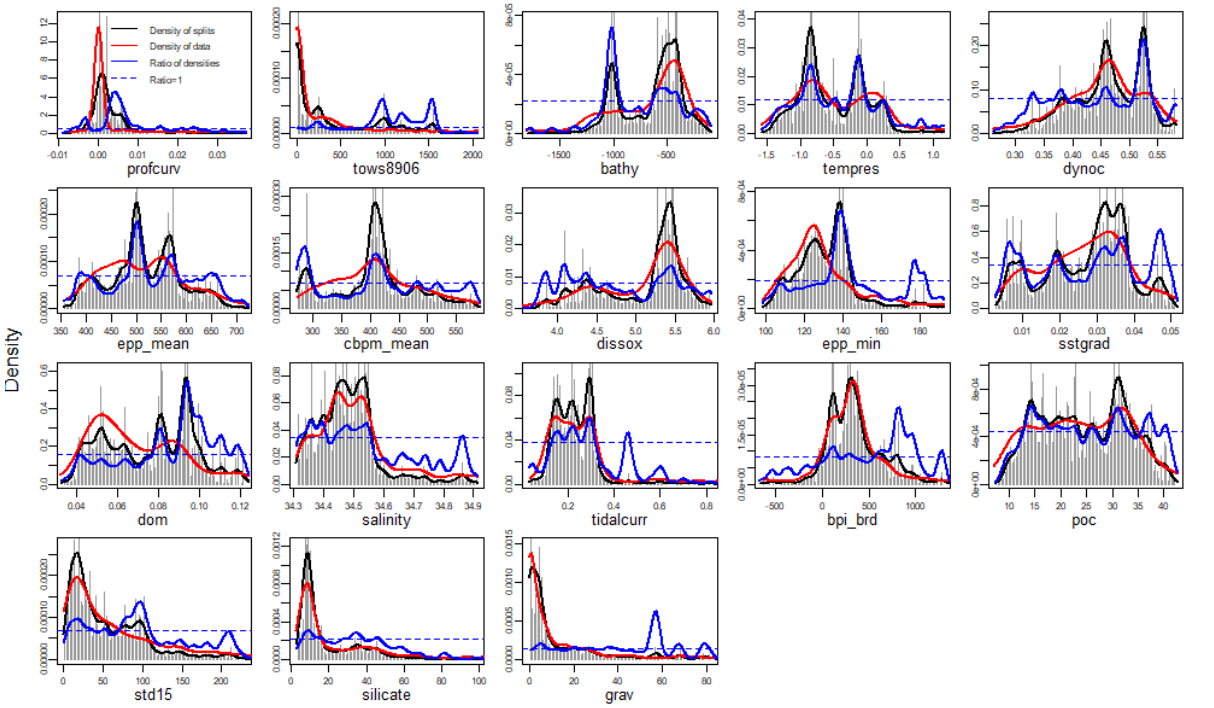

Figure A-4: Gradient Forests splits-density plot, showing the density of Random Forest splits along each of the 18 environmental predictor gradients as an indication of where changes in the abundances of multiple taxa occur. Bars show binned split importance and location on each gradient; black lines show kernel density of splits; red lines show density of observations; blue lines show the ratio of splits density to observation density, and dashed lines show ratio of 1.

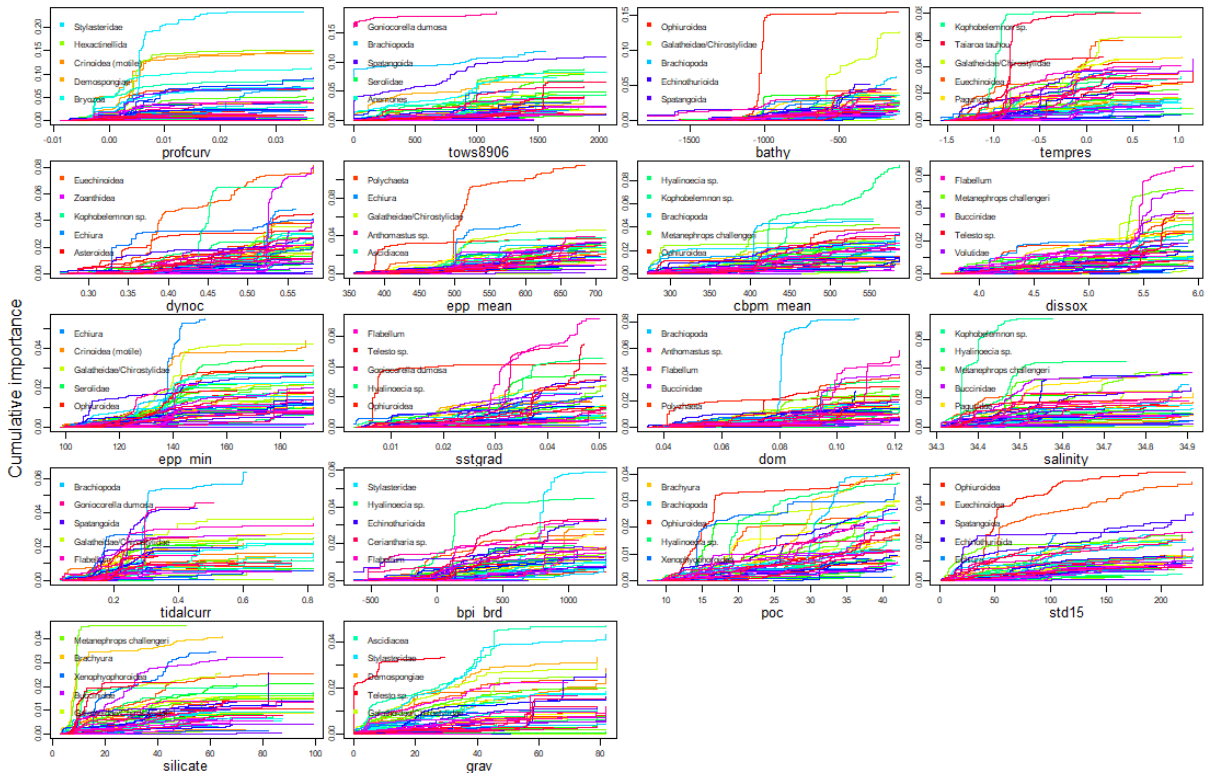

Figure A-5: Gradient Forests cumulative change in assemblage composition in relation to the 18 environmental gradients; coloured plots represent changes in individual taxa. The five most strongly responding taxa for each variable are labelled in the plot legends.

Table A-3: Gradient Forests. Taxon table, showing mean density of benthic taxa within each class of the 50-class classification developed using 17 predictor variables (i.e., excluding trawl history). Densities are numbers of individuals 1000 m^{-2} back-transformed from $log_{10}(1+x)$ sample data used in the GF model. Cut-off for inclusion here is 3 inds.1000 m^{-2}.

Class	Taxon	Density	Class	Taxon	Density
2	Spatangoida	23.10	17	Spatangoida	89.54
	Pennatulacea	18.77		Asteroidea	33.87
	Holothuroidea	14.95		Anthomastus sp.	26.91
	Radicipes sp.	13.64		Enypniastes eximia	16.70
	Galatheidae/Chirostylidae	13.33		Holothuroidea	7.89
	Caridea	10.24		Caridea	3.72
	Brachyura	9.02			
	Metanephrops challengeri	8.98	18	Bryozoa	518.02
	Taiaroa tauhou	6.59		Crinoidea (motile)	249.67
	Asteroidea	5.06		Zoanthidea	245.69
	Anemones	4.53		Primnoidae	136.11
				Ascidiacea	109.83
3	Demospongiae	67.86		Paguridae	78.90
	Bryozoa	26.70		Demospongiae	61.26
	Anemones	17.62		Anthomastus sp.	56.39
	Ascidiacea	15.42		Euechinoidea	46.17
	Taiaroa tauhou	14.98		Anemones	36.90
	Stylasteridae	12.13		Ophiuroidea	30.51
	Hydrozoa	10.62		Hexactinellida	24.36
	Galatheidae/Chirostylidae	10.03		Caridea	24.34
	Pennatulacea	7.52		Hydrozoa	20.08
	Hexactinellida	5.23		Galatheidae/Chirostylidae	16.29
	Paguridae	5.14		Stylasteridae	15.06
	Polychaeta	4.87		Pennatulacea	13.92
	Brachyura	3.87		Caryophylliidae	12.52
				Enallopsammia sp.	12.11
4	Caridea	27.32		Xenophyophoroidea	11.92
	Pennatulacea	21.74		Asteroidea	10.03
	Paguridae	20.27		Gastropoda	7.74
	Anemones	7.64		Gorgonacea	7.56
	Asteroidea	6.76		Madrepora sp.	6.50
	Kophobelemnon sp.	4.99		Alcyonacea	5.24
	Galatheidae/Chirostylidae	3.82		Holothuroidea	3.91
	Brachyura	3.82		Polychaeta	3.62
	Echinothurioida	3.82			
16	Euechinoidea	281.24			
	Asteroidea	17.82			
	Paguridae	8.32			
	Bryozoa	7.72			
	Demospongiae	6.59			
	Anthomastus sp.	5.97			
	Radicipes sp.	5.66			
	Caridea	3.90			
	Flabellum	3.40			
20	Bryozoa	1495.97	24	Bryozoa	426.16
	Crinoidea (motile)	979.01		Crinoidea (motile)	170.69
	Ascidiacea	425.35		Stylasteridae	97.11
	Zoanthidea	301.39		Demospongiae	71.90
	Polychaeta	225.03		Solenosmillia variabilis	62.99
	Demospongiae	210.70		Hexactinellida	49.63
	Paguridae	181.94		Paguridae	46.89
	Hexactinellida	135.24		Caridea	44.61

Class	Taxon	Density	Class	Taxon	Density
	Ophiuroidea	125.34		Primnoidae	43.93
	Anemones	123.31		Anemones	31.41
	Hydrozoa	102.32		Hydrozoa	30.88
	Solenosmillia variabilis	88.34		Ophiuroidea	21.36
	Galatheidae/Chirostylidae	60.99		Ascidiacea	19.70
	Caridea	58.24		Xenophyophoroidea	18.13
	Alcyonacea	41.58		Polychaeta	16.48
	Xenophyophoroidea	36.44		Galatheidae/Chirostylidae	14.78
	Primnoidae	31.69		Gorgonacea	13.50
	Gorgonacea	30.12		Isididae	9.85
	Anthomastus sp.	23.72		Buccinidae	8.75
	Gastropoda	18.03		Antipatharia	8.39
	Asteroidea	14.12		Gastropoda	7.66
	Caryophylliidae	13.90		Anthomastus sp.	7.62
	Isididae	12.22		Caryophylliidae	6.74
	Enypniastes eximia	9.50		Alcyonacea	6.58
	Euechinoidea	7.60		Cidaroida	6.47
	Ceriantharia sp.	6.78		Pennatulacea	4.22
	Worm indet.	6.35		Asteroidea	4.04
	Echiura	5.67		Hyalinoecia sp.	3.87
	Stylasteridae	5.51			
	Madrepora sp.	3.49	26	Spatangoida	31.46
	Cidaroida	3.21		Bryozoa	26.08
				Hyalinoecia sp.	23.03
22	Radicipes sp.	264.56		Pennatulacea	20.05
	Hyalinoecia sp.	37.17		Radicipes sp.	14.01
	Cidaroida	24.03		Hydrozoa	11.95
	Pennatulacea	17.43		Caridea	10.56
	Euechinoidea	11.01		Paguridae	8.44
	Primnoidae	10.21		Holothuroidea	8.05
	Caridea	9.99		Ceriantharia sp.	7.82
	Asteroidea	6.40		Asteroidea	6.91
	Paguridae	5.57		Stylasteridae	6.04
	Gastropoda	4.70		Anemones	5.40
	Brachyura	4.19		Demospongiae	4.60
	Buccinidae	3.52		Taiaroa tauhou	4.20
	Ophiuroidea	3.45			
	Ceriantharia sp.	3.22			
23	Enypniastes eximia	57.36			
	Xenophyophoroidea	26.90			
	Cidaroida	15.37			
	Asteroidea	5.62			
	Holothuroidea	4.73			
	Spatangoida	3.25			
27	Stylasteridae	88.59	30	Hyalinoecia sp.	63.58
	Demospongiae	69.29		Paguridae	35.91
	Crinoidea (motile)	25.49		Polychaeta	35.70
	Bryozoa	24.62		Flabellum	31.86
	Ophiuroidea	22.88		Bryozoa	28.24
	Caridea	19.83		Anthomastus sp.	26.14
	Ascidiacea	19.22		Buccinidae	25.87
	Paguridae	13.46		Spatangoida	25.69
	Goniocorella dumosa	12.68		Taiaroa tauhou	23.05
	Gorgonacea	11.41		Galatheidae/Chirostylidae	21.45
	Caryophylliidae	8.59		Anemones	19.22

Class	Taxon	Density	Class	Taxon	Density
	Cidaroida	8.11		Demospongiae	13.68
	Holothuroidea	8.06		Asteroidea	12.89
	Anemones	6.33		Hydrozoa	11.75
	Euechinoidea	6.22		Hexactinellida	9.83
	Antipatharia	6.13		Holothuroidea	9.57
	Hydrozoa	5.42		Stylasteridae	9.39
	Asteroidea	5.21		Pennatulacea	8.85
	Gastropoda	4.39		Radicipes sp.	8.66
	Primnoidae	3.38		Worm indet.	8.60
				Cidaroida	8.56
28	Spatangoida	70.96		Gastropoda	8.48
	Pennatulacea	32.99		Euechinoidea	7.94
	Radicipes sp.	23.60		Telesto sp.	7.44
	Hydrozoa	11.17		Ascidiacea	7.36
	Galatheidae/Chirostylidae	9.76		Psolidae	6.49
	Asteroidea	8.30		Echinothurioida	4.78
	Holothuroidea	7.86		Caryophylliidae	3.95
	Anemones	5.45		Caridea	3.18
	Metanephrops challengeri	4.14		Alcyonacea	3.14
	Goniocorella dumosa	3.51			
			31	Spatangoida	91.21
29	Stylasteridae	1634.04		Goniocorella dumosa	72.69
	Hexactinellida	375.22		Brachiopoda	49.54
	Demospongiae	66.60		Galatheidae/Chirostylidae	35.70
	Enallopsammia sp.	62.14		Hydrozoa	35.11
	Primnoidae	51.28		Taiaroa tauhou	17.87
	Anemones	46.69		Demospongiae	16.10
	Antipatharia	30.05		Cidaroida	13.02
	Paguridae	28.33		Ascidiacea	12.87
	Goniocorella dumosa	26.44		Paguridae	10.33
	Zoanthidea	25.16		Asteroidea	9.82
	Crinoidea (motile)	19.03		Caryophylliidae	9.35
	Echinothurioida	16.77		Polychaeta	7.77
	Caridea	16.74		Anemones	7.40
	Anthomastus sp.	12.14		Bryozoa	5.93
	Caryophylliidae	11.99		Stylasteridae	5.42
	Bryozoa	10.85		Caridea	5.12
	Radicipes sp.	10.52		Brisingidae	3.20
	Hydrozoa	9.59			
	Xenophyophoroidea	8.70			
	Crinoidea (stalked)	8.17			
	Asteroidea	7.34			
	Gastropoda	7.32			
	Pennatulacea	3.17			
32	Asteroidea	36.53	36	Kophobelemnon sp.	100.16
	Paguridae	28.72		Spatangoida	66.80
	Anemones	27.73		Galatheidae/Chirostylidae	53.00
	Demospongiae	23.11		Paguridae	42.26
	Brachiopoda	19.76		Demospongiae	28.10
	Stylasteridae	17.01		Taiaroa tauhou	27.98
	Crinoidea (motile)	15.03		Anemones	27.48
	Spatangoida	13.00		Caridea	25.01
	Hydrozoa	9.74		Polychaeta	23.55
	Scaphopoda	7.91		Goniocorella dumosa	19.90
	Alcyonacea	6.22		Euechinoidea	15.60
	Brachyura	5.19		Cidaroida	13.58
	Bryozoa	4.47		Bryozoa	12.72
	Gorgonocephalidae	3.60		Asteroidea	10.79

Class	Taxon	Density	Class	Taxon	Density
	Holothuroidea	3.11		Hydrozoa	9.44
				Ascidiacea	8.91
33	Galatheidae/Chirostylidae	48.06		Stylasteridae	8.24
	Spatangoida	42.65		Hyalinoecia sp.	7.95
	Demospongiae	14.75		Crinoidea (motile)	7.71
	Bryozoa	13.09		Echinothurioida	6.90
	Brachyura	12.40		Worm indet.	5.53
	Paguridae	9.97		Flabellum	5.02
	Asteroidea	8.55		Cladorhizidae	4.96
	Anemones	8.02		Primnoidae	4.75
	Echinothurioida	5.68		Caryophylliidae	4.31
	Cidaroida	4.54		Gorgonacea	3.96
	Hydrozoa	3.14		Buccinidae	3.50
34	Demospongiae	271.58	37	Taiaroa tauhou	319.42
	Brachiopoda	205.38		Paguridae	50.97
	Bryozoa	106.47		Hyalinoecia sp.	43.39
	Stylasteridae	85.66		Anemones	35.50
	Antipatharia	38.64		Kophobelemnon sp.	25.48
	Hydrozoa	37.29		Galatheidae/Chirostylidae	21.33
	Ophiuroidea	32.70		Flabellum	17.58
	Ascidiacea	27.56		Anthomastus sp.	17.50
	Brachyura	14.05		Polychaeta	15.82
	Gastropoda	9.73		Worm indet.	15.73
	Hexactinellida	9.19		Asteroidea	14.69
	Holothuroidea	5.67		Stylasteridae	9.67
				Hydrozoa	9.35
38	Hyalinoecia sp.	1108.69		Cidaroida	8.53
	Cidaroida	172.10		Caridea	8.41
	Anemones	8.95		Buccinidae	7.50
	Paguridae	7.28		Bryozoa	7.46
	Gastropoda	7.28		Goniocorella dumosa	6.79
	Taiaroa tauhou	3.08		Demospongiae	5.82
	Ceriantharia sp.	3.08		Telesto sp.	5.75
	Buccinidae	3.08		Ceriantharia sp.	4.36
				Gastropoda	3.40

39	Stylasteridae	69.35	42	Hyalinoecia sp.	198.76
	Demospongiae	45.21		Cidaroida	64.06
	Anemones	42.34		Paguridae	55.03
	Cidaroida	34.97		Anemones	31.21
	Brachiopoda	27.07		Hydrozoa	11.77
	Galatheidae/Chirostylidae	22.57		Holothuroidea	3.56
	Asteroidea	21.59			
	Corallimorpharia	18.34	44	Demospongiae	118.43
	Polychaeta	16.40		Anemones	93.22
	Spatangoida	16.34		Brachiopoda	51.44
	Bryozoa	13.71		Galatheidae/Chirostylidae	51.26
	Paguridae	11.28		Bryozoa	44.58
	Buccinidae	10.61		Stylasteridae	44.45
	Euechinoidea	10.60		Cidaroida	37.50
	Crinoidea (motile)	10.15		Polychaeta	32.51
	Brachyura	9.90		Asteroidea	28.39
	Caryophylliidae	7.33		Worm indet.	26.16

Class	Taxon	Density	Class	Taxon	Density
	Gastropoda	4.57		Bivalvia	22.98
	Goniocorella dumosa	4.51		Caryophylliidae	19.44
	Primnoidae	4.41		Caridea	12.28
	Antipatharia	3.69		Hexactinellida	11.78
	Gorgonacea	3.27		Goniocorella dumosa	9.79
				Holothuroidea	6.77
40	Xenophyophoroidea	59.00		Flabellum	6.61
	Hyalinoecia sp.	51.31		Hydrozoa	5.91
	Euechinoidea	42.50		Crinoidea (motile)	5.73
	Stylasteridae	36.99		Gorgonacea	5.03
	Demospongiae	18.50		Paguridae	4.30
	Alcyonacea	17.80		Euechinoidea	3.99
	Asteroidea	15.72		Ceriantharia sp.	3.58
	Paguridae	15.27		Gastropoda	3.56
	Gastropoda	9.88		Alcyonacea	3.41
	Cidaroida	9.60		Spatangoida	3.12
	Caridea	8.78		Ophiuroidea	3.08
	Holothuroidea	8.49			
	Gorgonacea	8.43	45	Demospongiae	211.44
	Anemones	5.73		Hyalinoecia sp.	107.78
	Hydrozoa	4.99		Xenophyophoroidea	82.56
	Flabellum	4.42		Gastropoda	63.38
	Bryozoa	4.04		Paguridae	58.80
	Primnoidae	3.49		Anemones	25.68
	Volutidae	3.41		Asteroidea	23.75
	Echinothurioida	3.35		Cidaroida	20.87
				Flabellum	15.32
41	Ophiuroidea	1812.74		Euechinoidea	14.81
	Euechinoidea	191.38		Primnoidae	12.90
	Taiaroa tauhou	38.00		Galatheidae/Chirostylidae	10.79
	Primnoidae	24.30		Crinoidea (motile)	6.29
	Caridea	19.96		Ophiuroidea	5.66
	Paguridae	12.48		Hexactinellida	5.34
	Asteroidea	11.64		Alcyonacea	5.05
	Gastropoda	7.90		Buccinidae	4.94
	Cidaroida	7.17		Anthomastus sp.	4.50
	Demospongiae	5.48		Holothuroidea	4.40
	Buccinidae	3.45		Stylasteridae	3.93
	Madrepora sp.	3.15			
46	Ophiuroidea	6011.77	49	Euechinoidea	108.90
	Xenophyophoroidea	47.42		Demospongiae	29.50
	Demospongiae	43.76		Asteroidea	22.25
	Holothuroidea	9.66		Ophiuroidea	17.88
	Asteroidea	6.05		Caridea	4.48
	Ceriantharia sp.	5.00			
	Echinothurioida	4.83			
	Anemones	3.69			
	Cidaroida	3.29			

Table A-4: Gradient Forests. Raw mean values of environmental variables for each class in the 50-class classification including trawl history. For variable descriptions, units, and sources, see Table 1.

GF class	profcurv	trawl	bathy	tempres	dynoc	epp_mean	cbpm_mean	epp_min	sstgrad	salinity	dissox	tidalcurr	dom	bpi_brd	poc	std15	silicate	grav
Grp_1	-4.41E-05	175	-139	0.909	0.446	762.8	343.5	234.3	0.016	34.86	5.545	0.402	0.096	568.40	34.48	116.7	4.55	14.60
Grp_2	-5.84E-04	2023	-408	0.401	0.476	700.4	200.1	233.9	0.025	34.69	5.166	0.302	0.082	583.37	25.69	243.4	7.67	7.14
Grp_3	3.30E-06	484	-439	0.103	0.478	555.6	367.9	152.6	0.032	34.64	5.295	0.247	0.063	619.54	27.11	42.2	8.56	6.37
Grp_4	8.14E-04	175	-852	0.173	0.463	696.9	209.9	217.8	0.025	34.50	4.795	0.170	0.078	145.81	25.62	342.5	23.88	3.40
Grp_5	2.72E-03	160	-458	0.025	0.426	797.8	376.0	232.6	0.012	34.62	5.358	0.079	0.116	64.34	21.37	350.7	10.29	15.23
Grp_6	3.35E-03	67	-1584	0.109	0.465	677.9	313.0	185.3	0.022	34.56	4.146	0.084	0.079	-433.48	15.65	364.8	74.93	4.62
Grp_7	8.62E-05	5	-1637	0.154	0.541	504.8	354.1	144.6	0.023	34.57	3.790	0.093	0.053	-10.56	9.35	198.7	88.21	7.09
Grp_8	1.25E-05	74	-1184	-0.083	0.515	535.3	394.4	148.4	0.025	34.47	4.211	0.130	0.057	259.45	13.23	130.1	44.95	4.91
Grp_9	4.76E-05	4	-1738	0.296	0.541	387.2	291.0	118.8	0.011	34.58	3.800	0.089	0.041	311.48	7.32	76.7	88.42	3.06
Grp_10	7.37E-05	234	-213	0.365	0.421	576.0	450.9	153.0	0.013	34.73	5.688	0.497	0.064	576.01	32.55	49.1	4.98	15.74
Grp_11	1.87E-06	286	-174	-0.247	0.402	752.2	505.4	189.0	0.020	34.61	5.857	0.270	0.093	187.75	36.66	105.3	4.38	10.61
Grp_12	-1.19E-02	99	-972	0.074	0.435	737.5	378.2	197.9	0.020	34.51	4.881	0.170	0.100	-137.13	23.57	464.8	22.46	8.83
Grp_13	-1.15E-03	224	-1209	-0.018	0.416	759.3	403.4	200.4	0.012	34.49	4.342	0.088	0.101	-511.97	19.84	320.7	48.55	10.92
Grp_14	1.21E-03	155	-791	-0.021	0.387	714.8	467.0	195.6	0.029	34.45	4.911	0.150	0.096	-294.08	19.97	200.4	26.39	1.61
Grp_15	-1.50E-04	15	-1682	0.126	0.394	666.5	442.1	169.7	0.013	34.58	4.172	0.092	0.085	-824.40	12.24	170.4	85.13	7.29
Grp_16	-5.31E-04	405	-420	-0.130	0.400	778.9	453.3	205.4	0.022	34.54	5.515	0.145	0.104	-20.64	21.57	244.7	8.08	5.13
Grp_17	2.75E-05	73	-1132	-0.120	0.390	665.5	463.3	175.5	0.014	34.47	4.349	0.126	0.086	-320.45	16.05	150.4	43.37	4.73
Grp_18	1.23E-03	1344	-582	0.123	0.419	753.3	409.2	185.2	0.013	34.58	5.119	0.144	0.101	249.45	26.45	282.9	14.92	24.17
Grp_19	-2.56E-06	296	-837	0.044	0.487	567.4	389.6	153.6	0.033	34.47	4.811	0.156	0.062	469.32	17.65	116.3	25.19	3.64
Grp_20	-4.32E-06	78	-1199	0.106	0.531	428.1	300.7	118.4	0.015	34.44	4.193	0.112	0.047	461.59	10.72	109.8	48.32	5.54
Grp_21	-3.50E-05	23	-778	0.202	0.542	453.7	331.0	119.7	0.021	34.45	4.644	0.153	0.050	464.83	16.33	53.9	22.80	2.89
Grp_22	-2.90E-04	213	-87	-0.230	0.411	826.6	536.6	239.3	0.018	34.65	5.936	0.290	0.103	219.71	29.80	51.4	3.40	19.32
Grp_23	1.46E-03	1224	-1121	-0.171	0.527	508.0	411.6	141.8	0.017	34.47	4.116	0.149	0.052	313.72	15.07	108.9	46.57	5.00
Grp_24	-2.36E-05	628	-653	-0.142	0.402	634.7	453.4	166.2	0.007	34.51	5.212	0.195	0.079	303.73	21.43	93.9	15.24	9.70

GF class	profcurv	trawl	bathy	tempres	dynoc	epp_mean	cbpm_mean	epp_min	sstgrad	salinity	dissox	tidalcurr	dom	bpi_brd	poc	std15	silicate	grav
Grp_25	-6.63E-07	1750	-533	0.181	0.496	552.9	371.7	150.5	0.048	34.61	5.129	0.237	0.065	677.02	23.10	101.7	9.22	8.87
Grp_26	2.01E-05	65	-492	0.095	0.535	475.7	377.0	120.7	0.026	34.57	5.175	0.246	0.055	451.45	22.24	37.3	9.26	7.27
Grp_27	1.27E-02	177	-831	0.227	0.522	415.6	290.1	108.4	0.011	34.42	4.523	0.142	0.045	678.27	12.41	109.9	31.02	5.05
Grp_28	1.59E-05	48	-422	-0.657	0.477	492.7	376.3	121.0	0.032	34.52	5.360	0.280	0.066	294.20	26.20	15.2	8.06	15.53
Grp_29	1.63E-05	1257	-486	-0.637	0.370	678.3	519.8	147.2	0.031	34.47	5.691	0.247	0.103	47.14	35.18	36.1	8.25	3.55
Grp_30	3.85E-05	451	-539	-0.642	0.374	650.3	501.7	150.2	0.035	34.43	5.633	0.216	0.103	38.60	31.36	25.3	10.26	2.62
Grp_31	6.79E-06	39	-323	-0.471	0.454	566.5	368.6	131.5	0.026	34.61	5.516	0.310	0.076	361.99	37.30	16.9	6.58	10.54
Grp_32	9.11E-05	64	-264	0.527	0.521	450.5	346.9	122.0	0.015	34.79	5.490	0.447	0.055	371.88	30.50	35.7	4.81	17.74
Grp_33	5.79E-08	1052	-357	0.454	0.539	498.0	341.4	127.8	0.024	34.72	5.223	0.131	0.064	389.65	31.54	47.4	5.79	5.89
Grp_34	-3.09E-05	15	-92	1.261	0.523	484.4	514.0	151.9	0.007	34.90	5.808	0.611	0.070	562.63	39.99	24.8	2.80	21.81
Grp_35	-4.56E-06	164	-102	-0.508	0.393	686.4	602.7	167.4	0.038	34.56	6.115	0.346	0.079	306.16	44.34	14.4	3.60	19.43
Grp_36	5.67E-05	244	-439	-0.957	0.421	579.1	456.0	121.2	0.039	34.46	5.547	0.239	0.089	198.93	32.07	43.3	8.01	5.72
Grp_37	-2.78E-05	2038	-197	-0.688	0.373	697.2	558.4	142.7	0.025	34.61	5.927	0.348	0.099	252.38	43.39	87.4	4.48	7.60
Grp_38	-5.12E-06	1244	-527	-0.896	0.436	526.3	446.4	126.9	0.035	34.43	5.423	0.196	0.075	235.51	24.80	49.4	9.31	12.98
Grp_39	1.25E-05	173	-731	-1.118	0.431	453.8	429.6	120.2	0.028	34.35	5.097	0.186	0.059	235.27	18.26	60.9	17.94	10.23
Grp_40	2.22E-03	1980	-1237	0.120	0.525	403.6	276.3	105.8	0.009	34.41	4.289	0.114	0.045	558.24	10.12	166.0	44.12	5.01
Grp_41	-9.81E-07	84	-70	-0.180	0.398	719.5	736.4	223.3	0.031	34.56	6.241	0.199	0.085	224.06	40.29	6.5	3.50	9.54
Grp_42	1.96E-04	60	-329	0.064	0.496	433.2	337.0	133.8	0.011	34.72	5.514	0.190	0.054	897.81	23.75	99.8	4.83	20.19
Grp_43	3.69E-04	60	-610	-0.386	0.477	412.0	300.0	129.4	0.023	34.46	5.204	0.154	0.047	655.04	18.02	104.4	11.11	12.22
Grp_44	-1.21E-05	2413	-262	-1.097	0.380	649.5	507.9	133.3	0.053	34.45	6.050	0.169	0.077	279.45	46.87	98.8	5.53	7.06
Grp_45	1.45E-04	70	-706	-0.920	0.364	566.4	555.8	119.3	0.028	34.33	5.317	0.164	0.083	31.82	28.19	38.2	18.66	1.75
Grp_46	1.50E-04	59	-905	-1.344	0.340	465.4	557.6	111.8	0.016	34.33	4.822	0.130	0.060	30.32	19.17	54.8	36.47	3.51
Grp_47	-2.75E-05	11	-1224	-1.180	0.327	374.4	478.1	108.1	0.008	34.43	4.307	0.108	0.039	44.19	11.71	41.4	54.17	4.79
Grp_48	-1.26E-05	690	-508	-0.941	0.369	613.6	520.8	119.3	0.044	34.40	5.880	0.159	0.069	100.22	38.61	84.3	10.20	3.45
Grp_49	-8.87E-06	0	-1574	-0.401	0.262	322.6	460.8	95.0	0.005	34.57	4.082	0.084	0.031	-42.58	8.01	57.7	77.73	1.75
Grp_50	2.09E-05	184	-816	-0.873	0.342	500.8	494.7	117.9	0.048	34.33	5.068	0.089	0.047	-156.80	25.87	204.3	29.11	2.63